TRANSMOTOR APPLICATIONS FOR ELECTRIC VEHICLES

A Dissertation

by

AHMET YASIN YEKSAN

Submitted to the Office of Graduate and Professional Studies of
Texas A&M University
in partial fulfillment of the requirements for the degree of

DOCTOR OF PHILOSOPHY

Chair of Committee,	Mehrdad Ehsani
Committee Members,	Robert S. Balog
	Shankar P. Bhattacharyya
	Alan B. Palazzolo
Head of Department,	Miroslav M. Begovic

May 2018

Major Subject: Electrical Engineering

ABSTRACT

Efficient energy storage and cost-effective solutions are vital for electric vehicle applications. As it is widely known, the battery pack of an electric vehicle is a significant component that determines the range and price of the electric vehicle mostly. The recent trend in electric vehicles is using Li-Ion battery packs as the primary energy source. However, Li-Ion battery technology is still immature and its cost is higher than other battery solutions. Although the range of recent electric vehicles has been improved significantly with this recent battery type, their range is still less than conventional vehicles and their market price is almost twice of a gasoline fueled-vehicle. This has brought about new electric powertrain configurations to increase the vehicle energy efficiency.

Regenerative braking is a feature that increases the energy efficiency of an electric vehicle by capturing the kinetic energy and storing it in the electrical energy storage unit. This unique feature leads to drive some extra miles with an electric vehicle. However, the round-trip efficiency of the regenerative braking is quite low in applications. The powertrain components in an electric vehicle have more than 90% efficiency values. Improving the efficiency of the electrical machine or the power processor unit would not increase the regenerative braking efficiency because of the overall energy efficiency chain. In addition, regenerative braking has a power limitation that is the rated electrical power. Because of these reasons, if we would like to improve the range of an electric vehicle, we need to increase the regenerative braking capability. Energy form conversions should be avoided and mechanical form of the energy in the vehicle should be kept the same as much as possible.

In this study, we introduced a magnetically coupled three-port electric machine, the transmotor. The transmotor consists of two mechanical ports that are decoupled and an electrical port for the power processor unit connection. In vehicle applications, the first mechanical port can be connected wheels. The second mechanical port in the machine can be connected a mechanical energy storage device such as a flywheel. Hence, the structure of the transmotor creates two mechanical paths for the energy exchange. This two-path energy exchange feature can be used to

enhance the regenerative braking capability of electric powertrains.

We developed a new powertrain configuration for electric vehicles that is called Flywheel Transmotor (FWT) powertrain. Application of the transmotor and a flywheel in an electric powertrain was presented. This new powertrain configuration was applied in a commercial electric vehicle, Nissan Leaf 2012 that is currently in the electric vehicle market. Simulation models were developed for the existing powertrain of the vehicle and flywheel transmotor powertrain. Standard drive cycles were used to run simulations. Simulation results of the new powertrain configuration were presented and compared with the conventional Nissan Leaf 2012 powertrain simulation results. Effect of the new parameters that are flywheel moment of inertia and flywheel initial speed was investigated. Performance tests were also performed and outcomes were presented. We optimized the flywheel powertrain configuration of Nissan Leaf 2012 with the acquired simulation data.

According to simulation results, the range of the Nissan Leaf 2012 can be increased by 14.2% with flywheel transmotor powertrain configuration. In addition, the rated electrical power of the traction motor and power electronics can be decreased by 25%. In other words, a Nissan Leaf 2012 can travel 14.2% more with a smaller electric power rating compared to its original powertrain. The required flywheel weight for this powertrain is around 1-2% of the vehicle weight. The stored energy in the flywheel is 2-3% of the battery pack energy. The control complexity of the new powertrain configuration is less compared to existing electric flywheel powertrains in the literature. Since we only utilize one electric motor/generator and one power electronics circuit in the powertrain, it is a cheaper and more reliable solution than other flywheel powertrain applications. The flywheel transmotor powertrain can be a competitive alternative for existing electric powertrains by providing a better regenerative braking capability.

DEDICATION

To my mother Fatma Nurten, my father Mehdi, my sisters Ayse Nur and Merve, and my grandmother Hatice.

To my dear future wife Elham.

CONTRIBUTORS AND FUNDING SOURCES

Contributors

This work was supervised by a dissertation committee consisting of Professor Mehrdad Ehsani and Professors Robert S. Balog, Shankar P. Bhattacharyya of the Department of Electrical and Computer Engineering and Professor Alan B. Palazzolo of Mechanical Engineering. All work for the dissertation was completed independently by the student.

Funding Sources

Graduate study was supported by a fellowship from The Scientific and Technological Research Council of Turkey (TUBITAK) from 2014 to 2016 for 24 months.

TABLE OF CONTENTS

Page

LIST OF FIGURES

FIGURE Page

LIST OF TABLES

TABLE Page

1. INTRODUCTION AND LITERATURE REVIEW

1.1 Introduction

The history of automotive goes back to the 17^{th} century. It started with steam powered cars and continued with internal combustion (IC) engine vehicles, with electric vehicles (EVs) gaining popularity in the late 19^{th} century. However, their popularity had not last long because of the cheap fuel gasoline that was used by IC engine vehicles. IC engine vehicles have dominated the last 150 years of the automotive market. During this time, the world has witnessed the industrial revolution two World Wars, and the digital transformation. The world has been in a competition to industrialize every day more and the effect of the vehicle technology cannot be ignored. However, excessive usage of fossil fuels has drained away resources and caused many environmental problems.

Fossil fuel restriction and environmental issues have raised many concerns about IC engine vehicle usage. Because they are the primary consumer of oil products and the worst contributor in air pollution. In addition, many people have believed that vehicle usage is one of the main reasons for global warming. Automakers have tried to increase the fuel efficiency and decrease the tailpipe gas emissions of their products for the last three decades; however, it was not a permanent solution. Meanwhile, the digital transformation has started to show its affect on the automotive products as well. Every year automotive companies added electronic features in their models like automatic braking system, electric steering, electronic stability control, road computer, infotainment systems, lane change assistant, and automated driving systems etc.. Each new feature has made vehicles more of a digital product and a compatible electric powertrain was required. The need of revolutionizing the vehicle technology was not avoidable.

Electric vehicles do not generate power by combustion and they do not release any exhaust gases. Furthermore, electric motors can be controlled by electronic control units easily, which makes them more preferable for autonomous vehicle applications. The idea of zero emission vehicle that does not pollute the air and high technology vehicles have motivated some entrepreneurs

to start new automotive companies that produces only electric vehicles. Especially the success of Tesla Model S has brought millions of people's attention on EVs in the United States. In the meantime, Nissan Motor Company's all electric vehicle Nissan Leaf have achieved a great success in European countries with a more affordable price but less range compared to Tesla Model S [1, 2]. The success of these two companies can be assumed as the milestone of the automotive industry. Because the number of drivers who are convinced that a conventional gasoline fueled car can be replaced by an EV after the recent developments in the market have increased. Hence, the increasing demand on EVs could not be ignored by main automobile manufacturers anymore and most of them have launched their fully electrified models.

EVs have brought their own concerns and one of them is on-board energy storage. The range of an EV, battery requirement, and correspondent cost of the battery are all related. Electro-chemical batteries have been the most reliable and cost effective solution for the vehicle applications so far. Lead-acid batteries and NiMH batteries have been used for different electric and hybrid electric vehicles (HEVs). However, their energy density and power density levels are low. Because of this reason the number of battery packs that are used in electric vehicles are high. Hence, the battery weight, volume, and cost numbers increase dramatically. In the last decade, Li-Ion batteries have become a better option for electric vehicles [3]. Energy density of a Li-Ion battery is around 120 Wh/kg whereas this number is around 50 Wh/kg for lead-acid batteries [4]. The difference is more than twice and most of the EV makers preferred them to achieve a better range in their products. Although the cost of Li-Ion battery packages makes upto 50% of the full price of an electric vehicle, the industry still relies on them.

Flywheel energy storage is another alternative for vehicle applications. Their simplicity and low cost make them an attractive option for EVs as well. Using them as a primary energy source may not be a feasible idea because of the weight issue. However, recent developments in flywheel materials have made flywheels a competitive candidate in energy storage systems [5, 6]. In addition, flywheels have a high power density compared to electrochemical batteries thanks to their mechanical structure. Yet, very large amount of energy can be delivered instantly and repeatedly

by flywheels without performance degradation [7]. Unlike their rivals electrochemical batteries, flywheels energy density is low and not enough to supply the complete energy demand in vehicles.

Utilizing flywheels in electrical energy storage systems requires an elaborate topology such as using two electrical machines and related drives. This concept is mostly known in the literature as flywheel battery (FWB) and can be seen in Fig. 1.1 [8]. In this concept, the wheel of a vehicle drives an electrical machine and generates electrical power. The generated power is processed by a rectifier/inverter group and another electrical machine is supplied by this power. The latter machine is connected to a flywheel that stores the energy finally. As a result, the kinetic energy of the load again is stored in mechanical form through an electrical system. Batteries are not necessary for this system. Hence, the energy stored in the vehicle is not transformed into the chemical form. Since the energy conversions are avoided, the efficiency of energy storage process is considerably higher than a conventional battery system.

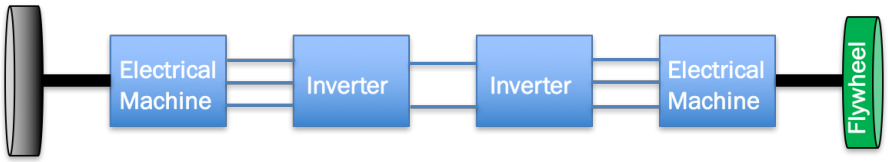

Figure 1.1: Flywheel battery concept

Most of EVs on the market utilize a synchronous ac motor/generator or an induction motor/generator in their powertrain. Generally speaking, electric machines in EVs are two-port-machines that consist of a mechanical port, which is the shaft of the machine, and an electrical port, which is connected to the electric drive system. Using a flywheel directly in an electrified powertrain requires an extra mechanical port which is not possible by using a conventional two port electrical machine.

Three-port electrical machines (TPEM) consists of two mechanical ports and an electrical port. The extra mechanical port in the machine brings another degree of freedom into the system. Weisenburger automobile is one of the oldest application of a TPEM and it was used as

an electromagnetic gear [9]. A separately excited DC machine that had slip rings to supply both the field and armature winding was used in that application. Another early vehicle application of TPEM is Dey automobile. It was exactly the same topology with Weisenberger automobile but the machine was an integrated part in the rear axle [10].

Around a decade ago, a new double-shaft machine with two electrical ports was invented and instead of TPEM term the term: Dual-Mechanical-Port (DMP) was adopted [11]. The principle of the operation of a permanent magnet DMP topology was explained in [11] and further study on control strategies and operation modes of DMP machines were given in [12]. The application in that paper was a hybrid electric vehicle. It was shown that the IC engine in the driveline can be kept at optimum operating conditions by using a DMP machine. A DMP machine does not have to be a permanent magnet machine. Instead of permanent magnets, windings can be utilized in the rotor. In this case, it would be an induction type DMP machine. A good analysis of squirrel cage outer rotor DMP machine can be seen in [13]. The brushes of the DMP machine can be seen as a disadvantage for automobile applications. This problem is discussed in [14] and a novel brushless DMP machine topology is offered in their study. Analysis, modeling and control strategy optimization of DMP machines can be found in the literature [15, 16].

Researchers from Texas A&M University, proposed a new three-port electrical machine as an electromagnetic gear in a HEV. They named their invention as transmotor and presented its modes of operation, for a switched reluctance machine, in a hybrid vehicle [17]. A design example of a mild HEV with a transmotor was reported by Gao and Ehsani in 2002 [18]. In their study, they presented the results of a specific drive cycle simulation and showed that the fuel efficiency of the HEV could be increased significantly. A more recent study of the transmotor application to HEVs and comparison of different three-port machine topologies can be found in [19].

In our study, we purposed to use a flywheel in the electric powertrain to increase the range of EVs by the capturing more kinetic energy. Since we are to use a flywheel in the powertrain, we can combine merits of mechanical and electrical energy storage systems. The lack of power density of electro-chemical batteries can be compensated by flywheels. Thus, the regenerative braking

capability of an EV can be improved. A better regenerative braking capability increases the range of the EV. In addition, the stress on the battery decreases since the charge and discharge depth is lower. Hence, an improvement can be obtained on battery life, cost and weight as well. We used the transmotor as the TPEM in the electric powertrain for traction. We applied the flywheel transmotor powertrain to a current EV which is Nissan Leaf 2012. We compared our results with the original Nissan Leaf 2012 data that we obtained in our simulation model. Lastly, we made different designs to optimize the vehicle and shared our results.

1.2 Literature Review

1.2.1 Flywheel Energy Storage in Electric Vehicles

The flywheel electrical powertrain is not a new concept. The first major application of the flywheel energy storage in an electric vehicle is the Gyrobus in Switzerland in the 1950s. The Oerlikon Company used a 1500 kg flywheel which had a 1.6 m of diameter and 32 MJ of energy storage capacity. The maximum speed of the flywheel was 3000 rpm. The Gyrobus could cover up to 1.2 km with a single charge from a 360 V, 50 Hz utility. This concept had been used around 16 years in European cities and as well as in some African cities. However, the heavy flywheel caused frequent maintenance problems and the operation of the bus was over-complicated. Moreover it needed to be charged many times during the daily operation. Hence, it disappeared from the streets [20].

In 1972, one of the early concepts of the flywheel battery (electromechanical battery) was proposed by Whitelaw. FWB concept refers to electrical connection of the flywheel (and its motor/generator set) to the powertrain. The main application of this concept was the local duty vehicles in the United States as most journeys in the US cities were less than 50 miles. The flywheel battery would supply the average power and the batteries were supposed to provide the peak power [21].

After 1973 oil crisis, the US Department of Energy (DOE) initiated the first symposium, encouraging the researchers from all around the world to develop flywheel energy storage systems.

The outcome of the symposium was that Flywheel Energy Storage Systems (FESS) could be a competitive choice to extend the area of hybrid and all electric transportation applications from large vehicles to small vehicles [22]

In 1977, the US Postal Service and US Department of Energy developed a delivery vehicle that utilized a flywheel-batery powertrain [23]. The flywheel was connected to the traction motor shaft through a fluid coupling. The other side of the traction motor shaft was connected to a variable v-belt through a fixed gear. The proposed topology decreased the peak battery current (demanded by the traction motor) from 600 A to 270 A and improved the acceleration performance of the vehicle as well. The maximum speed of the flywheel was 36000 rpm and the energy storage capacity was 0.5 MJ. Demerit of the system was that the vehicle had to be started by the electric motor.

In 1980, the DOE evaluated 4 different continuous variable transmission (CVT) concepts that was used in a 1700 Kg electric vehicle assisted by a flywheel with a speed range of 14000 to 28000 rpm. The CVT was located between the flywheel and the electric motor, and the other shaft of the motor was connected to the wheels via a clutch and a differential. The evaluated CVT types can be listed as: v-belt CVT, flat belt CVT, toroidal traction CVT, and continuous variable roller cone traction CVT. The results of comparison was reported in a different study indicated that the steel (V-belt) was the most efficient one under the averaged power of 16 KW and the shaft speed of 3000 rpm [24].

In 1991, BMW suggested a new concept in which a high energy battery and a high power flywheel coexist. The proposed system included a planetary gear system with several clutches and brakes to connect the flywheel to the electric motor and the drive shaft. The power flow was determined by the torque and the speed of the electric motor. At standstill, the brake is activated and the electric motor speeds up the flywheel. The vehicle was accelerated using the flywheel and the motor acted as a generator to absorb the excessive energy from the flywheel. Then, at the right speed, the electric machine changed its role to become a motor, and help the flywheel to drive the vehicle forward. The utilization of the flywheel was only during the acceleration/deceleration, meaning that it was not used for cruising. This system lacks enough flexibility and the efficiency

is low due to the energy conversions [25].

In 1993, a group of researchers from University of Warwick reported a hybrid electric car design in which an internal combustion engine was connected to the wheels through a dual rotor brushless DC motor [26]. A steel flywheel was fixed to the stator of the motor. During acceleration (in electric mode) the engine was disconnected from the wheels via a clutch and the flywheel would accelerate the vehicle. In dual mode, the IC engine was operated in its most efficient point and in case of an extra power the flywheel would absorb it. It was claimed (based on their simulations) that the flywheel was able to stop the car and could help the IC engine start and accelerate the vehicle. A 1600 kg car was used in the simulations and according to the simulation results the car reaches to the speed of 60 mile/h in 5 seconds and from 60-80 mile/h in less than 4 seconds. The maximum speed of the car was 110 mile/h. The full electric range of the car was reported to be 40 miles, and the maximum speed in electric mode was 70 mile/h.

In 1994, an electric drive system with a flywheel battery was presented where the flywheel was used a load leveler (energy buffer). It means that the average power comes from the battery and the rest (peaking power) is provided by the flywheel battery. The results show that energy consumption of the vehicle decreased by 20% on the UDC (European driving cycle) [27].

In 2000, it was shown that with a variable DC link voltage it was possible to connect power buffers such as a supercapacitor and a flywheel battery to the drive system of traction motors. Reported results showed that it could reduce the demanded current from the battery and increase the range travelled by the vehicle. Furthermore, it will extend the life span of the battery. On the other hand it is also reported that an advanced energy management technique is necessary to control the limited energy storage capacity of the power buffer effectively [28].

In 2005, another bus application for FESS was reported by University of Texas at Austin. The flywheel unit was capable of accelerating a bus with a full load to 100 km/h with a peak power of 150 kW. The energy storage capacity of the flywheel was 7 MJ (1.93kWh) at 40000 rpm. Its specific energy was reported to be more than 120 kJ/kg while its specific power was 2.5 kW/kg. The results showed that the usage of FESS doubled the acceleration of the bus whereas 25% less

power demand from the engine [29].

The super energy efficient electric vehicle concept was proposed by a group of researchers. This concept design includes flywheel battery, Li-Ion battery, photovoltaic cells, fuel cell and IC engine (as a prime mover for on board generator). The reported fuel consumption of the system was 188 km/l for urban driving and 50 km/l for long driving (highway) [30–33].

Another area of usage for FESS was trams. FESS allowed to operate trams beyond the wires, which was applied by Alstom. A carbon fiber flywheel that is connected to a permanent magnet motor/generator set recovers braking energy of the tram and enables it to reuse the energy. Furthermore, 1.2 mile of the 7 mile-long line is wireless and only the FESS supplied the power demand of the tram for that wireless distance [20].

In 2011, a new flywheel battery design for a full electric powertrain was presented by a research group from Uppsala University [34, 35]. A fully integrated flywheel was utilized in the FWB unit where the machine connected to the flywheel had two separate sets of windings, one high voltage and the other low voltage. The low voltage winding was connected to batteries (via a DC-AC converter). The high voltage windings was connected to the traction motor via power electronic converters. This new configuration offers lower battery charge and discharge currents, and, as a result, lower resistive losses. Also, since lower voltage levels are desired for the batteries, this topology enables the system to work with low voltage battery packs while having high voltages for traction motor drive simultaneously. However, this design requires at least three power electronic converters (inverters) and one DC-DC converter that increases the complexity of the system and needs complicated control algorithm. Moreover, since both high voltage and low voltage windings coexist on the same stator, insulation and cooling will be difficult which can lead to reliability problems. Since all topology is in series, in case of any faults in any component, the whole system will stop working. The last but not least, the power electronic converters and the flywheel machine all need to be full sized (their power must always match the traction motor power) .

A high power high energy FWB system was developed by William's Formula 1 team. Their system was never used in Formula 1 race. However, It was used some other races such as Le Mans

24h race in 2012 and they won the race. The energy storage capacity was 140Wh and the rated power was 150 kW [20].

1.2.2 Flywheel Energy Storage in Conventional Vehicles

The first flywheel hybrid internal combustion powertrain appeared for vehicular applications in England In 1964. The transmission that utilized 104 kg flywheel was named as Gyreacta. The maximum speed of the flywheel was reported to be 15000 rpm. Gyreacta had some integrating and differentiating gears to connect the flywheel to the wheels. Several planetary gearsets were used in the unit as well. The planetary gear sets were engaged and disengaged via a clutch. For each speed shift there were some unavoidable flywheel kinetic energy loss. Although the system was efficient, the output shaft speed was discontinuous (stepped), and the topology was over complicated and costly [36].

In 1971, a flywheel usage for a parallel hybrid topology for a family car was reported. In that parallel hybrid topology either the internal combustion engine or the flywheel or both at the same time could propel the car. The energy storage capacity of the flywheel was 0.5 kWh. The proposed system was prototyped and tested, and the result was satisfactory for city driving conditions [37].

Another research in 1971 presented the super flywheel concept in mechanical hybrid powertrains. In that study, four different classes of cars were considered: commuter cars, family cars, city buses, and vans. It was found that the hydromechanical CVT was the most efficient and controllable transmission type. The internal combustion engine was controlled in on-off modes to recharge the flywheel. The IC engine was operated to recharge the flywheel when its speed was halved. Both the flywheel and internal combustion engine were connected to the driveline via clutches. In the proposed design, there was also an electric flywheel charging unit to charge the flywheel externally. According to authors, the hybridization with flywheel was beneficial for all mentioned car classes but the control was challenging due to lack of affordable digital controllers and the computer technology level at that time [38].

In 1975, a more practical work was done by the University of Wisconsin-Madison. They used a 2.3 liter Ford Pinto powertrain and a power split hydrostatic CVT. The topology was basically

a parallel hybrid powertrain. The main purpose of their control strategy was to run the engine in its maximum efficiency point (brake specific fuel consumption) and recovering the braking energy while the engine is idling. In EPA urban driving cycle, 58% range improvement was reported [39].

In 1976, a series hybrid topology with a small internal combustion engine and a big flywheel was presented. The rated power of the IC engine was about 7.5 kW, and the energy capacity of the flywheel was 10kWh. Two CVTs existed in the powertrain. One small CVT between the IC engine and the flywheel, and a big one between the flywheel and the differential. The engine was running at its most efficient point and it was aimed to charge the flywheel. The flywheel was able to drive the car by itself until its state of charge was more than a threshold value. Afterwards, the engine restarted to recharge the flywheel and drive the car together. Only in case of fully depleted flywheel, the engine would drive the car by itself [40].

In 1981, a hybrid bus was developed by MAN in Germany. The topology consisted of a 100 kW diesel internal combustion engine, a flywheel with .750 Wh energy capacity, and an infinite varibale transmission (IVT). The flywheel was connected to the IVT. The authors reported that up to 16% fuel saving was achieved as well as the engine downsizing. The system drawbacks were poor efficiency in low speed range and noisy operation of the drivetrain [41].

In 1986 another flywheel hybrid bus was presented using a Perbury transmission. This type of transmission offers a wider speed ratio range with slightly lower efficiency. The engine and the flywheel are connected together but before the connecting point, there is a sprag clutch on the engine shaft to ensure the unidirectional flow of power from the engine. The engine can recharge the flywheel as well [42].

In 1986, A flywheel internal combustion engine was developed and presented by General Motors in which a V-belt CVT was used. The configuration had a high speed flywheel which was able to accelerate the car up to 100 km/h. The flywheel was able to recover the braking energy at braking events too. Also, the configuration had a low speed mode in which the engine would drive the car by itself while charging the flywheel. The test results show that the system was too complex and losses were high, and the IC engine was not always at its best efficiency point. According to

analysis and test data, and a fuel economy benefit of 13% was predicted for the system on the EPA cycle. Since the fuel economy benefit was not enough to justify the associated costs, the research was stopped [43].

In 1987, a research study in which a flywheel hybrid internal combustion powertrain concept (similar to the GM concept) was done in the University of Eindhoven. The vehicle used a 47 kW 1.4 IC engine, a v-belt CVT, and a flywheel. An urban driving fuel economy benefit of 15-25% was predicted for the system. The vehicle was prototyped and tested (on a test rig) in their laboratory. They reported 30% fuel consumption reduction when the engine was doing stop-start with a flywheel. According to the authors, the fuel savings were mostly due to the more optimal operation of the IC engine, not due to the regenerative braking [44].

In 2001, researchers from the University of Eindhoven developed 'the zero inertia powertrain'concept for internal combustion engines [45]. In this concept, an additional flywheel connected to the powertrain tries to avoid the inertia effect of the IC engine during acceleration periods. The inertia effect of the engine has a tendency to drag the vehicle during aggressive accelerations. The flywheel plays an important role by compensating a great part of the engine inertia, and consequently, making it possible to minimize fuel economy in cruising without sacrificing drivability in transients (acceleration periods). Generally speaking, the CVT is used to allow the engine to run at its sweet spot This means that there would be almost no (or very little) reserve power to be used for acceleration. During aggressive accelerations, the engine has to develop much more power necessary for the acceleration, and the only way of doing it would be increasing its speed. Since the engine has a considerable amount of inertia, this speed ramp up will need energy. Therefore, the engine will take some kinetic energy from the car, and consequently decelerates the car a little, to increase its own speed. Needless to say, this unavoidable deceleration during the acceleration period is undesirable and sacrifices the drivability.

In 2008, a new flywheel assisted powertrain was presented by Imperial College researchers. In their proposed concept a flywheel was connected to a CVT and the CVT was connected between the output conventional gearbox and the final drive (differential). This system was used to recover

the kinetic energy of a car at braking events and supply it back during the next acceleration when the engine is off. Achieved fuel economy benefits were up to 22-33% more. Due to the shorter IC engine operation time rather than the IC engine operating at its sweet spot [46] continuously.

Formula 1 management allowed to use kinetic energy recovery system (KERS) in racing cars in 2009. Although most of the KERSs were essentially electrical systems, Flybrid-Torotrak employed a mechanical flywheel kinetic energy recovery system. According to the company figures, a flywheel assisted full size car could save up to 18% fuel on the new European driving cycle (NEDC). The reported fuel saving benefit for a 2600 kg SUV was around 35% on the FTP driving cycle [47].

Since 2011, Jaguar has been utilizing a flywheel powertrain that is made by Flybrid in its mechanical hybrid vehicle model Jaguar XF. The weight of the flywheel is 65 kg and its energy storage capacity is 120Wh at 60 krpm. The maximum deliverable power is 60kW. This hybrid model offers 20% fuel saving benefit. Moreover, Volvo has declared their interest in Flybrid's flywheel technology for their Volvo S60 model [8, 20]. Also, currently many European companies are developing and implementing flywheel energy recovery systems for their road vehicles.

In 2011, in a joint project, several companies and Technical University of Eindhoven collaborated together to develop a mechanical hybrid technology named EcoDrive that utilizes a flywheel and a push-belt CVT. The diameter of the flywheel unit was 0.15 m and the weight of this unit was 20 kg. The flywheel speed was 35000 rpm. Despite the high rotational speed of the unit, bearings of the systems was conventional and simple [48].

The EMAFER (Electro Mechanical Accumulator for Energy Reuse) system is another project that Technical University of Eindhoven and CCM company worked together. The aim of the system was utilizing an electromechanical flywheel to enable the regenerative braking in mobile applications [20].

1.3 Problem Definition

Existing hybrid and electric vehicles are not able to recover a great part of the kinetic energy of a vehicle during a braking event. For example, Nissan Leaf that has a full size electric

motor/generator and battery pack has a 25 % regenerative braking efficiency [49]. The overall efficiency is even worse for HEVs. There are two main reasons for this issue. The first one is that the braking power is usually much higher than the rated power of electric machine and power electronics in the vehicle. For instance, accelerating a medium size vehicle, which is around 1500 kg, from 0 speed to 60 mph takes 9s-12s and the acceleration power would be around 70 kW-120 kW. If we want to brake this vehicle and stop it completely, we should do that in less than 4s to remain in braking safety standards. Then, we have to apply a greater torque to stop the vehicle that increases the braking power 250 kW to 500 kW. This power can reach up to megawatts if we need severe deceleration. However, powertrain components like electrical machine, power electronic converter and battery is designed for the propulsion power. In this case, the vehicle control unit decides to use the friction brakes to meet the desired braking torque. Since the rated power of the electric powertrain in vehicles is restricted, the utilization of the friction brakes happens very often, and that means lower efficiency for kinetic energy recovery. As a result, majority of the kinetic energy of the vehicle is lost during the braking event. Fig. 1.2 illustrates a typical acceleration and braking event for a medium size EV.

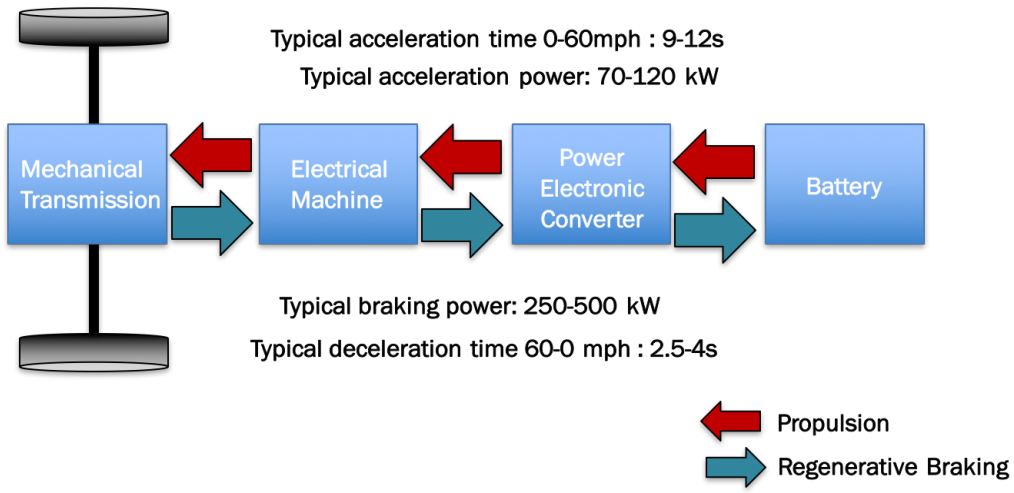

Figure 1.2: A braking and acceleration example for medium size EV

The second reason is that multiple energy conversions occur during the acceleration and braking. Fig. 1.3 shows the energy conversions in EVs. As we can see from the picture, kinetic energy of the vehicle is processed by the electro-mechanical power processing unit and stored in the electrochemical battery. Each process and each device in this process has an efficiency. Thus, the efficiency of regenerative braking is determined by an efficiency chain in the vehicle [50].

In other words, the mechanical power of the car is transformed to electrical power via a generator then it is processed by power electronics converter and it is chemically stored in a battery pack. For the next acceleration, the whole procedure is repeated in the reversed direction. Hence, during the whole circulation path (wheels to wheels) form of the energy has been transformed four times. The resultant overall efficiency is a multiplication of each energy transformation efficiency. It should be mentioned that every single one of the four energy transformations has a relatively high value but the multiplication makes the result dramatically low [50].

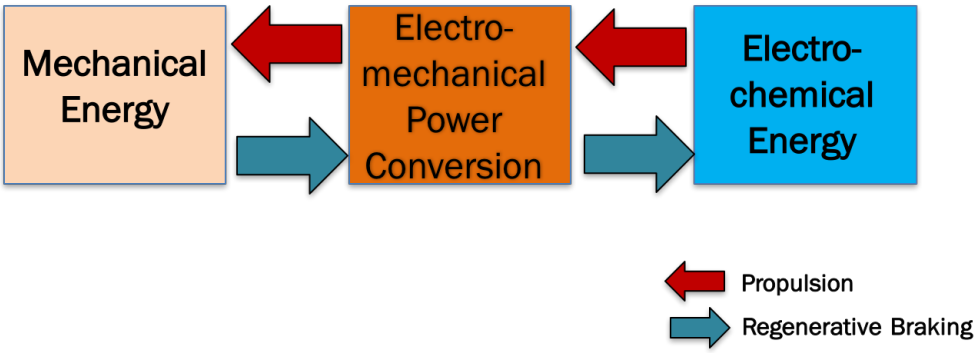

Figure 1.3: Regenerative braking in EVs

In vehicle applications, majority of the power demand, particularly in urban driving, is related to acceleration and deceleration of the vehicle. The average power demand of a medium size vehicle on the federal test procedure (FTP75) driving cycle is 2.2 kW while the maximum power demand is 33.5 kW [35]. The peaking power is almost 16 time greater than the average power that has to be supplied by the power source to satisfy the driving cycle. This fact shows that the load

characteristic is mostly inertial. If there was no inertial load in a vehicle, the power supply only would have to provide the average power which is necessary to overcome the mechanical frictions and electrical losses.

The average power (base power) can be supplied by an electrical machine and the peaking power (instantaneous power) can be delivered by a power buffer in EVs. A power buffer can be a flywheel or any other device such as ultra-capacitors and batteries. In this study we used a flywheel as the power buffer since it has a higher power density than other electrical energy storage devices. In the literature review, we presented both mechanical and electrical flywheel powertrains. Using a complete mechanical system or an electrical system brings many disadvantages. A better engineering product can be delivered by combining mechanical and electrical systems. In this way we can increase the regenerative braking power capability, avoid energy conversions, and deliver the power demand of a vehicle in all conditions. In the following sections, disadvantages of both systems are given.

1.3.1 Disadvantages of Mechanical Flyheel Topologies

Mechanical flywheel powertrains usually utilize mechanical components for energy transmission and a flywheel for energy storage. Due to its smooth shifting behavior, a continuously variable transmission (CVT) is preferred to charge and discharge the flywheel. While their energy storage capacity is low, they are still capable of capturing a great part of the vehicle kinetic energy during the braking period. Although mechanical flywheels have already been applied to racing cars and buses, their mass production of hybrid passenger cars still awaits [7]. This can be due to several reasons:

- The accurate and robust control of the mechanical continuous variable transmission and its clutches is hard to achieve due to dynamic operating conditions and lack of torque sensors, while in electrical hybrid systems torque sensors are not necessary.

- The design of powertrain controller is complex due to the existence of multiple driving modes and kinematic constraints that are imposed by mechanical connections.

- Since the commercial continuously variable transmission is a young technology. More research studies are necessary including cost, packaging, modularity, comfort, and lifetime.
- CVTs are limited in terms of turn ratio and power.
- Based on the literature, the suggested schemes have to utilize a high number of clutches that inversely affects the reliability and maintenance of the whole system. Also, suitable CVT for flywheel hybrid applications require expensive materials which can tolerate high stresses and frictions between the connections.

1.3.2 Disadvantages of Electrical Flywheel Topologies

The existing electric flywheel regenerative energy systems have to use two electric machines, usually one high-speed and one low-speed with similar power levels, and two power converters sharing one energy storage device: a battery in most cases. As a result they are rather expensive, bulky and inefficient. Another problem with the examples from the literature is reliability. Electrical machines and power processors in those systems are connected in series. In case of a machine failure or power processor unit failure, the whole system becomes dysfunctional.

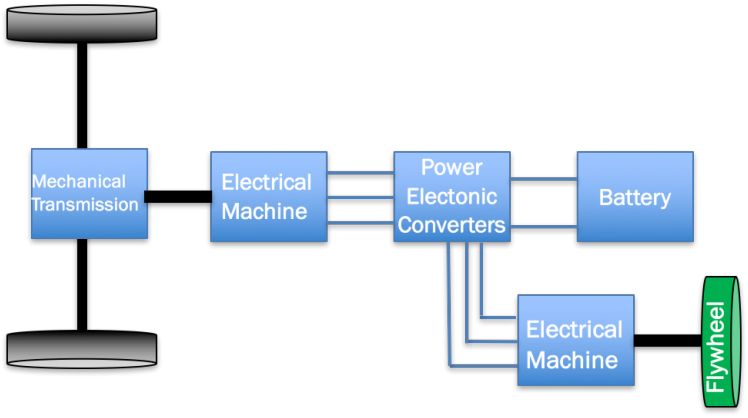

Figure 1.4: Flywheel assisted electric powertrain

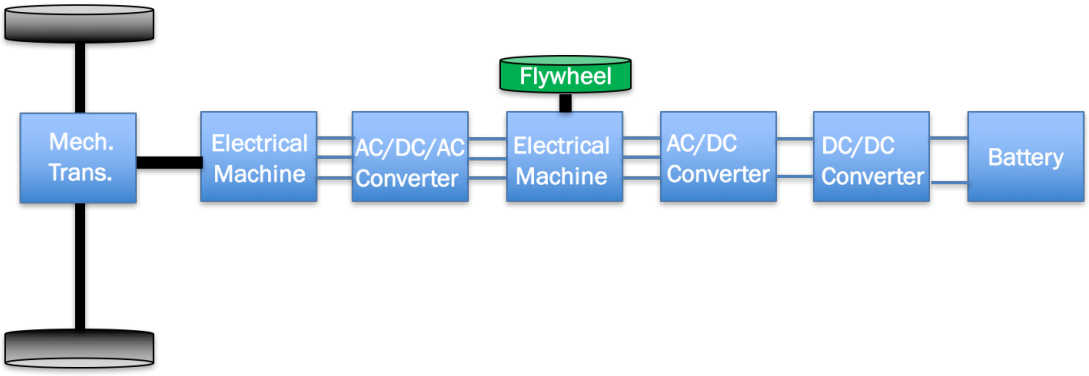

Figure 1.5: Flywheel electric powertrain example from literature

Fig. 1.4 and 1.5 are examples from the literature [8, 51]. In both examples at least 2 electrical machines are used. All electrical machines should be full power and related power electronics should be designed for full power as well. In the second example, a special electrical machine that has two different voltage level stator winding is used. Battery side of the topology works with lower voltage. However, this topology uses too many power electronics converters. Consequently, control complexity and cost of the topology is much higher than a conventional topology. The all-series-connected structure of the topology increases the reliability problem. These two examples summarizes all different applications of the electric flywheel powertrains because the basic idea and components are more or less the same.

1.3.3 Expected Criteria from Power Buffers

A good power buffer has to satisfy the following:

- Recover the majority of the kinetic energy during the braking period and boost the motor when necessary
- Substitute the inefficient part of the internal combustion engine efficiency map for hybrid electric vehicles
- Have a reasonable cost, weight and volume without excessive additional control complexity
- Since braking usually happens in short periods, high power absorbing density and high effi-

ciency (low overall impedance) is expected from the power buffers.

1.4 The Suggested Solution

The energy conversion is a costly process in EVs. As we mentioned before, During the regenerative braking, mechanical energy changes its form several times. As a result, the final recuperated energy in the vehicle is very low. In addition, electrical power limitation during the braking event also decreases the captured energy. A powertrain topology that is able to transfer and store the energy in mechanical form can increase the regenerative braking capability of an EV significantly. An addition of a mechanical power buffer in the powertrain can be suggested as an effective solution. Existing electric vehicle powertrain schemes are not able to transfer the energy in the mechanical form.

We introduce a dual mechanical port electrical machine that is named transmotor in the powertrain of an electric vehicle. Since the transmotor has two mehcanical ports, we can connect a flywheel to its second shaft to store the braking energy in the vehicle. Fig. 1.6 below shows the suggested scheme for an electric vehicle. Transmotor enables us to transfer the energy in the me-

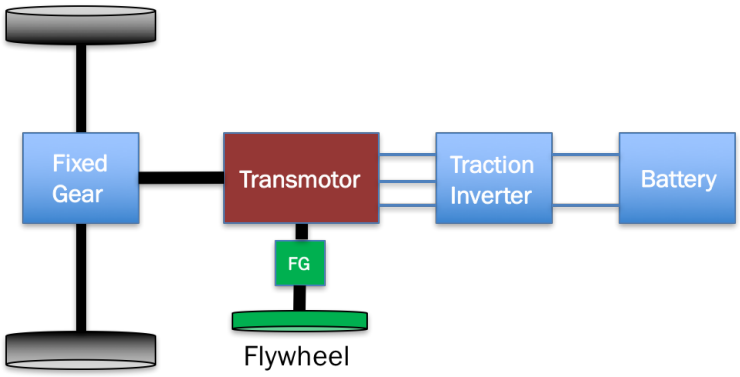

Figure 1.6: Flywheel transmotor powertrain topology

chanical and electrical form at the same time thanks to the magnetic coupling. Fig. 1.7 shows energy conversion paths in a flywheel transmotor (FWT) powertrain. As we can see from the

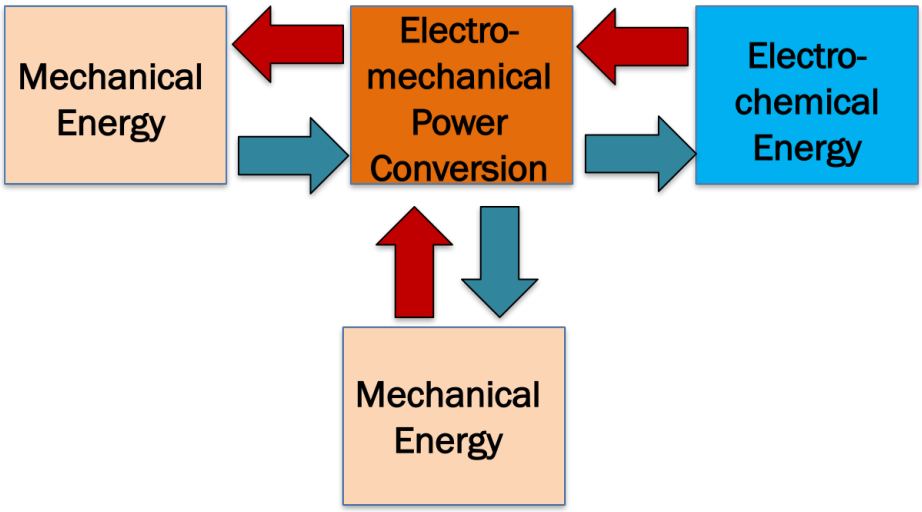

Figure 1.7: Flywheel transmotor powertrain energy conversions

picture, the integrated flywheel through the transmotor creates a second path for the energy transfer. Every time the vehicle accelerates or decelerates, the flywheel in the powertrain contributes a mechanical power. Hence, it increases the energy capturing capability during the braking and decreases the power required from the battery during the acceleration. This two-path energy transfer can increase the available regenerative braking power. As a result, with a better regenerative braking capability, the range of an EV can be improved.

The transmotor, principal of operation, how to drive a transmotor, flywheel specifications, application of the FWT powertrain in a commercial vehicle are given in following sections.

2. TRANSMOTOR

The term transmotor was first coined at Texas A&M in the 1990s. The transmotor is an electromagnetic device in which both the rotor and the stator can rotate freely [52]. A transmotor can be treated as a three-port device, one electrical port and two mechanical ports as is shown in 2.1. These devices obey the same electromagnetic energy conversion principles that apply for conventional electric machines. According to the Newton's third law of motion, the developed torque on both rotating rotor and stator has the same magnitude but opposite directions. As a result, the transmotor is able to transfer torque from rotor to stator and vice versa, magnetically through the air gap.

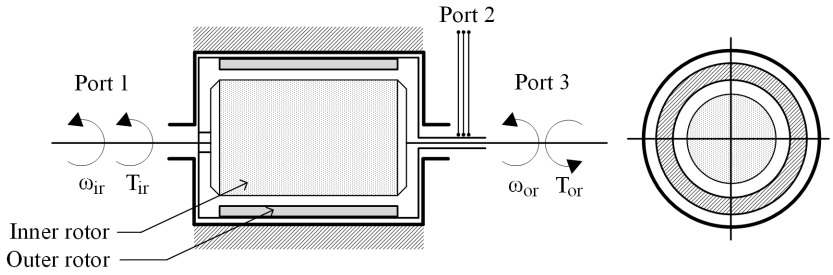

Figure 2.1: Transmotor (reprinted from [52])

The conventional electric machine principals apply for the transmotor as well. The most important difference is the reaction torque that is generated in the machine is free to rotate the stator. The equations (2.1)-(2.3) governs the basic principals of a transmotor.

$$\omega_{elec} = \omega_{ir} - \omega_{or} \tag{2.1}$$

$$T_{elec} = |T_{ir}| = |T_{or}| \tag{2.2}$$

$$P_{elec} = P_{ir} - P_{or} \tag{2.3}$$

The key point to drive a multi-phase AC transmotor is adjusting the electrical frequency. The electrical frequency applied by the power processor must be the relative speed of the outer rotor to the inner rotor that is multiplied by the pole pair number in order to create the proper magnetic coupling. In the case of a speed difference between the inner and outer rotor, the transmotor can run as a motor and a magnetic transmission or a generator and a magnetic transmission. The operation mode depends on the reference torque direction and the speed gradient. It should be mentioned that the torque transmission ratio is always unity regardless of the supply frequency. Alternatively, if the supply is a DC voltage source, acts as a synchronous coupler [52]. In this case, the relative speed of the rotor and the stator must be zero. In this case, the relative speed of the rotor and the stator must be zero. Detailed information about the operation modes are given in Section 2.1.

2.1 Operating Modes of a Transmotor

A transmotor can operate in all four quadrants below in Fig.2.2. The graph shows the relative speed of the inner rotor to the outer rotor, as well as, the induced torque defines the operation quadrant of the machine.

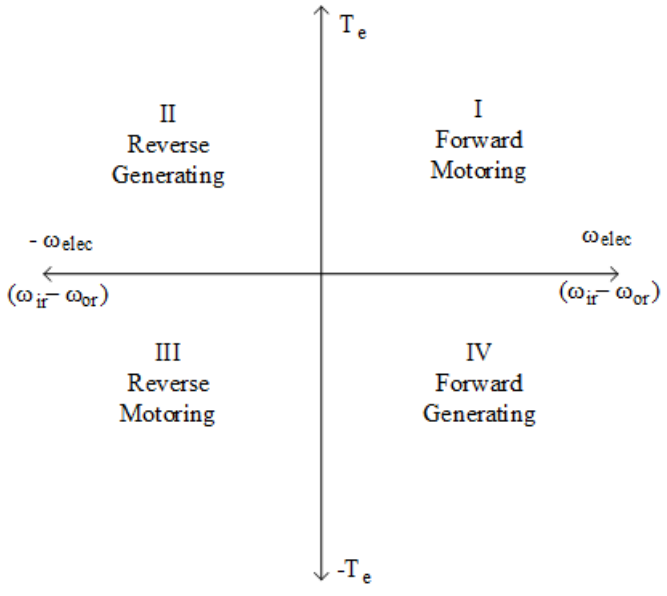

Figure 2.2: Four-quadrant operation mode of a transmotor

A transmotor mainly operate in 9 different modes in steady state and they can be listed as [17]:

- Mode 1 $\omega_{or} = 0$, $\omega_{ir} > 0$ or $\omega_{ir} < 0$
- Mode 2 $\omega_{ir} = 0$, $\omega_{or} > 0$ or $\omega_{or} < 0$
- Mode 3 $\omega_{ir} = \omega_{or}$
- Mode 4 $\omega_{or} > 0$, $\omega_{ir} > 0$ and $\omega_{ir} > \omega_{or}$
- Mode 5 $\omega_{or} > 0$, $\omega_{ir} > 0$ and $\omega_{or} > \omega_{ir}$
- Mode 6 $\omega_{or} < 0$, $\omega_{ir} > 0$
- Mode 7 $\omega_{or} > 0$, $\omega_{ir} < 0$
- Mode 8 $\omega_{or} < 0$, $\omega_{ir} < 0$, and $|\omega_{ir}| > |\omega_{or}|$
- Mode 9 $\omega_{or} < 0$, $\omega_{ir} < 0$, and $|\omega_{ir}| < |\omega_{or}|$

Depending on the application, a transmotor can be operated in certain modes as a motor or a generator. Detailed explanation for each mode can be found in [17]. A specific example is given in Section 2.5.

2.2 Mathematical Model of an AC Permanent Magnet Transmotor

A transmotor can be any type of electrical machine such as an induction motor, permanent magnet motor, dc motor etc. In this study, we used an AC permanent magnet motor. A well-known method of modeling of AC electric machines is using direct-quadrature(dq) axes modeling. DQ modeling in AC machines transforms three phase variables into two-phase variables. Eliminating one of the variables is significant because AC variables in the machine can be treated as DC variables eventually. Once we have DC parameters in the machine, we can apply control techniques easily. In other words, DC current or torque control methods with controllers would apply to AC machines as well.

In DQ modeling, we use a reference frame that is either stationary or rotating. There are different applications of the reference frame theory in the literature. The important point is that being consistent in transformations. Being consistent means that if we start to use a reference frame model, say it uses stationary reference frame, then we have to stick to related forward and reverse mathematical equations every step of the modeling.

Stationary reference frame, also known as stator reference frame, measurements are made at the stator of the AC machine and converts them into two-phase varibles. This transformation is known as Clark's transformation in the literature. When we apply Clark's transformation, resultant variable would be still AC parameters. Howvever, if we are to use PI regulators in the control system, we should convert the variables into DC form by using another transformation method. Park's transformation transforms the stationary reference frame parameters into a rotating frame parameters. Basically, we rotate the the reference frame with the rotor. Once we start rotating the reference frame with the rotor, the steady-state variables in the stator would appear as DC values. The following equations 2.4 and 2.5 combines Clark's and Park's transformation and presents the forward and reverse transformation matrices.

$$\begin{bmatrix} f_d \\ f_q \\ f_0 \end{bmatrix} = \sqrt{\frac{2}{3}} \begin{bmatrix} \cos\theta & \cos\left(\theta - \frac{2\pi}{3}\right) & \cos\left(\theta + \frac{2\pi}{3}\right) \\ -\sin\theta & -\sin\left(\theta - \frac{2\pi}{3}\right) & -\sin\left(\theta + \frac{2\pi}{3}\right) \\ \frac{\sqrt{2}}{2} & \frac{\sqrt{2}}{2} & \frac{\sqrt{2}}{2} \end{bmatrix} \begin{bmatrix} f_a \\ f_b \\ f_c \end{bmatrix} \tag{2.4}$$

$$\begin{bmatrix} f_a \\ f_b \\ f_c \end{bmatrix} = \sqrt{\frac{2}{3}} \begin{bmatrix} \cos\theta & -\sin\theta & \frac{\sqrt{2}}{2} \\ \cos\left(\theta - \frac{2\pi}{3}\right) & -\sin\left(\theta - \frac{2\pi}{3}\right) & \frac{\sqrt{2}}{2} \\ \cos\left(\theta + \frac{2\pi}{3}\right) & -\sin\left(\theta + \frac{2\pi}{3}\right) & \frac{\sqrt{2}}{2} \end{bmatrix} \begin{bmatrix} f_d \\ f_q \\ f_0 \end{bmatrix} \tag{2.5}$$

where θ represents the electrical location of the reference frame.

Now, we can describe general differential equations for AC machines. Likewise, we write expression for three phase voltage equations considering the voltage drop on the winding resis-

tance, the flux linkage change and back emf voltage. The following set of equations establishes the mathematical model of an AC motor [53].

$$v_{q_s} = R_s i_{q_s} + \frac{d\psi_{q_s}}{dt} + \omega\psi_{d_s} \tag{2.6}$$

$$v_{d_s} = R_s i_{d_s} + \frac{d\psi_{d_s}}{dt} - \omega\psi_{q_s} \tag{2.7}$$

$$\psi_{q_s} = L_{q_s} i_{q_s} \tag{2.8}$$

$$\psi_{d_s} = \psi_m + L_{d_s} i_{d_s} \tag{2.9}$$

$$T_e = \frac{3}{2} p[i_{q_s}\psi_m + (L_{d_s} - L_{q_s}) i_{d_s} i_{q_s}] \tag{2.10}$$

After writing these equations for an AC machine, we can apply them to a permanent magnet AC transmotor. As we know from the previous sections, transmotor has two rotating mechanical parts. While we are applying the reference frame theory we should match the electrical speed of the flux in the machine to align PM flux with d axis. The following figure shows the application of the reference frame theory in a transmotor.

In figure 2.3 a,b,c axes represents the inner rotor that rotates with the mechanical speed of ω_{ir} and we have three-phase windings in the inner rotor.Permanent magnets that are represented by N and S are fixed in the outer rotor and it rotates at the mechanical speed of ω_{or}. Lastly, we have the dq plane that rotates at the electrical relative speed, ω_e. Electrical relative speed is defined by the mechanical speed difference between the rotors multiplied by pole pair number.

In a transmotor the outer rotor and inner rotor can have different mechanical speed values. Since we want to obtain DC values for variables in the machine, we need to set the speed of the reference frame at the electrical relative speed ω_e. If we are supplying the transmotor at the inner rotor terminals, than we should set the reference frame speed at the electrical relative speed of the inner rotor, ω_{ir}, with respect to the outer rotor speed, $\omega_o r$. Similarly, if we supply the transmotor at the outer rotor terminals, then we should rotate the reference frame at the relative speed of the outer rotor with respect to the inner rotor. In our study, we assumed that we supply the transmotor

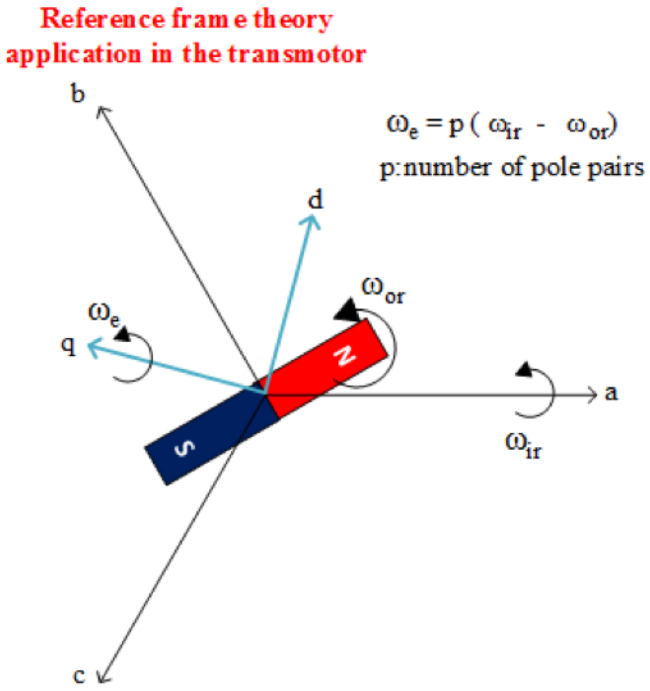

Figure 2.3: Application of the reference frame theory in the transmotor

at the inner rotor terminals.

In the light of these explanations, we can rearrange the general differential equations of an AC motor and establish a complete model for a permanent magnet AC transmotor. Expressions 2.11-2.15 governs the electrical equations.

$$v_{q_{or}} = R_{or} i_{q_{or}} + \frac{d\psi_{q_{or}}}{dt} + p(\omega_{ir} - \omega_{or})\psi_{d_{or}} \tag{2.11}$$

$$v_{d_{or}} = R_{or} i_{d_{or}} + \frac{d\psi_{d_{or}}}{dt} - p(\omega_{ir} - \omega_{or})\psi_{q_{or}} \tag{2.12}$$

$$\psi_{q_{or}} = L_{q_{or}} i_{q_{or}} \tag{2.13}$$

$$\psi_{d_{or}} = \psi_m + L_{d_{or}} i_{d_{or}} \tag{2.14}$$

$$T_{e_{or}} = -T_{e_{ir}} = \frac{3}{2} p(i_{q_{or}} \psi_m + (L_{d_{or}} - L_{q_{or}}) i_{d_{or}} i_{q_{or}} \tag{2.15}$$

$$T_{e_{or}} = T_{e_{or}} + J_{or} \frac{d\omega_{or}}{dt} + B_{or}\omega_{or} \tag{2.16}$$

$$T_{e_{ir}} = T_{e_{ir}} + J_{ir}\frac{d\omega_{ir}}{dt} + B_{ir}\omega_{ir} \tag{2.17}$$

Equations 2.16 and 2.17 are mechcanical expressions for the transmotor. Compared to conventional machine models one more mechanical equation for the second rotating part of the machine is introduced. The electromagnetic torque that is developed in the machine applies to both rotors equal in magnitude and opposite in direction.

As it can be seen from the equations, the mathematical model of an AC permanent magnet transmotor is very similar to a permanent magnet synchronous motor. However, there is an additional mechanical block and relative speed term is used in the transmotor mathematical model.

2.3 Torque Control in AC Permanent Magnet Transmotor

Torque control in AC machines is more complex than DC machines since voltage and current values are time variant. In DC machines, controlling the armature current means directly controlling the torque in the machine and controlling the excitation current leads to control the field in the machine. On the other side, in AC machines we only have access to the supply current that is mostly the stator current. For example, in induction machines the stator current both magnetizes the rotor and generates torque. It is obvious that magnetizing current and torque generating current is combined in a single current in induction machines. If torque control or field weakening is required in these machines, related component is needed to be decomposed from the supply current [54].

We explained the dq modeling of AC machines in the previous section. It was stated that as a result of reference frame transformations, we obtain two-phase values that are direct axis value and quadrature axis value. Quadrature axis current I_q and direct axis current I_d appear in equations 2.11-2.14. Since we align the direct axis with the magnetic field in the machine, I_d current represents the magnetizing current. We also know that the current perpendicular to the field in the machine generates torque. Then, I_q current represents the torque generating component in AC machines.

If we are to control the torque in an AC machine, we can produce reference torque command

for I_q. Likewise, we can control the flux in the machine by commanding I_d value in the machine. Since I_q and I_d values are DC, we can use PI regulators in the system conveniently. Figure 2.4 presents torque control in AC machines.

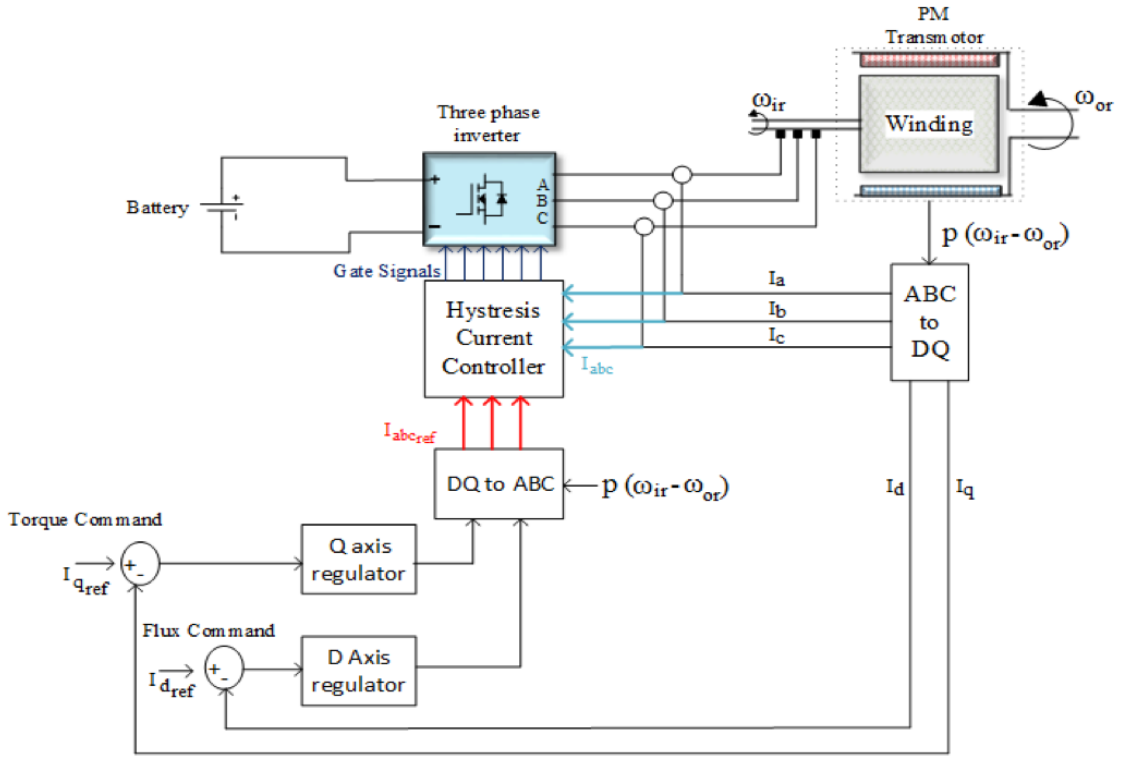

Figure 2.4: Torque control in AC machines

Torque control in an AC permanent magnet transmotor is quite similar to conventional AC machines. The difference comes from the second rotor in the machine. An extra speed sensor is needed to determine the the location of the flux. As long as we have the relative speed difference information, we can perform the transformations and apply any kind of control technique to a transmotor.

A permanent magnet (PM) machine can be surface PM (SPM) or interior PM (IPM) in construction that also applies to a transmotor. Magnets in SPM machines are placed on the surface of the rotor whereas they are buried in the magnetic material of the rotor in IPM machines. This

physical difference affects the dynamics of the machine.

In SPM configuration, the surface of the rotor is covered by the magnets. The permeability of a magnet is almost equal to as of air. As a result, a magnet behaves like air and creates a relatively big airgap that forms the big portion of reluctance in the magnetic circuit of SPM machines. Compared to conventional electrical machines, inductance of SPM machine is lower because of the high reluctance. This low inductance results in high current ripple. As a result, controlling the current becomes more problematic. Higher switching frequencies are required in power electronics circuits to deal with the current ripple. Besides, if the controller is not triggered by the power electronic circuit's current limit, drive system can result in failure. Another aspect of having high current ripple is torque ripple in the machine. Torque ripple cause vibration and noise in the machine and it would lead to reliability problems.

Since the d-axis path and q-axis path are identical in the SPM structure, related inductance values are equal as well. Equal and low L_d and L_q inductance values in SPM machines make the field weakening operation very limited. In the equation 2.18, first term is called magnet torque and second term is called reluctance torque. The reluctance torque is ignored in SPM machines due to symmetry of flux paths.

$$T_e = \underbrace{\frac{3}{2}pi_{q_s}\psi_m}_{\text{Magnet Torque}} + \underbrace{\frac{3}{2}(L_{d_s} - L_{q_s})i_{d_s}i_{q_s}}_{\text{Reluctance Torque=0}} \tag{2.18}$$

The torque is developed by only the PM flux linkage in SPM machines. Because of this reason, magnetizing current reference $I_{d_{ref}}$, in these machines is set to 0 and torque equation becomes a function of I_q.

$$T_e = \frac{3}{2}pi_{q_s}\psi_m \tag{2.19}$$

In the case of an IPM machine, d-axis flux path is different than the q-axis flux path. This difference would make the reluctance different and L_d and L_q would become different as well.

Since inductance values are not equal, saliency is introduced in IPM machines. The following equation defines the saliency ratio in a IPM machine [55, 56].

$$\xi = \frac{L_q}{L_d} \tag{2.20}$$

Field weakening operation can be realized applying negative values of magnetizing current that cancels the permanent magnet flux in the machine. If the saliency ratio is high in a PMSM machine, the range of the field weakening operation can be extended [55, 57].

In our study, we preferred to use an IPM structure for the transmotor to take the advantage of wider field weakening operation and reluctance torque development in the machine.

2.3.1 Maximum Torque per Ampere Operation

Current control schemes in electric machines have different goals. Most common methods can be listed as torque angle control, maximum torque per ampere (MTPA) control, unity power factor control, constant stator flux control. Among these control schems, MTPA control is the most proper one for vehicle traction applications. It is because that MTPA control ensures minimum supply current is applied for the demanded torque. As a result, copper losses in the machine is minimized and maximum efficiency is obtained. MTPA control can be used for IPM transmotors as well [58].

Restrictions for MTPA control comes from the inverter in the electric drive system. The maximum current in the transmotor can not exceed the maximum inverter current.

$$i_q{}^2 + i_d{}^2 \leq I_{max}{}^2 \tag{2.21}$$

The equation above defines a circle that has radius of I_max and I_d and I_q current values should remain in this circle.

On the other hand, DC bus voltage defines another constraint for the driver and it is given in following equation.

$$v_q{}^2 + v_d{}^2 \leq V_{max}{}^2 \tag{2.22}$$

For the steady state operation we can rearrange equations 2.11 and 2.12:

$$v_{q_{or}} = R_{or} i_{q_{or}} + p(\omega_{ir} - \omega_{or})\psi_{d_{or}} \tag{2.23}$$

$$v_{d_{or}} = R_{or} i_{d_{or}} - p(\omega_{ir} - \omega_{or})\psi_{q_{or}} \tag{2.24}$$

If we ignore the voltage drop on the windings and combine equations 2.21,2.23, and 2.24, we get:

$$(L_d i_{d_{ir}} + \psi_m)^2 + (L_q i_{q_{ir}})^2 = \left(\frac{V_{max}}{p(\omega_{ir} - \omega_{or})}\right)^2 \tag{2.25}$$

As is seen in 2.25 the maximum voltage is inverse function of the speed and defines an ellipse whose center is $\frac{-\psi_m}{L_d}$. The operation of the transmotor is constrained by the maximum current circle and maximum voltage ellipse. Intersection of these two function defines the operation region of a transmotor under MTPA schme and MTPA curve can be expressed by the following equation [55, 59]

$$\begin{aligned} i_{d_{ir}} &= \frac{-\psi_m + \sqrt{\psi_m{}^2 + 8(L_q - L_d)^2 I_{max}^2}}{4(L_q - L_d)} \\ i_{q_{ir}} &= \sqrt{I_{max}^2 - i_{d_{ir}}^2} \end{aligned} \tag{2.26}$$

Equations above ignore magnetic saturation in the machine. Saturation in the magnetic material in the machine would affect inductance values and as a result, changes the MTPA curve. MTPA curve depends on machine parameters. If we know machine parameter, we can create look up tables to determine reference current commands. Any kind of nonideality can be included in these look-up tables.

2.4 Mechanical Energy Transfer Through a Transmotor

The kinetic energy transfer from one shaft to another is possible by proper control of the transmotor. If the inner rotor has an initial speed, while the outer rotor is at standstill, a developed torque that decrease the speed of the inner rotor will cause an equal reaction torque in the opposite direction on the outer rotor due to the magnetic coupling. The electromagnetic torque that is developed in the machine controls the energy transfer rate.

The speed difference between the shafts induce a voltage due to permanent magnets across the windings at the beginning of the process. The transmotor operates as a generator and sends energy to the energy storage source through a power processor unit until both shafts have the same speed. If we still need to transfer the energy from the inner rotor to the outer rotor, the same torque, and the corresponding voltage should be applied to the transmotor which defines the motoring mode. The captured energy in the energy storage source is released during the motoring mode. In an ideal case, no net energy is needed from the energy storage source.

As a result, different from the conventional electric machines, a transmotor can transfer the kinetic energy in two separate ways. If we rearrange (3), we can observe this fact better.

$$P_{ir} = P_{elec} + P_{or} \tag{2.27}$$

During the kinetic energy transfer, the transmotor splits the initial mechanical power into two and processes the power in electrical and mechanical forms which is a novel method to transfer the mechanical energy.

Fig. 2.5 demonstrates an example topology for the mechanical energy transfer. In the proposed system, two flywheels are connected to shafts of the transmotor. If any of the flywheels are charged the mechanical energy can be transferred through the transmotor in the system. The performance of the system and a comprehensive explanation are given in Section 2.5.

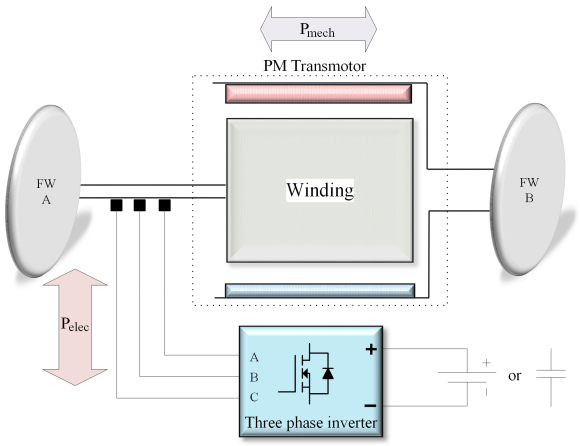

Figure 2.5: Proposed system overview

2.4.1 Regenerative Braking

The most remarkable quality of the energy transfer in the transmotor topology is that some of the mechanical energy keeps its form and is transferred mechanically. The rest is captured by the power processor unit and stored in the battery. This two path energy transfer can be used to increase the efficiency of a regenerative braking system in an EV or HEV. Fig. 2.6 illustrates the difference between the conventional regenerative braking system of an electric vehicle and the proposed system's regenerative braking system [50].

The two-way energy efficiency of a conventional regenerative braking system is only 36%, and the reason for this low number is multiple energy transformations during the process [50]. In this example, mechanical losses of the drivetrain are ignored, and in a practical application the efficiency decreases dramatically. For instance, the braking energy recovery of a Nissan Leaf electric vehicle is around 25% [49].

On the other side, the transmotor topology can process the kinetic energy in mechanical form. The efficiency of the mechanical energy transfer is higher than the other energy transfer processes. The efficiency of the mechanical energy transfer for this process is above 90% since most of the losses are in the windage of the transmotor. If we assume that 50% of the initial kinetic energy is

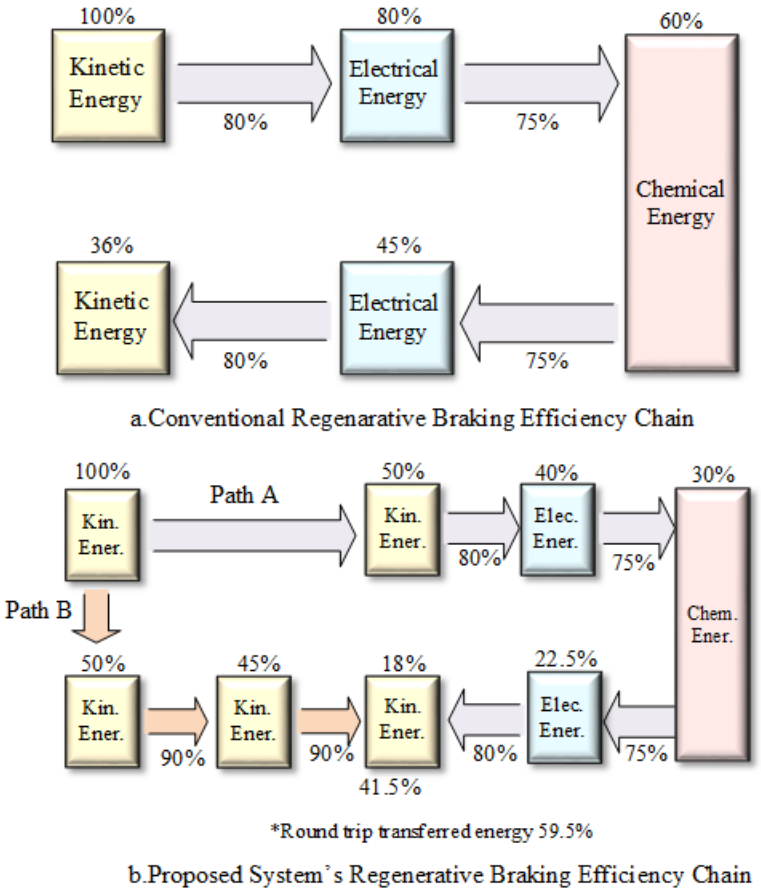

Figure 2.6: Comparison of two regenerative braking systems

processed in the electrical form that follows Path A, and the rest is transferred in the mechanical form that follows path B in Fig. 2.6, the resulting round-trip energy recuperation efficiency is increased to around 60% of the initial energy.

2.5 Performance Tests

A simulation model was built to observe the kinetic energy transfer through a transmotor. The simulation model consists of two flywheels, an electrical machine, a bi-directional power electronic converter and a storage device that can be a battery or an ultra-capacitor. In this study, we preferred to use a battery. For the simplicity, it is assumed that both flywheels are identical and have the same moment of inertia. Overview of the system can be seen in Fig. 2.5.

In these performance tests, the transmotor operates in modes 2-5, in forward motoring and

forward generating quadrants. Table 2.1 ddescribes the different operation modes for this specific application, and Table 2.2 gives the transmotor and system parameters [60].

Table 2.1: Transmotor operation modes in mechanical energy transfer

Condition of FW B	$\omega_A > \omega_B$	$\omega_B > \omega_A$	ω_A=ω_B
Acceleration of FW B	Generating mode ($P_{elec} < 0$)	Motoring mode ($P_{elec} > 0$)	$P_{elec} = 0$
Deceleration of FW B	Motoring mode ($P_{elec} > 0$)	Generating mode ($P_{elec} < 0$)	$P_{elec} = 0$

2.5.1 Ideal Case Results

The ideal case tests ignores any kind of mechanical and electrical losses in the system. Flywheel A spins at 120 rad/s and flywheel B has no speed at the beginning. Constant torque is applied to the transmotor and results are given in Fig. 2.7-2.10.

Referring the Table 2.1, the transmotor is operating as a generator and the phase sequence as ABC, which can be seen in Fig. 2.7, at start-up. The electrical frequency is high due to the speed difference.

The speeds of the flywheels become equal after 0.62 s and the transmotor electrical power, P_{elec}, hits the 0 value. Furthermore, phase currents of the transmotor at that moment become DC. Since the deceleration of flywheel A speed continues, transmotor switches to motoring mode right after 0.62 s and phase sequence becomes CBA as shown in Fig .2.7. The transition from generating mode to motoring mode can be observed from the Fig. 2.9 as well.

The energy exchange of the flywheels and the battery can be seen in Fig. 2.10. During this process, the battery receives some energy from flywheel A and then transfers the stored energy back to the flywheel B. In other words, battery buffers the energy received from flywheel A due to flywheel B's inability to receive energy and later releases that extra energy when flywheel B needs

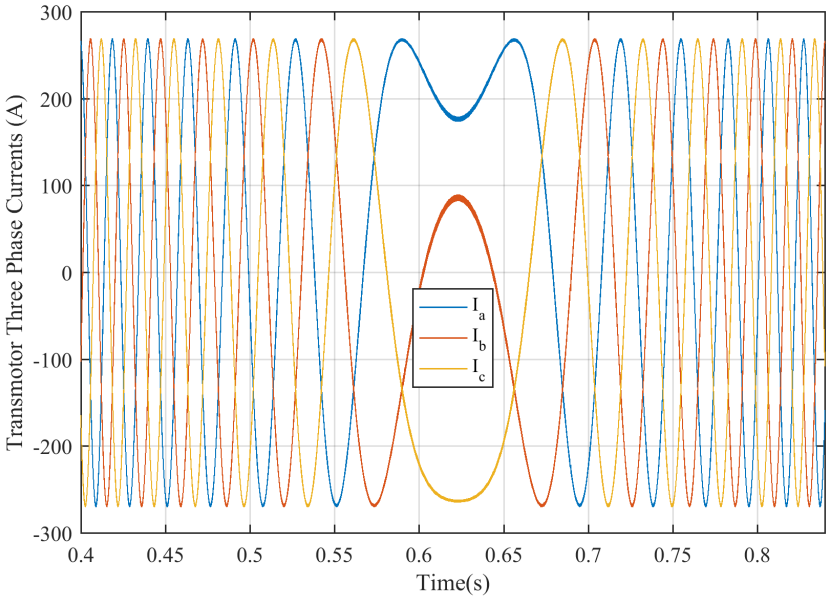

Figure 2.7: Ideal case-transmotor three phase currents

more energy for acceleration. During the energy exchange process, no net energy is needed as seen from the E_{elec} in Fig. 2.10.

2.5.2 Practical Case (Non-ideal Case) Results

Practical case simulation considers the winding resistance and viscous friction losses. Initial speed conditions are the same as the previous case. Due to the viscous friction, the speed changes are slightly slower than the ideal case and the final speed of the flywheel B is 118.5 rad/s. Consequently, the three phase currents pattern is a little different from the ideal case as can be seen in Fig. 2.11 and 2.12. Since the torque profile is the same as the ideal case, the slight slower speed change will affect the power profile but this effect is negligible. According to Fig. 2.14, the electrical energy profile is noticeably different. In this case, the electrical energy hits zero before the end of the process and takes negative values indicating that some pre-stored energy is necessary by the drive system to complete the process. As is seen in Fig. 2.14 the net required energy amount is 1471J due to losses.

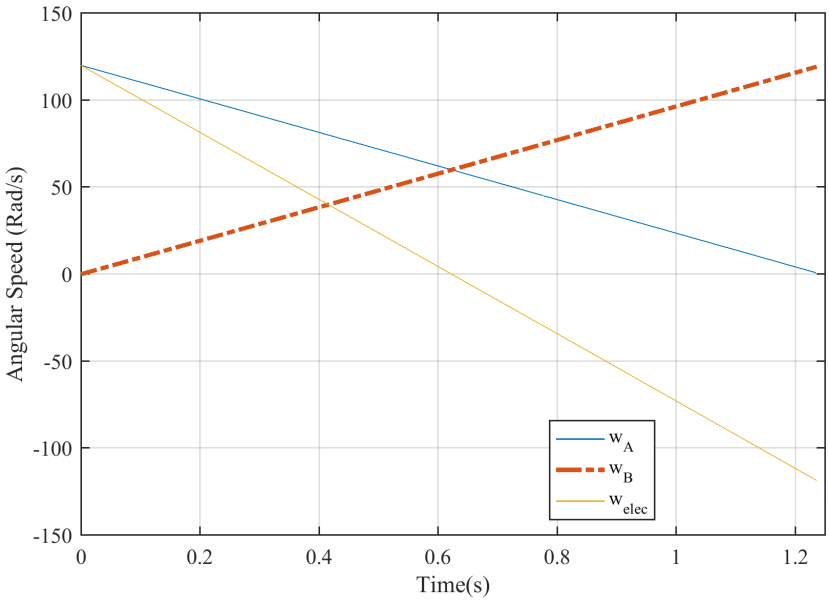

Figure 2.8: Ideal case-speed graph

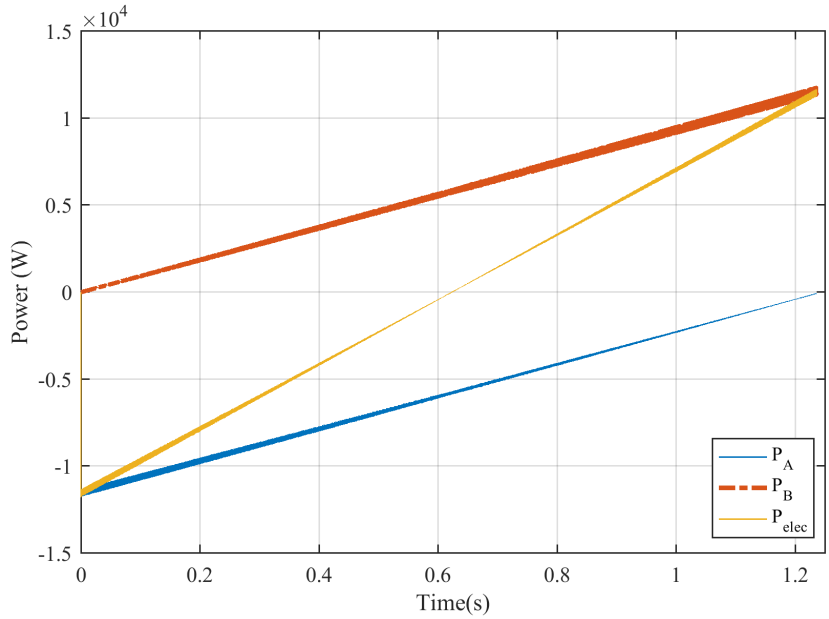

Figure 2.9: Ideal case-power graph

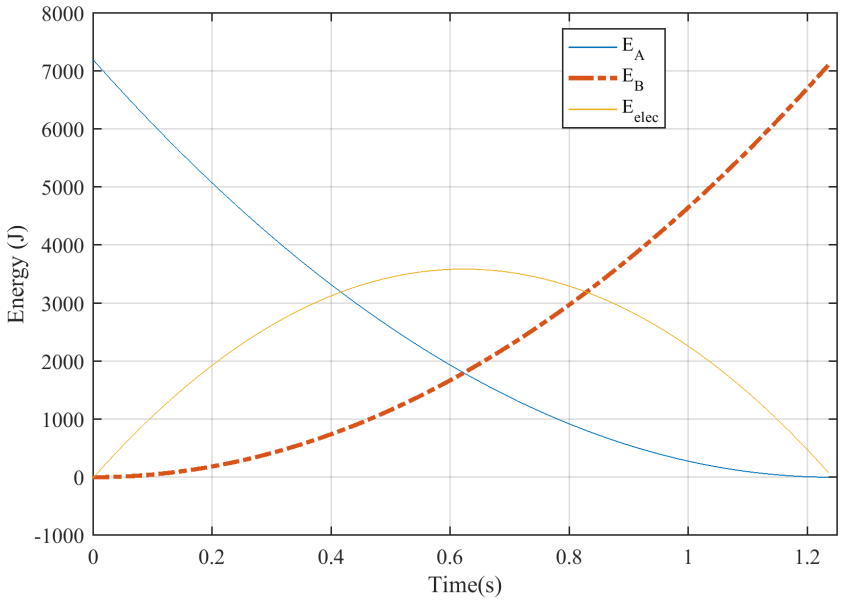

Figure 2.10: Ideal case-energy exchange curves

Table 2.2: Transmotor-based energy exchange system specifications

Winding Resistance	0.011 ohm
L_d	0.12 mH
L_q	0.23 mH
Magnet flux	0.034 Wb
Pole Pair Number	8
Base Speed	1200 rpm
Rated Power	12 kW
Phase Current	190 A
DC Bus Voltage	200 V
Viscous friction coeffient (B)	0.01 Nms/rad
Flywheel A&B moment of inertia	1 kgm^2

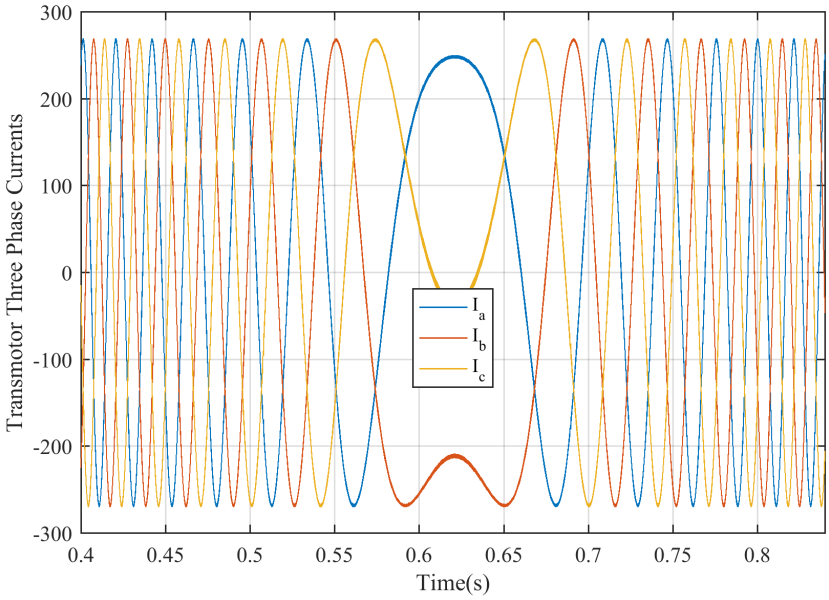

Figure 2.11: Practical case-transmotor three phase currents

2.5.3 Effect of the Initial Flywheel Speed

In the previous tests initial speed of FW A was 120 rad/s whereas FW B was at rest initially. For the following simulations, initial speed of FW B is increased from 0 speed to 100 rad/s step by step, and FW A initial speed is kept at 120 rad/s for each step. When FW B's speed reaches FW A's initial speed value, simulations are terminated. The same losses are considered with the practical case from the previous section. The detailed results are given in 2.3.

According to the simulation results, the initial speed values of the flywheels change the ratio of the mechanical to mechanical energy transfer. If FW B is at standstill at the beginning of the energy exchange process, around 49% percent of the total energy is transferred in mechanical form whereas this percentage reaches 94.3 for the initial speed of 100 rad/s. A better interpretation can be made if we normalize FW B's initial speed to FW A's initial speed. Fig. 7 presents the mechanical to mechanical energy transfer ratio with respect to normalized initial speed values of FW B.

Fig.2.15 shows that the mechanical to mechanical energy transfer ratio saturates around half

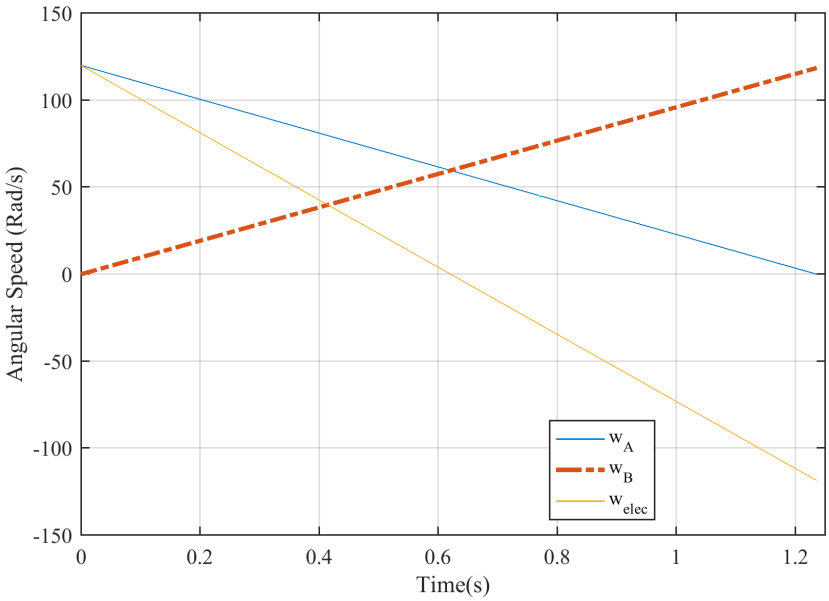

Figure 2.12: Practical case-speed graph

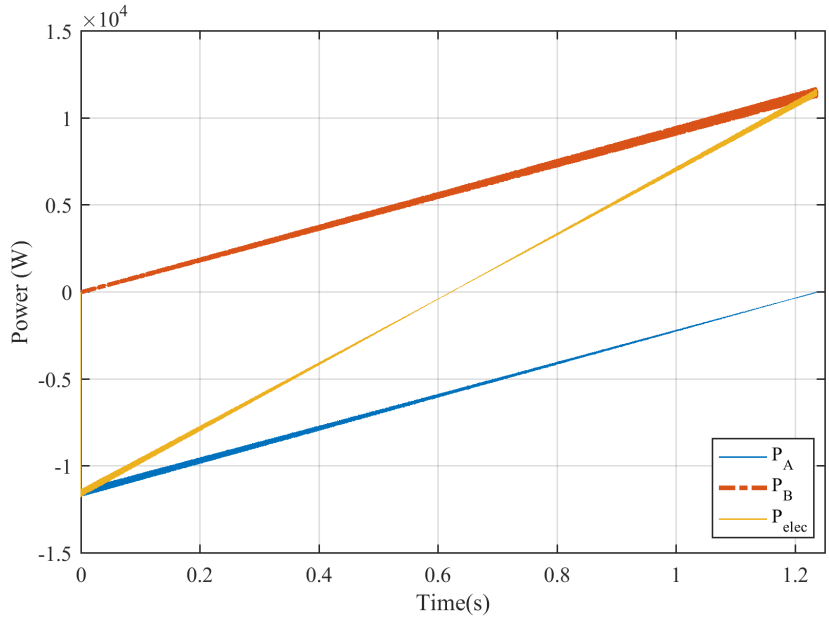

Figure 2.13: Practical case-power graph

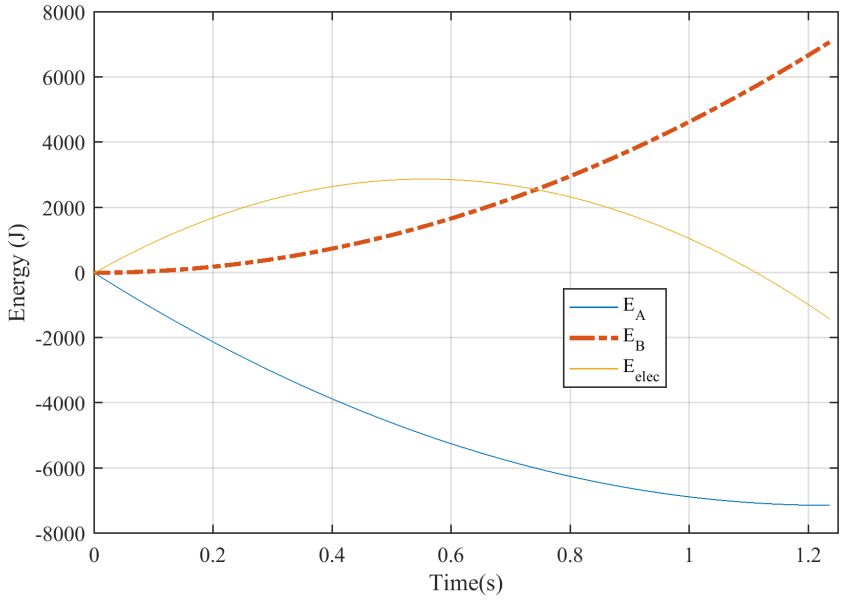

Figure 2.14: Practical case-energy exchange curves

Table 2.3: Simulation results of different FW B initial speeds

FW B ω rad/s	R_s Loss (J)	Max. E_{elec}	FW B ΔE_{mech}	Max. P_{elec}	Max. P_{FW}
0	1465	2875	7100	11500	11500
20	1237	1900	7000	9750	11500
40	990	1140	6455	7750	11500
60	732.4	725	5340	5760	11500
80	488	490	3970	3850	11500
100	247.5	263	2216	1920	11500

the speed of FW A's initial speed, and the ratio is 82.7%. Increasing the initial speed of FW B after the halfway point, does not increase the mechanical to mechanical energy transfer ratio significantly. As a result, we can say that to get the maximum efficiency from the system FW B should not be depleted completely, and should be operated at a certain speed value that is half of FW A's speed. The mechanical to mechanical energy transfer ratio can be in the range of 49% to 82.7% for practical application.

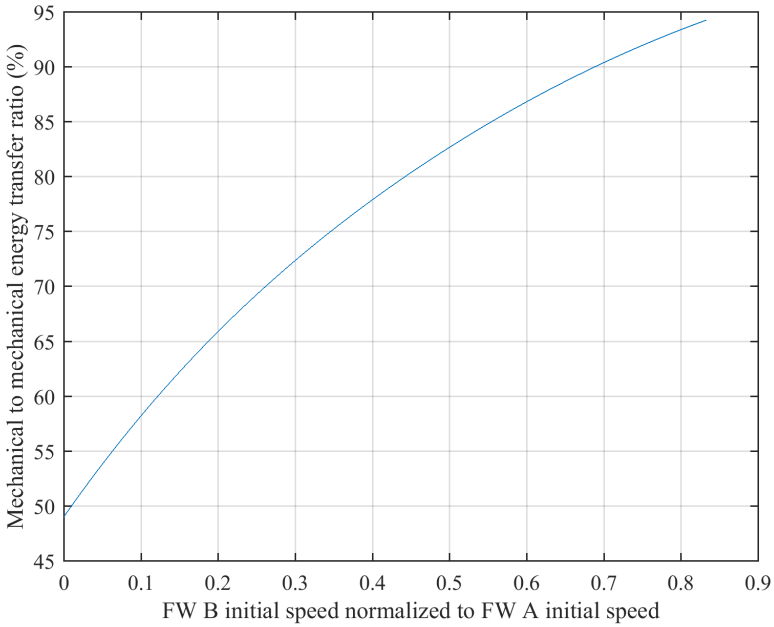

Figure 2.15: Mechanical to mechanical energy transfer ratio

It should be noted that the inner rotor mechanical power (P_{ir}) is much higher than the outer rotor mechanical power (P_{or}) at the beginning of this process ($P_{ir} >> P_{or}$). As the speed difference decreases, the electrical power (P_{elec}) becomes smaller. We can say that adjusting the speed difference between the two shafts of the transmotor, we can minimize the required electrical power in the system. Thereby, decreasing the required power from the power processor unit and the battery.

3. ELECTRIC VEHICLES

Road vehicle technology has evolved into a new form in the last two decades that is electric vehicles. Many studies in the literature project that carbon fuel sources are going to be extinct in next 50 years. As a result, fuel prices will rise dramatically and conventional gasoline or diesel fueled cars will be obsolete due to high fuel prices. In addition, conventional cars emit high amount of carbon dioxide gases and pollutes the air. According to the Environmental Protection Agency (EPA), the annual carbon dioxide production of a conventional car is around 4.7 metric tons. If we consider the number of the vehicles all around the world, we can understand the significance of this carbon dioxide generation, and its danger to the environment. Governmental facilities like Environmental Protection Agency, California Air Resources Board who pioneered the recognition of the global warming in the United States set a zero emission vehicle target for car makers. Auto companies are now in a very aggressive competition to satisfy the new goal and lead the electric vehicle market. As a result, new and more developed EV models are released by the companies every year.

A full electric vehicle uses an electrical machine for traction power and batteries for the energy storage in the vehicle. As we know electric vehicle term is very broad and can be used for hybrid electric vehicles, fuel cell electric vehicles, and range extended electric vehicles. To prevent any confusion, electric vehicle term will be used for battery electric vehicles and we will focus on battery electric vehicles in this study.

The main advantage of an EV is traction motor efficiency. Compared to internal combustion engines (ICE), electrical machines' efficiency is significantly high. The efficiency range of an electric motor in a vehicle application is between 80% to 95% whereas the efficiency of an ICE is around 40% in the sweet spot of the engine. An electric vehicle relies only on batteries and uses an electric machine. Therefore, there is no combustion process during power generation in the car. Hence, they do not generate any greenhouse gases that cause air pollution and they are environmentally friendly. On the other hand, a conventional car burns gas to operate and the in-

ternal combustion engine produces exhaust gases. Torque generation in ICE cars is intermittent due to the combustion process. However, EVs generate torque continuously from the standstill. Because of this reason EVs are more quiet and smoother in operation that increases the driving comfort of the vehicle. ICE cars only rely on fossil fuel resources and these sources are limited. On the other hand, EVs can use clean and renewable energy sources like solar energy, wind energy, hydro energy, and nuclear energy. EVs also can use different energy storage units on board such as batteries, ulta-capacitors, fuelcells, and flywheels. The last advantage of an EV is its regenerative braking capability. As we know, ICE vehicles uses only mechanical friction brakes to stop the vehicle and dissipates the vehicle energy on brake pads. Some recent conceptual ICE vehicle models introduces regenerative braking in their cars. However, mechanical regenerative braking systems utilizes too complicated and expensive components in the their drivetrain. On the other side, EVs are natural in regenerative braking. They do not need any extra component for regnerative braking because an electric motor can operate as a generator as well. Hence, EVs are high efficient vehicles compared to ICE cars.

We should mention disadvantages of EVs to make a fair comparison with ICE vehicles. Due to high technology use in EVs, such as electrical machine, power electronic converters, sensors, and batteries, the cost of the vehicle substantially high. Lithium-Ion batteries are widely preferred in EVs and cost of the battery pack makes around 30% of the vehicle price. Furthermore, the longest range of an EV, Tesla Model S, in the market as of the year 2017 is around 250 miles and MSRP of that vehicle is around $68,000. A 2017 model Toyota Camry can drive upto 600 miles with a full tank. MSRP of a 2017 Toyota Camry is around $23,000. Besides, charging an EV from an empty battery to full state requires around 2 hours in the best case scenario that is using Tesla's superchargers. In the last decade, reaching EV charge stations have become very convenient however it is still not sufficient to travel long distances. On the other hand, filling up an empty tank of any ICE vehicle do not take more than a couple of minutes and thousands of gas stations are located very frequently.

We can see that a customer would pay 3 times more than an ICE car to purchase an EV whose

range is less than half of an ICE car and requires hours to recharge it. Still, they would have a hesitation in their mind that if the range of the vehicle is enough for their trips. At this point, we should accept that ICE vehicles are much more convenient to buy as of today. The range and cost are main issues with EVs. When the energy storage issue is solved economically in an EV, the age of ICE vehicles will come to an end. Relentless research are being made on EV technology and the competition between the automakers will decrease the time to transform the transportation.

3.1 Electric Powertrain Topologies

The powertrain of an ICE vehicle consists of an engine, a transmission, clutches, a differential and final gear in general aspect. Engine generates the power and transmits it to the wheel via a transmission,shaft, clutches and gears. In conventional EVs, the engine and gas tank is replaced by an electric machine, a battery pack, and a power processor and control unit. Although ICE vehicles' power train topologies are more or less the same, EV powertrain topologies can be in various configurations. Followig figure shows different powertrain topologies for EVs.

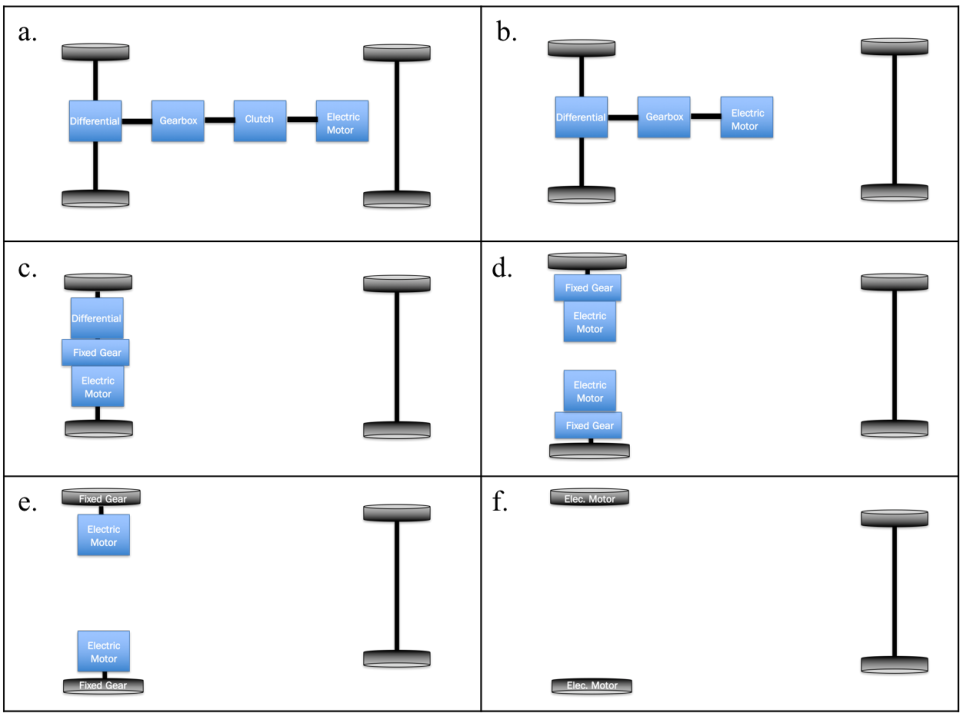

Figure 3.1: Electric vehicle powertrain configurations

In figure 3.1.a we see a conventional EV powertrain that consists of a electric motor, clutch, transmission, and a differential. In terms of mechanical complexity,this powertrain is similar to as of ICE car powertrain. A simpler version of this powertrain can be seen in figure 3.1.b. In this configuration, the clutch is avoided.

It is possible to avoid the transmission in the powertrain as well. However, in that case the electric machine that propels the vehicle in the powertrain is subject to operate in a wide speed range. Figure 3.1.c shows that a fixed gear can replace the transmission and a more simple drivetrain can be utilized in the vehicle.

First three powertrains uses only one electrical machine in the powertrain. Multiple electrical machines can be used to propel the vehicle as well..Figure 3.1.d shows an example of 2 electrical machines in the powertrain. As is seen, this topology does not use a differential. Generated torques is applied to the wheel through a fixed gear.

The fixed gear and electric machine can be directly mounted in the wheels. This topology is called as in-wheel drive and it decreases the mechanical components in the powertrain significantly. Figure 3.1.e shows in-wheel drive application with a fixed gearbox and figure 3.1.f shows is application of it without a fixed gear box. The last one is known as direct drive application and the generated torque in the machine directly applied to the wheels. Wheel angular speed is equal to the motor shaft speed that means the electrical machine should be able to generate high torque in a wide speed range. In-wheel direct drive application can utilize 4 machines for each wheel. In this case, the weight of the vehicle decreases significantly, regenerative braking capability increases and turning radius decreases. However, each electrical machine requires seperate controllers, which increases the cost and control complexity. Also, extra weight in wheels would cause extra maintenance problems for the suspension system of the vehicle [52].

3.2 Electric Powertrain Components

An EV powertrain consists of different electrical and mechanical components but we can talk about three main components that are electric motor-generator, power processing and control unit, and energy storage unit. Following sections briefly presents these main powertrain components.

3.2.1 Electric Motor-Generator

The electric motor-generator in the powertrain develops torque and generates power. It is mainly responsible for the traction. Electrical traction motors are required to satisfy some criteria in EV applications. These can be listed as following [4].

- High specific power (kW/kg)
- High power density (kW/L)
- Low cost ($\$/kW$)
- High temperature operation
- Harsh environment operation
- Wide field weakening operation

Designing an electrical traction motor that satisfies all the criteria above is not possible. A high torque machine with a high power density is not likely, because it needs more magnetic material that increases the volume of the machine. Similarly, high specific power demand would reflect on the insulation and thermal design of the machine. Because of these reasons design of an electric motor requires different aspects of knowledge and experience and it is usually trade off process.

The electric traction machine can run as a generator as well. In the generator operation, wheels drive the machine and generates voltage. In this way, electric machine captures the vehicle energy and sends it back to the battery. That is why they are usually called as electric motor/generator in different vehicle applications.

As we know, different type of electrical machines are in use for various daily and industrial applications. Any type of electrical machine can be used in EV applications such as DC or AC machines. However, because of the cost and dimension restrictions in a a vehicle, most of the automakers prefer to use AC machines in their products. Induction motors and synchronous motors can be used in traction applications. Majority of the known auto-makers prefer to use permanent magnet synchronous machines and its various topologies.

3.2.2 Power Processing and Control Unit

In order to control the flow of power to and from the storage devices, it is necessary to have a power processing unit (PPU) in the powertrain. The power processing unit usually consists of a dc/dc converter and a three phase inverter. However, depending on the application number of the dc-dc converters can be higher or none.

PPU relates the electrical machine with the energy storage unit, therefore power rating PPU is at least equal to the electrical machine power rating. PPU is basically a power electronic circuit that consists of switches. In EV applications IGBTs are widely used due to their high voltage ratings (up to 1600V) and lower conduction losses.

The dc-dc converter is usually connected to a high-voltage traction battery. As it is known, battery voltage varies during operation. A dc-dc converter can be used to regulate the DC bus voltage and keep it constant at the desired voltage value. Typical DC bus voltage values are in the range of 225-650V in EV applications [4]. In some car applications, dc-dc converters are avoided between the traction inverter and the battery (Fiat 500e). In terms of PPU complexity and cost, this latter one is better but performance of the electric motor is directly influenced by the battery output.

A control unit in the powertrain is a vital component. Speed of the vehicle, electrical machine voltage and current, battery voltage, current, and state of the charge, demanded torque, temperature data, etc. should be always measured and under control. A control unit receives data from all the sensors in the vehicle, performs digital signal processing and generates control signals for related components.

3.2.3 Energy Storage Unit

Energy storage unit is the most restricting element in the powertrain. Range of the EV is directly related to the amount of the energy stored on-board. Current energy storage units in electric vehicles are not enough energy dense. Energy density of the gasoline is 12.9 kWh/kg. The best alternative to the gasoline is Li-Ion batteries and their energy density is around 265 Wh/kg [4].

Numbers show that Li-ion batteries are around 50 times less energy dense. When this low energy density number is combined with low specific power, it results in a very heavy and high volume storage device in EVs.

EV applications do not need the energy density of the gasoline. The investments are focused on developing a better material technology for Li-Ion batteries and decreasing their cost by mass production. US government imposes manufacturers to decrease the Li-ion battery costs in next 10 years to around 150 $ per kg [3]. Therefore the price of EVs are expected to decrease significantly in the next decade. The cost reduction would lead to use more battery packs as well as increase in the range of EVs.

Following sections presents different energy storage devices used in EVs and gives some more insight for electrochemical batteries, ultra-capacitors and flywheels.

3.2.3.1 Electrochemical Batteries

The most widely known application of energy storage in electric vehicles is batteries. A chemical battery stores energy in chemical form and when it is needed transfers the energy in electrical form. Since electric vehicles have become a significant actor in the vehicle market, the research and investments on the electric vehicle batteries have significantly increased.

In traction applications, lead-acid, nickel cadmium, nickel metal hydride and lithium ion batteries have been utilized commonly. The energy density of a battery is the key parameter in electric vehicles because it affects the cost, weight and range of the vehicle. Lead-acid batteries' energy density value is considerably low which is 30-50 Wh/kg.Whereas, this number is more than 120 Wh/kg for lithium ion batteries. Because of this reason most of the electric car makers prefer to use these batteries in their powertrains. However, the cost of lithium ion batteries is still very high. The recent number of production cost of lithium ion batteries is around 350$ per kWh and this number can reach up to 500 $ per kWh with the profit margin [3].

An ideal battery should have a high specific energy, specific power, and low cost. Unfortunately, recent battery technologies suffer from the specific power values mostly. As a result, high number of battery packs are used to supply the power demand to propel the vehicle. Another draw-

back of chemical batteries is their lifetime. A typical number for lifetime for lithium ion batteries is 1000 cycles that is a very low number if we compare it flywheels or ultra-capacitors. Moreover, Li-Ion batteries are sensitive to rapid discharge and charge events. Their performance degrades as they get charged and discharged.

3.2.3.2 Ultracapacitors

Ultracapacitors consists of two charged plates and a dielectric material between the oppositely charged plates. Unlike the batteries, they do not employ ion move in their structure but they store energy under a certain electric field. Ultra-capacitors use electrostatic double layer deielectric materials that incresase their capacitance. Since their capacitance is high they can reach higher specific power values.

Ultra-capacitors, known as super-capacitors as well, are usually used as power buffers that requires rapid charge and discharge. Their specific power is around 14 kW/kg which is a great value compared to the batteries. However, their energy density is between 4-10 Wh/kg which is a small value to be used as a main storage device for vehicle applications [4, 7].

Ultra-capacitors can be used for regenerative braking in EVs, cranes, or trains. Their electrostatic energy storage structure makes them capable of capturing and releasing very high current values. Ultra-capacitors are usually hybridized with batteries in EV application to decrease the stress on the battery during the regenerative braking.

3.2.3.3 Flywheels

Flywheels are high-inertia rotating masses that store energy in mechanical (kinetic) form. The speed values can be 20,000 rpm 50,000 rpm depending on the application and material. Depending on the material, their energy density varies between 20-90 Wh/kg. This number is significantly better than ultra-capacitors. Their specific power that calculated in some constructed applications is 2-8 kW/kg [5, 7]. It is important to say that flyhwheels are able to receive and deliver limitless power. This feature makes them very unique in energy storage applications. Their performance do not degrade over the time and can be charged and discharged at very high power levels. Their

lifetime is also very long compared to the batteries (more than 1000000 cycles).

Flywheels are usually related to an electrical machine in energy storage applications. They drive the machine while they delivers power and they are driven by the machine when they receive power. Electrical machine and the flywheel can be fully integrated or the flywheel can be connected to the shaft of the electrical machine.

Similar to the ultra-capacitors they are not used as primary energy resource in EV applications. They are also hybridized with the battery in the vehicle to improve the regenerative braking performance and to decrease the stress on the battery.

Their specific power is slightly lower than ultra-capacitors while their specific energy is relatively higher. The most interesting point about sub-critical flywheels is that they are much cheaper than any other energy storage devices while they can tolerate high number of deep charge and discharge cycles. Having more than one storage devices with different power and energy specifications gives the designer some degrees of freedom to improve the performance of the system.

3.3 EV Performance

The performance of the car is related to the demanded power for traction and available power in the powertrain. The power generated in the traction motor should overcome the tire friction, air resistance, and grading resistance of the road and should generate additional power for desired acceleration and all mechanical and electrical losses in the vehicle.

Longitudinal model of the vehicle can be used to show the forces applied on a vehicle. If we assume this vehicle is front-wheel driven, we can write the acceleration equation of the vehicle by using Newton's second law.

$$\frac{dV_x}{dt} = \frac{1}{\delta M}(F_{xf} - F_r) \tag{3.1}$$

where V_x vehicle is the vehicle speed in m/s, δ is coefficient to convert rotational masses into translational masses, M is vehicle mass in kg ,F_r is resistive force, and F_{xr} is longitudinal force. F_r is expressed by the following equation:

$$F_r = (F_{zf} + F_{zr}\cos(\theta)C_r + F_d + Mg\sin(\theta)) \tag{3.2}$$

where F_d is aerodynamic drag force and C_r is rolling resistance coefficient. Aerodynamic drag force can be expressed as the function of the vehicle speed.

$$F_d = \frac{1}{2}C_d\rho A V_x^2 \tag{3.3}$$

where C_d is aerodynamic drag coefficient, ρ is air density, and A is frontal area of the vehicle. The force required to accelarate the vehicle can be expressed as following:

$$a = \delta M\frac{dV_x}{dt} \tag{3.4}$$

A simple vehicle mathematical model can be expressed by one force equation.

$$F_{traction} = \delta M\frac{dV_x}{dt} + \frac{1}{2}C_d\rho A V_x^2 + Mg\cos(\theta)C_r + Mg\sin(\theta) \tag{3.5}$$

The required power for the vehicle can be calculated by multiplying the equation 3.5.

$$P_{traction} = V_x\left[\delta M\frac{dV_x}{dt} + \frac{1}{2}C_d\rho A V_x^2 + Mg\cos(\theta)C_r + Mg\sin(\theta)\right] \tag{3.6}$$

The power equation above can be used to calculate the required motor power in an EV as well as instantaneous required power required by a vehicle. A driving cycle schedule can be used to generate a power profile. Detailed information can be found in following sections.

3.4 Drive Cycle Tests

Driving cycle is a velocity data that changes in a certain time of interval. This data is used for testing conventional cars and determining their fuel economy. A driving cycle usually contains at least one stop and go pattern and some idling time. The frequency of stop and go pattern depends on the type of driving cycle. A city driving is different than highway driving. In a city driving,

vehicles comes to a full stop and accelerates more often. On the other hand, in a highway driving, a vehicle cruises at high speed and accelerates in case of an overtake or lane change. Because of different driving conditions, a vehicle's fuel economy is usually given for three different conditions that are city driving, highway driving, and city-highway mixed driving [61].

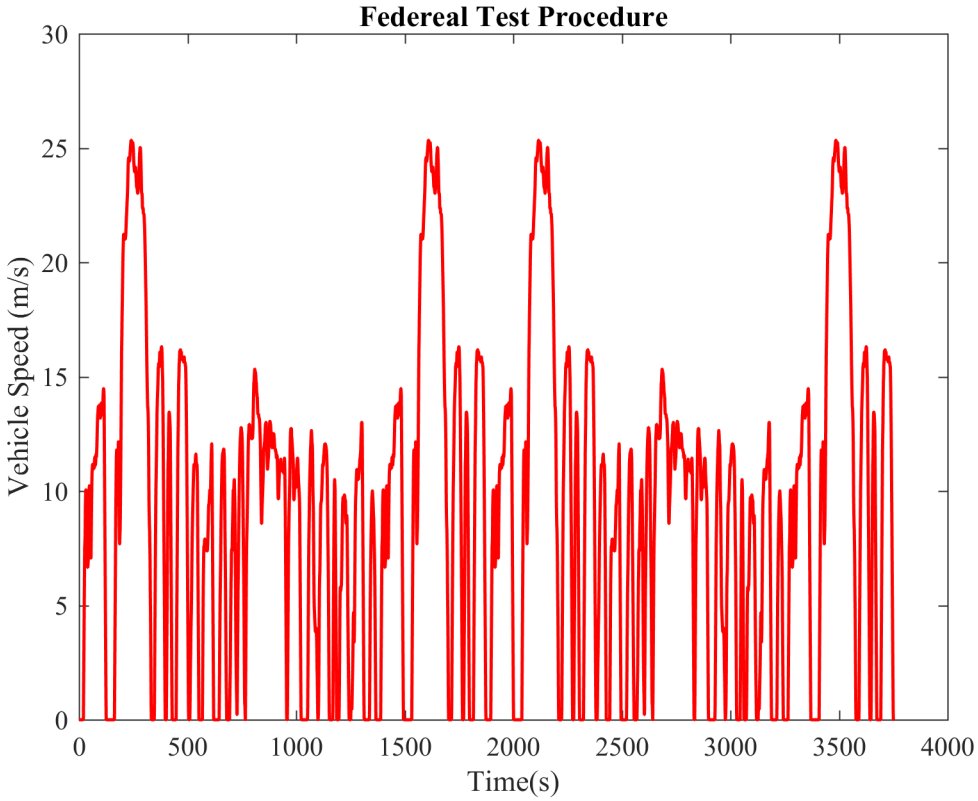

Figure 3.2: Federal test procedure

Standard driving cycle test procedures are defined by official organizations like Environmental Protection Agency (EPA) in the United States, or Association for Emissions Control by Catalyst (AECC) in Europe. Drive cycle data is gathered from different drivers that has different driving habits for various driving conditions. The gathered data is statistically processed and eventually a standard driving cycle is generated. Agencies from different countries have published different driving cycle data because driver habits change in different countries.

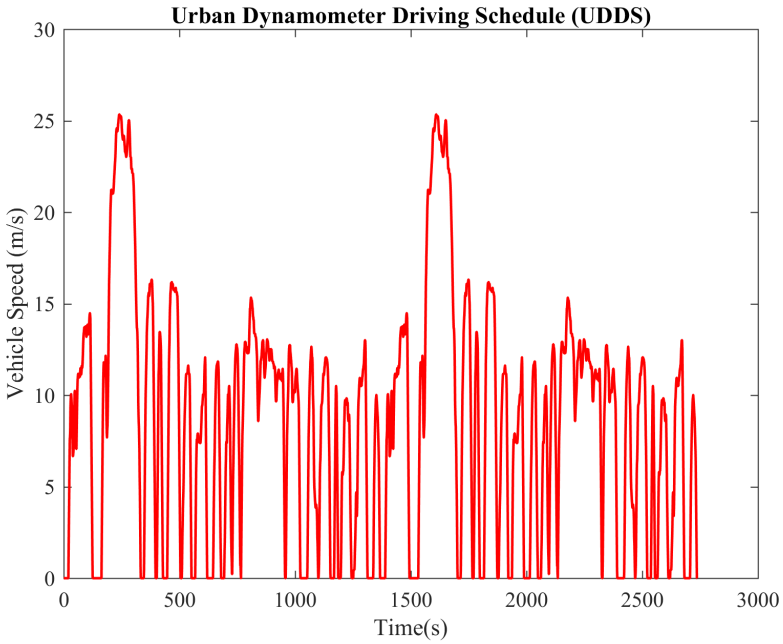

Figure 3.3: Urban dynamometer driving schedule

Driver behavior depends on many parameters such as driver's age, education, weather condition, or vehicle type etc. That is why driving patterns can change from one city to another or from one country to another. Although real world driving cycles are not easy to predict and can not be decided by only traffic parameters, standard driving cycles are still very useful to determine a vehicle's fuel economy and they are imposed to use by automakers to inform customers and satisfy environmental regulations. Following pictures 3.2-3.4 show three driving cycle schedule that EPA and AECC published.

Standard driving cycle tests are generated and intended to use for ICE cars. However, these tests are also used for EV fuel economy as well. EV range is decided by these standard test procedures. In different studies we can see different numbers for range tests. Since the performance of a battery sensitive to environment conditions, EVs range depends on different environment conditions like outside temperature. Standard driving cycles are repeated for EVs for various scenarios such as room temperature environment, cold and hot environment that is air conditioning or heater is on/off. Idling time becomes important in different weather conditions for EVs. Even

though EVs do not release any exhaust gases, their energy efficiency is obtained by these tests that is also a significant output for their effect on the environment.

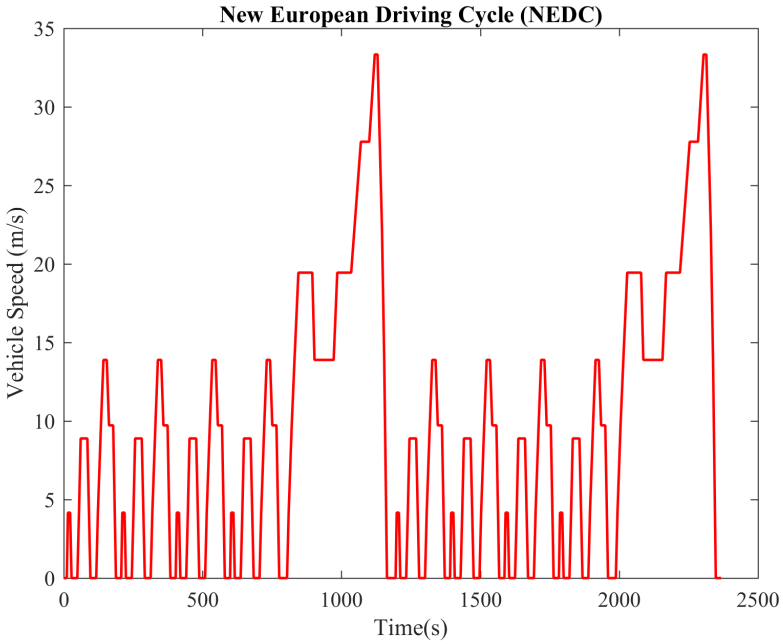

Figure 3.4: New european driving cycle

4. APPLICATION OF THE FLYWHEEL TRANSMOTOR POWERTRAIN IN ELECTRIC VEHICLES

4.1 Flywheel Transmotor (FWT) Powertrain

The main structure of the powertrain that is used in EVs basically has a single power processing path. It starts with the battery, goes through a power processor transferred to the electric motor/generator, and finally received by the wheels via mechanical components. Figure 4.1 shows the conventional EV powertrain.

The configuration that is presented in the picture above is in use more than a hundred years. As we mentioned in previous chapters, EVs suffer from their range problem and it is mostly related to the current battery technology. Most of the research on EVs focused on developing the battery technology; however, there is another path to follow to improve the range of EVs that is developing a new powertrain configuration.

Energy transformation process is not cheap and EVs transform energy 4 times at every start and stop event. Each transformation happens with a certain efficiency and all energy transformations describe an energy efficiency chain in the powertrain. We can easily say that propelling an EV from a mechanical energy source and decelerating and storing the vehicle energy in the mechanical form

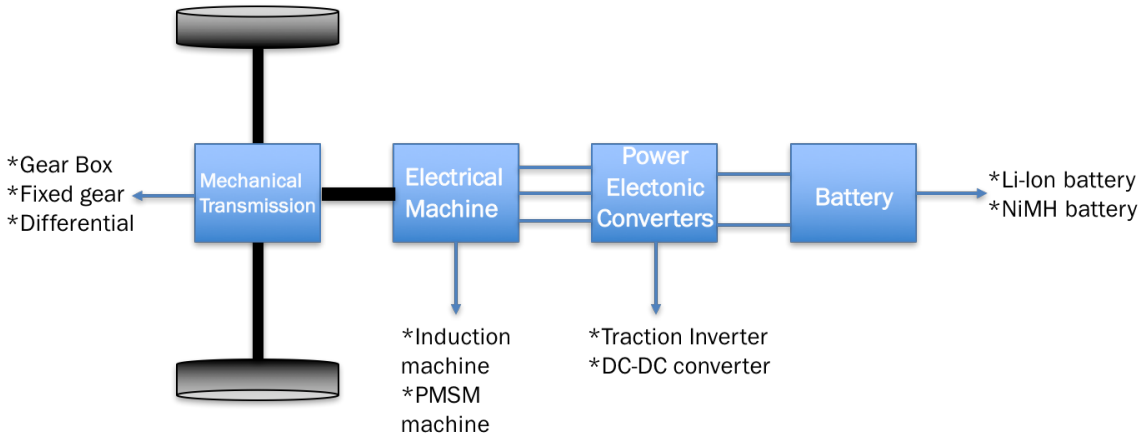

Figure 4.1: Conventional EV powertrain configuration

is the ideal method for EVs.

Regenerative braking in EVs is a very beneficial feature but it is very limited. If we were able to recuperate 100% percent of the vehicle energy, EV's range today would be roughly double in city driving. Hence, a powertrain topology that improves regenerative braking as well as propels the vehicle can revolutionize the EV design.

One of the best mechanical energy storage device option for vehicle applications is flywheels. However, as we explained in Chapter 3 they cannot be used as primary energy storage devices. As a result, they are used as auxiliary energy storage in vehicle applications. In the introduction chapter, we introduced previous studies on both electrical and mechanical flywheel powertrains. Both the electrical and mechanical flywheel powertrains have their own advantages and disadvantages.

On the one hand, electrical flywheel powertrain is easy to control and flexible, more compatible to digital processors, and have fast response time which makes them suitable to address dynamic operating conditions. Moreover, advanced electric machines are almost maintenance free and affordable.

On the other hand, mechanical flywheel powertrains do not need any energy transformation since the energy is always in the mechanical form and is just transferred from wheels to the flywheel and vice versa. Furthermore, they offer relatively high energy density and low cost.

In order to combine the merits of these two flywheel powertrains, namely the mechanical and electrical, a novel system has been invented and developed at Texas A&M University. The proposed system consists of four main parts and demonstrated in Fig.4.2.

- Transmotor

  The transmotor, first invented at Texas A&M in the 1990s, is an electromagnetic device in which both the rotor and the stator can rotate freely [17, 52]. A transmotor can be treated as a three-port device, one electrical port and two mechanical ports as is shown in Fig.4. These devices obey the same electromagnetic energy conversion principles that apply for conventional electric machines. According to the NewtonâĂŹs third law of motion, at steady state, the developed torque on both rotating rotor and stator has the same magnitude but

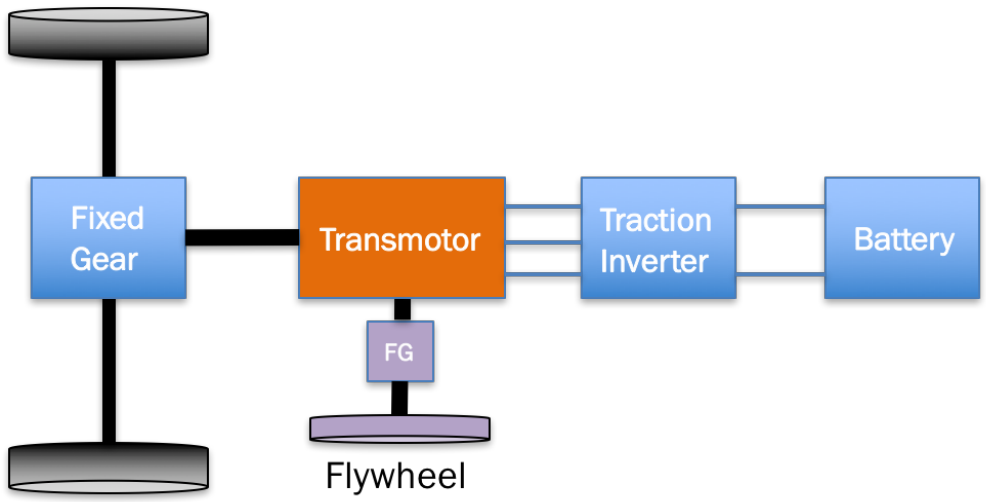

Figure 4.2: Flywheel equipped transmotor powertrain topology

opposite directions. As a result, the transmotor is able to transfer torque from rotor to stator and vice versa, magnetically through the air gap. In multiphase ac transmotors, the electrical frequency applied to the stator windings must be the relative speed of rotor to stator in order to have an effective magnetic coupling between those two rotating parts.

- Power processor unit

  The PPU provides the necessary output voltage and frequency to drive the transmotor based on the driver's desired torque, availability of energy in storage devices, and road conditions. It is also possible to supply the inverter with a dc/dc converter to achieve a regulated dc bus voltage.

- Battery

  The battery in the powertrain supplies the required energy to the propel the vehicle and stores the energy when it brakes. A Li-Ion battery pack is preferred in the FWT configuration as well.

- Flywheel

  The flywheel that is utilized in the proposed scheme does not need to have very high rota-

tional speeds as it is a sub-critical flywheel and the maximum speed is less than 20000 rpm. As a result, it can be very cheap as it does not need a vacuum chamber and special housing or magnetic bearings. Another remarkable aspect of the proposed scheme is that gyroscopic effects are not significant due to the low rotational speeds. It should be mentioned that even if the gyroscopic forces are not negligible, it is possible to have two counter-rotating cylinders in the same housing to cancel out the effect [50].

4.2 A Simple Drive Cycle Test

Drive cycle tests are performed to obtain a vehicle fuel economy. These cycle data are results of statistical studies gathered from different drivers. Basically a driving cycle represents a driver's behavior. In the United States, Environmental Protection Agency publishes the standard dynamometer drive cycles. Federal test procedure (FTP), Urban dynamometer driving schedule (UDDS), and New York city cycle (NYCC) are very well known standard driving schedules.

Standard driving schedules are used to obtain an electric vehicle's range also. Although they are aimed to use for conventional vehicles, they are used for electric vehicles as well. We will also run our simulations with these standard driving schedules. However, before we apply those long complicated driving cycles, we created our simple test driving cycle to test the system. This driving cycle is shown in Fig. 4.3. Results are shown in the following figures.

The power characteristic of the vehicle, flywheel and transmotor is given in Fig.4.4. Results show that the proposed system can significantly reduce the electrical power ratings. The demanded power is around 115 kW for the given vehicle parameters. Transmotor only delivers 58 kW power and the rest is supplied by the flywheel in the system. This result shows that FWT powertrain can improve the propulsion power in the vehicle. Since the high speed values of the wheel matches the flywheel speed closer, required electrical power is almost 50% less in the vehicle. This result also supports the previous results obtained in energy exchange simulations. Figures 4.5-4.7 presents and give detailed information about the operation of the novel powertrain.

Simulation results show that, the proposed system can follow a given driving cycle successfully with the proposed control systems in the simulation model. Simulation model considers tire

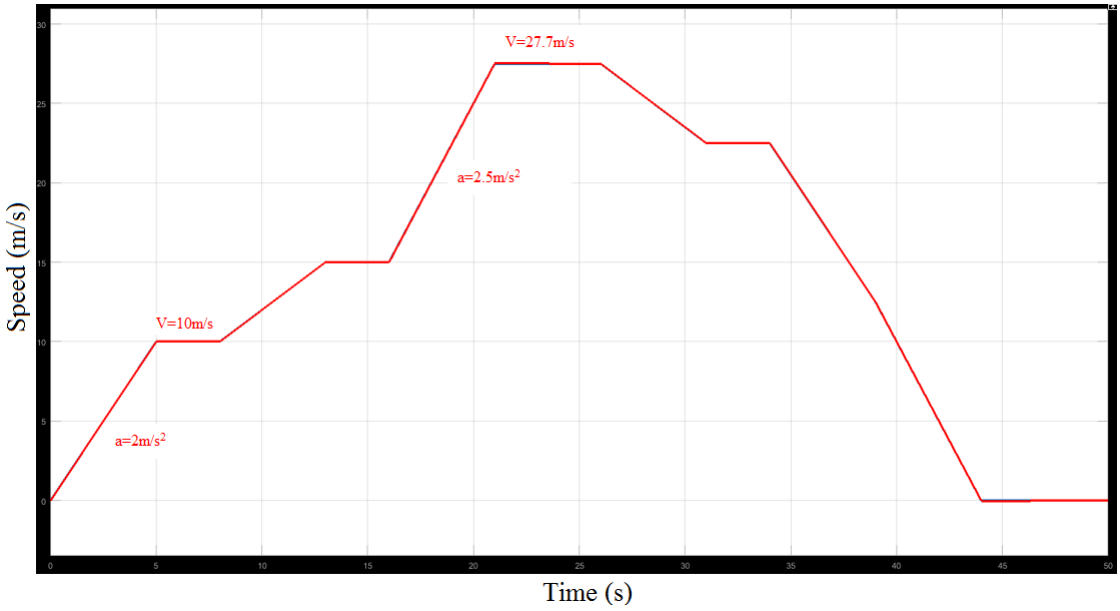

Figure 4.3: A simple drive cycle to test the proposed powertrain

friction, air friction and electrical losses. Because of these losses, the net energy change is never zero. We can see this result in Fig. 4.6 clearly. Overall, we can say that the proposed solution gave promising results for upcoming simulations. The next step is going to be working with actual vehicle parameters and standard driving cycles.

4.3 Case Study: Application of the New Powertrain to Nissan Leaf 2012

A simple application and details of the FWT topology are given in above sections. Early results show that this novel configuration can be a good alternative for current e-powertrain topologies. In this purpose, we applied the FWT powertrain to a commercial vehicle and performed standard driving cycle schedules.

Nissan Leaf 2012 was chosen as the case study. Nissan Leaf is the best selling EV model in Europe and it is one of the oldest commercial product in the EV market. Mechanical, electrical, and performance parameters of the vehicle can be found in the literature in many studies [62–71].

Nissan leaf 2012 is a 1500 kg compact size full electric car. The range of the vehicle is around 92 miles with 24kWh battery which shows it is mostly designed for urban driving. Since FWT

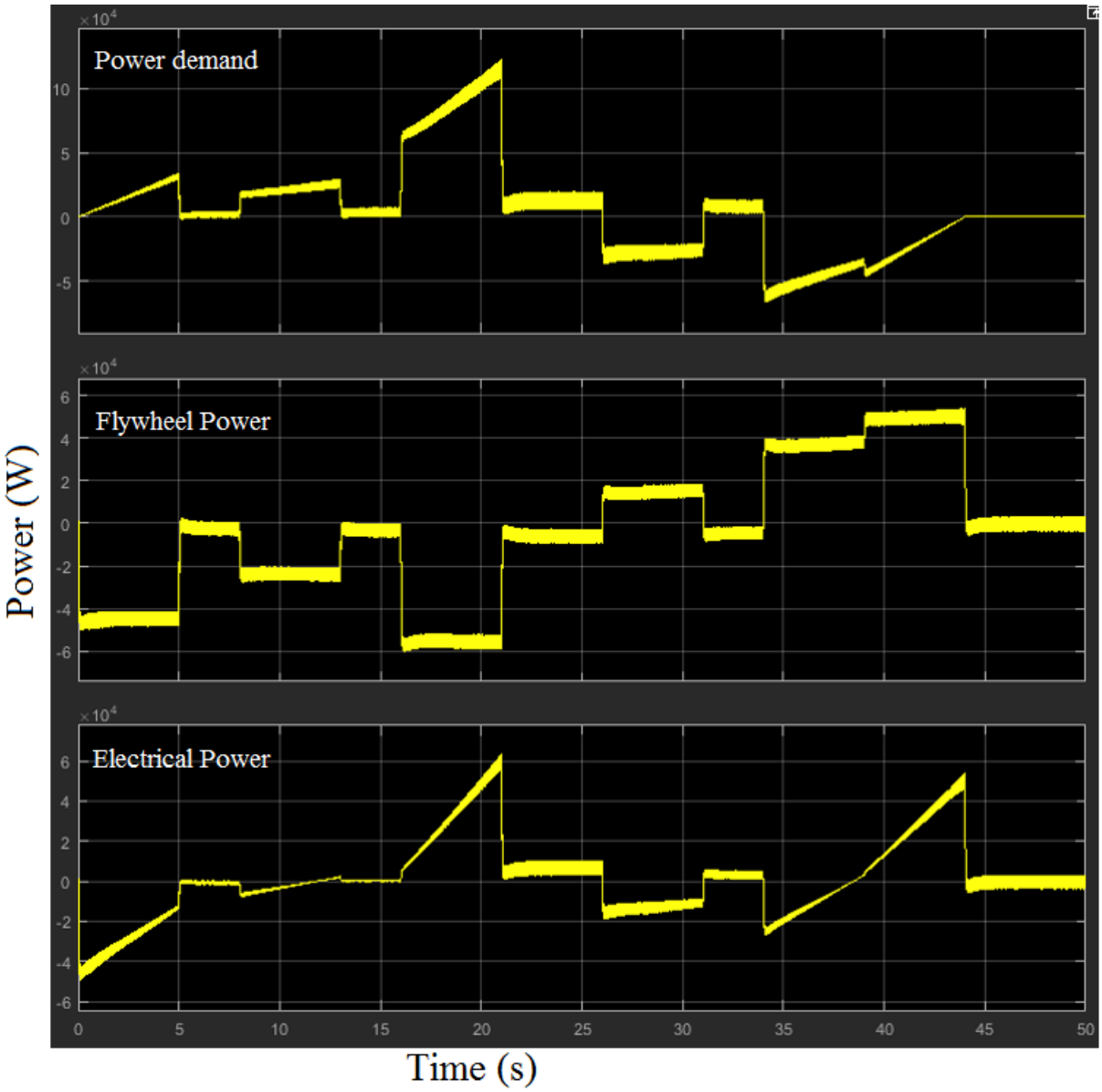

Figure 4.4: Simple drive cycle test power results

topology aims to recover most of the braking and accelerating power, Nissan Leaf EV is a perfect match with our research purpose. Nissan Leaf 2012's vehicle parameters, battery parameters, and motor parameters are given in tables 4.1-4.3.

A comprehensive simulation model for Nissan Leaf 2012 EV and Nissan Leaf 2012 with FWT powertrain was built in Matlab/Simulink by using the information given in Chapter 2. Figure 4.8 presents Simulink model. Transmotor model includes winding losses and windage losses. Battery

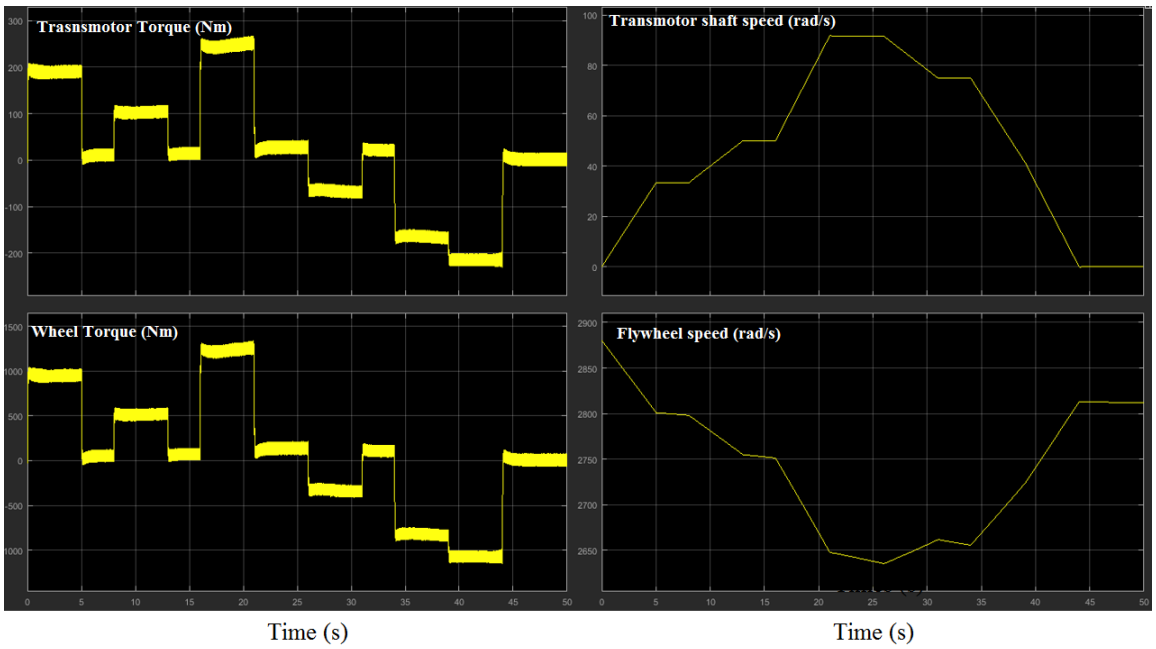

Figure 4.5: Simple drive cycle test torque-speed results

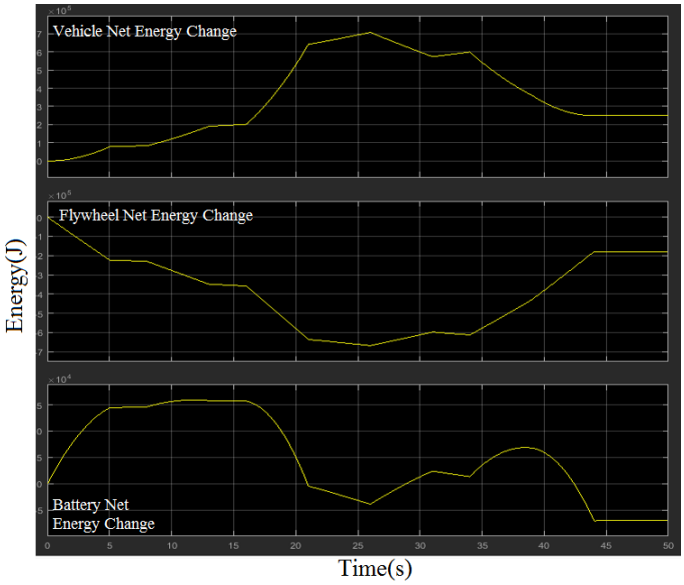

Figure 4.6: Simple drive cycle test energy exchange results

is modeled with resistive losses. Vehicle model includes wind and tire losses. Simulations were performed under standard drive cycles. Inverter losses are neglected.

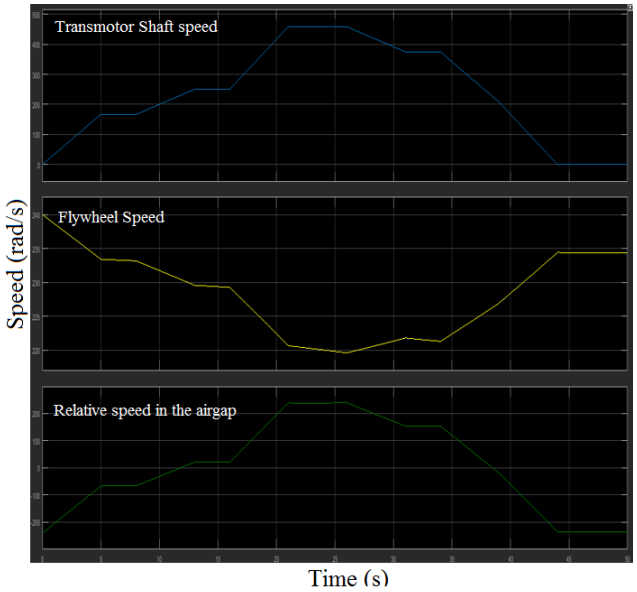

Figure 4.7: Simple drive cycle test speed results

Table 4.1: Nissan Leaf 2012 vehicle parameters

Vehicle Curb Weight	1521 kg
Frontal Area	2.27 m^2
Aerodynamic Drag Coefficient	0.29
Wheel Radius	0.315m
Rolling Resistance	0.00915
Final gear ratio	7.94

In the simulation model, field weakening operation and MTPA control scheme was applied. These blocks can ben seen in Figure 4.8 lower left corner. MTPA control block generates I_d and I_q reference current values. A look-up table was used for this control strategy, since motor parameters are known and assumed they do not change by any thermal effect or magnetic saturation. According to the given torque-speed characteristic of the motor, field weakening operation was introduced in the model.

The simulation model picture demonstrates tranmsotor mathematical model. Extra mechanical speed block is canceled for conventional EV simulations. Rest of the parameters were kept the same for first drive cycle simulations.

Table 4.2: Nissan Leaf 2012 battery module parameters

Type	Li-Ion
Construction	2 parallel x2 series
Average Voltage	7.2V
Capacity	66.2 Ah (0.3C)
Charge Power	>1900W
Discharge Power	>1900W
Energy Density	213 Wh/L
Specific Energy	132Wh/kg
Module Weight	3.8 kg
Total battery weight	182.4 kg
Total battery capacity	24 kWh

Table 4.3: Nissan Leaf 2012 electric motor parameters

Type	PMSM
Electric Power	80 kW
Torque	280 Nm
Base Speed	40 km/h
Top motor Speed	10390 rpm
Motor Weight	58 kg
Peak motor efficiency	97%
Combined eff. motor and inverter	96%
Number of poles	8

Table 4.4: Electric motor estimated parameters

L_d	0.55 mH
L_q	0.8 mH
R_s	280 Nm
ϕ_m	0.17 Wb
B	0.005 Nms/rad
J	0.01 kgm^2

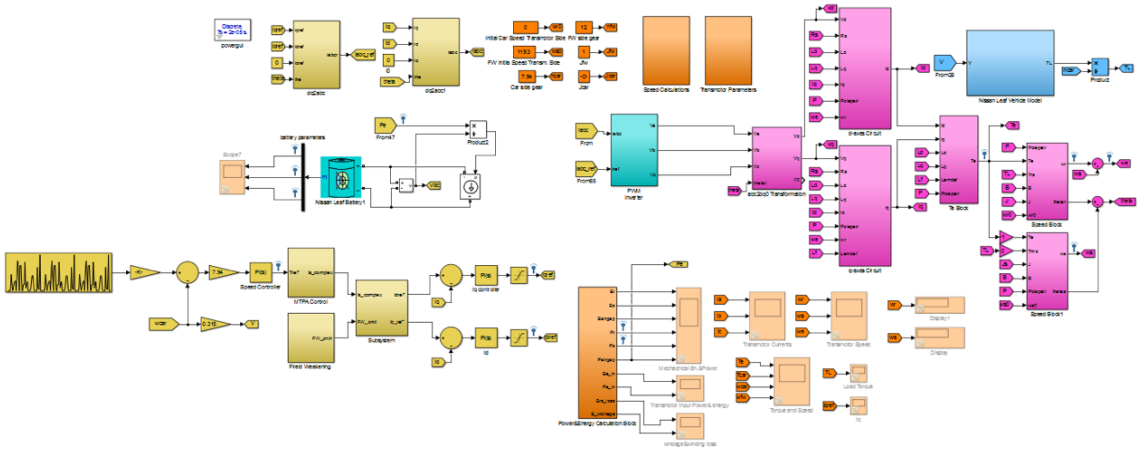

Figure 4.8: Simulation model

4.4 Simulation Results

Simulations were done for different scenarios. Two standard drive cycles that are UDDS and NYCC are chosen for vehicle tests. UDDS is EPA's federal test procedure for city driving. Since it has many stop-and-go patterns, it is a suitable drive cycle for our application. NYCC has more severe acceleration and braking events. It is also a slower driving schedule. This drive cycle is chosen to obtain results under more aggressive driving conditions.

In FWT powertrain we introduce a flywheel and a dual mechanical port machine into the vehicle. Essentially, we introduce two more new parameters in the vehicle that are flywheel mass and flywheel rated speed. Because of this reason, different flywheel inertia values and different rated speed values are tested to determine their effect on the vehicle and design.

Performance of a vehicle is a key parameter for vehicle design. Maximum motor power and required torque values are usually determined by the desired performance. Effect of the flyhweel parameters was tested as well.

Before we started our simulations, we made some assumptions. to simplify the model and make the results more understandable. Those assumptions can be listed as following:

- Vehicle's full energy is available to recover.
- Flywheel in the powertrain is assumed initially charged.
- Thermal effects were neglected.
- Magnetic saturation was neglected.

4.4.1 UDDS Drive Cycle Tests

UDDS drive cycle tests were performed for changing flywheel inertia and rated speed values. Drive cycle power and battery current characteristics, battery state of charge, flywheel speed change are presented in the following figures 4.9 - 4.18.

4.4.2 NYCC Drive Cycle Tests

NYCC drive cycle tests were performed for changing flywheel inertia and rated speed values. Drive cycle power and battery current characteristics, battery state of charge, flywheel speed change are presented in the following figures 4.19 - 4.28.

Drive cycle tests gives us very important insight about the FWT powertrain. First of all in drive cycle results we see that transmotor decreases the electrical power ratings. We can see this from figures 4.9,4.15, 4.19, and 4.25. In these figures, electrical power supplied by the transmotor and battery currents are decreased around 30% to 50% compared to Nissan leaf conventional topology. This result is a significant improvement for power electronics and battery in the powertrain. Less current means lower conduction losses on the switches that is in the traction inverter. Also, lower battery current decreases the stress on the battery. As we know, electro-chemical battery performance and life degrades by deep discharge and charge events. Since we have more than 30% less peaking current values, battery performance in FWT powertrain can remain healthy for a longer time.

Flywheel inertia has not a severe effect on electrical ratings. Electrical power supplied by the transmotor is not affected by the change of flywheel inertia. Increasing the inertia increases the stored energy and lasts longer. That is why power levels and battery currents remain lower in high

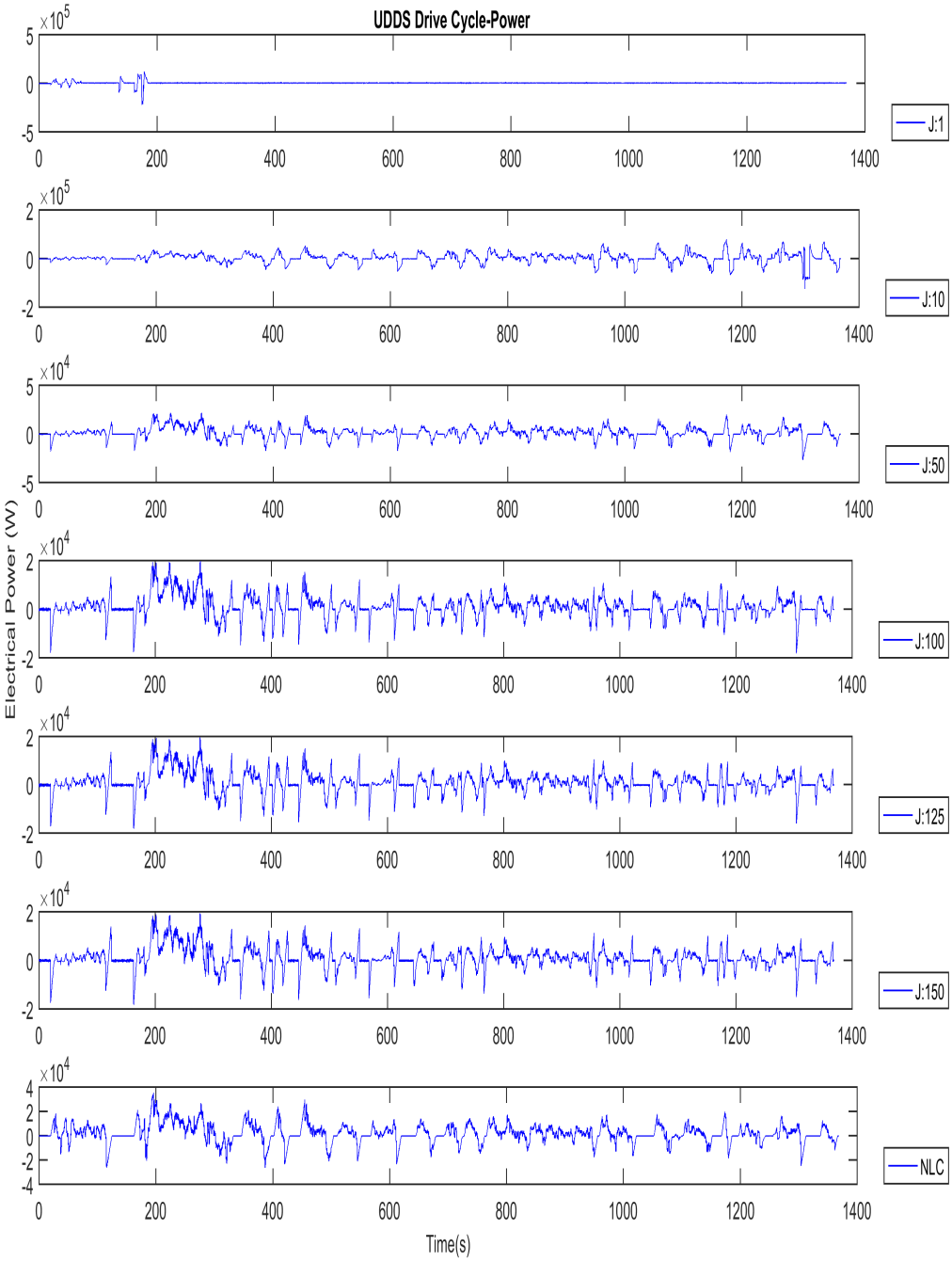

Figure 4.9: UDDS drive cycle power graph-effect of the moment of inertia

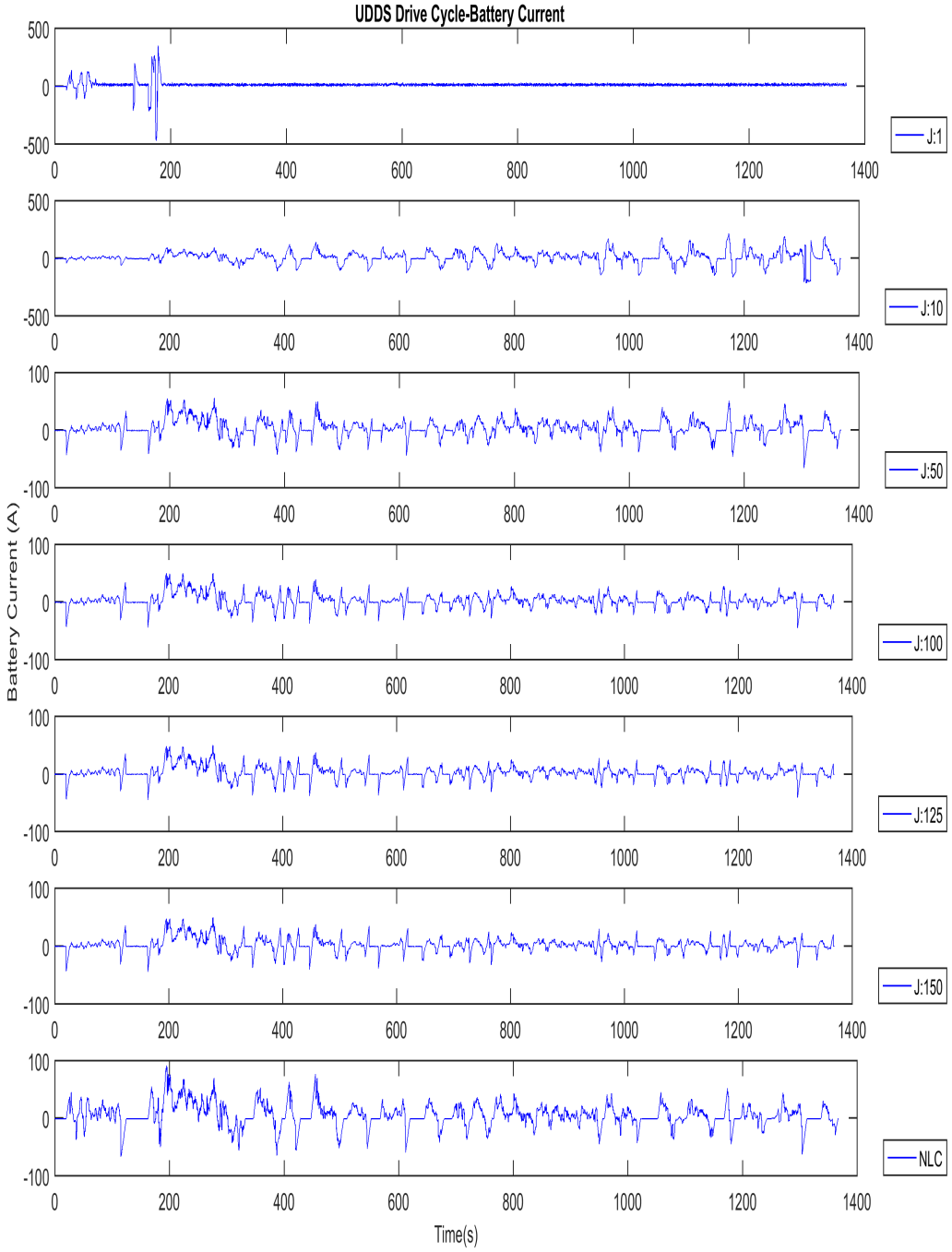

Figure 4.10: UDDS drive cycle battery current graph-effect of the moment of inertia

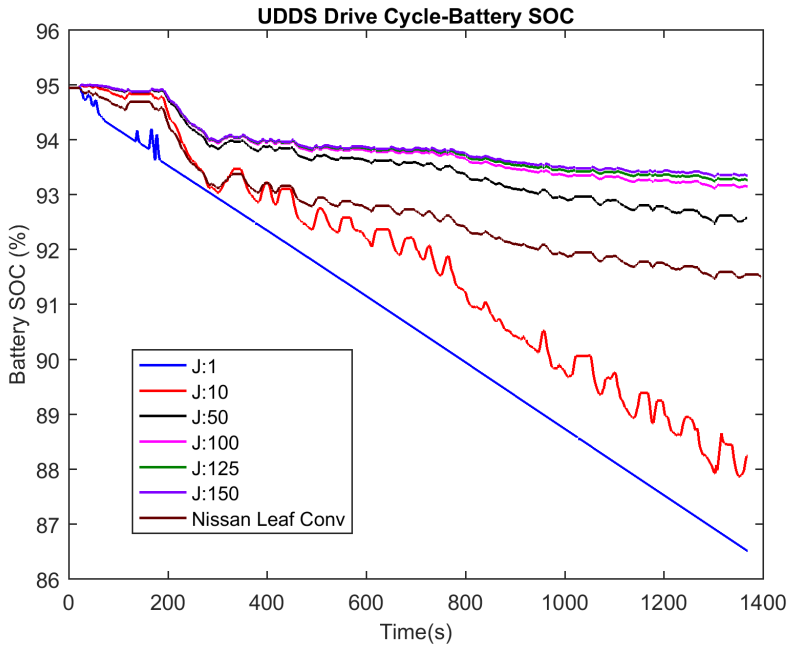

Figure 4.11: UDDS drive cycle SOC graph-effect of the moment of inertia J:1-150 kgm^2

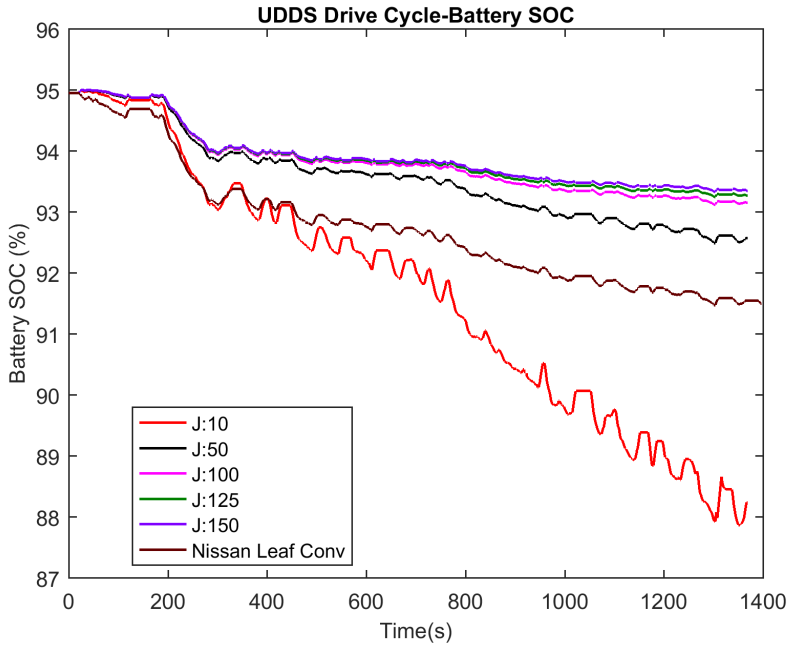

Figure 4.12: UDDS drive cycle SOC graph-effect of the moment of inertia J:10-150 kgm^2

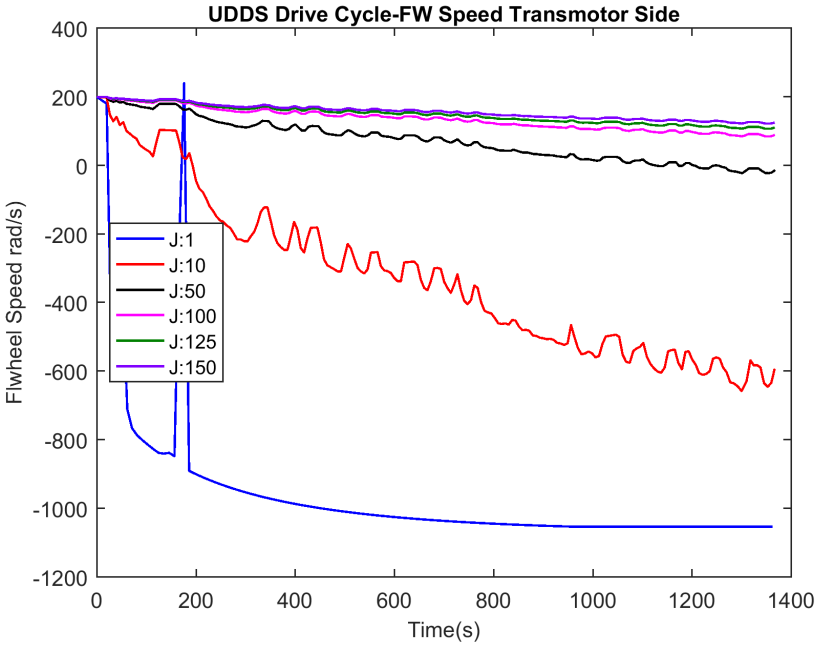

Figure 4.13: UDDS drive cycle FW speed graph-effect of the moment of inertia J:1-150 kgm^2

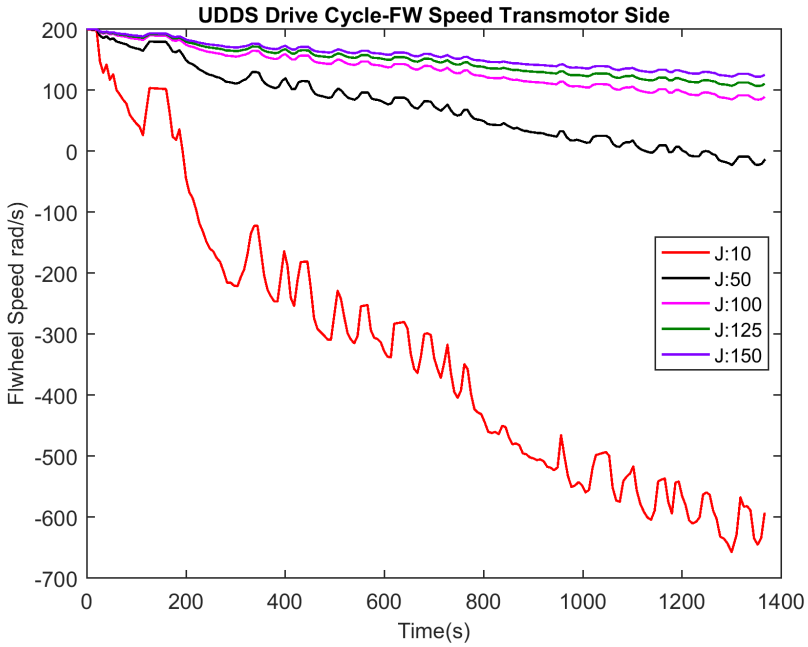

Figure 4.14: UDDS drive cycle FW speed graph-effect of the moment of inertia J:10-150 kgm^2

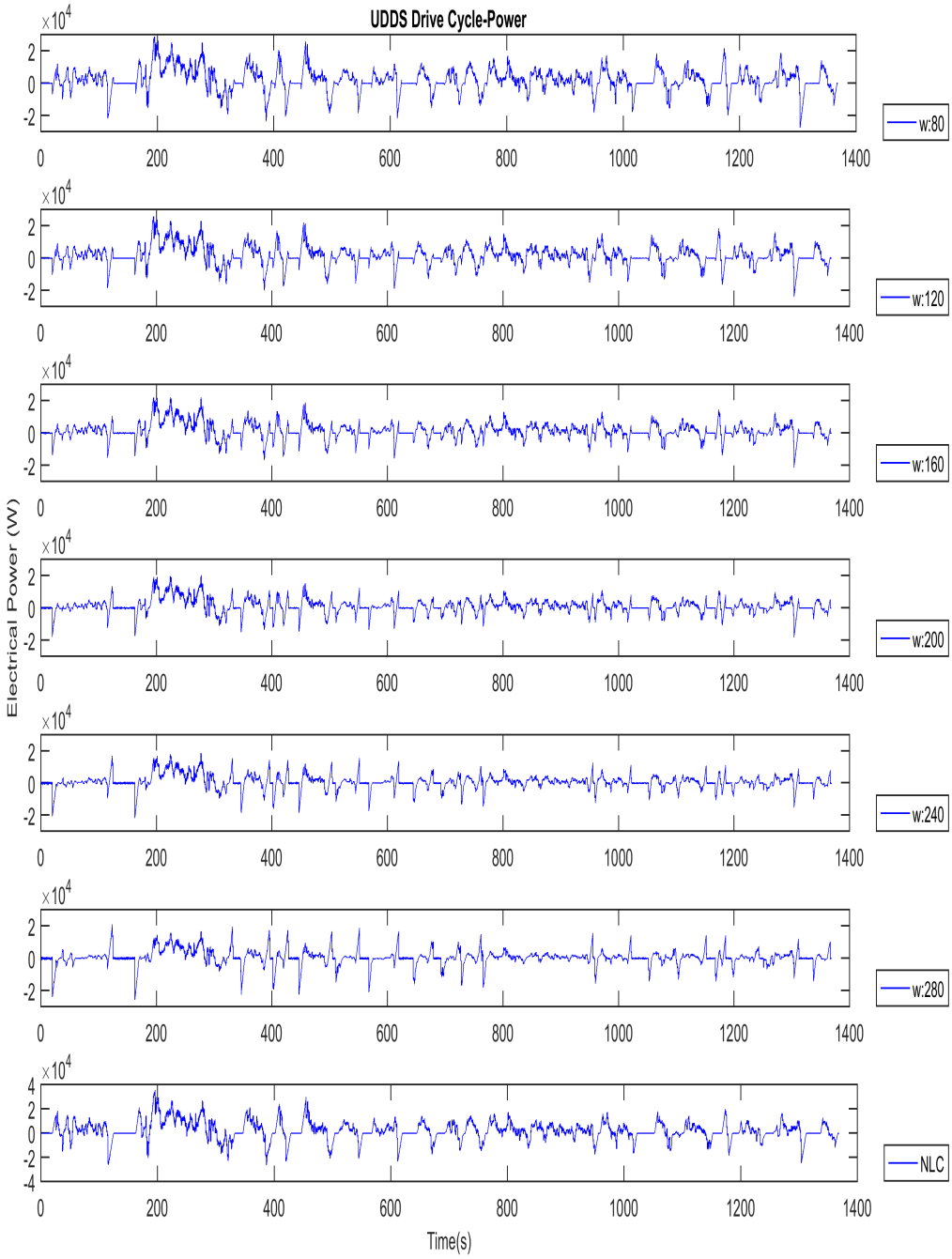

Figure 4.15: UDDS drive cycle power graph-effect of the flywheel initial speed

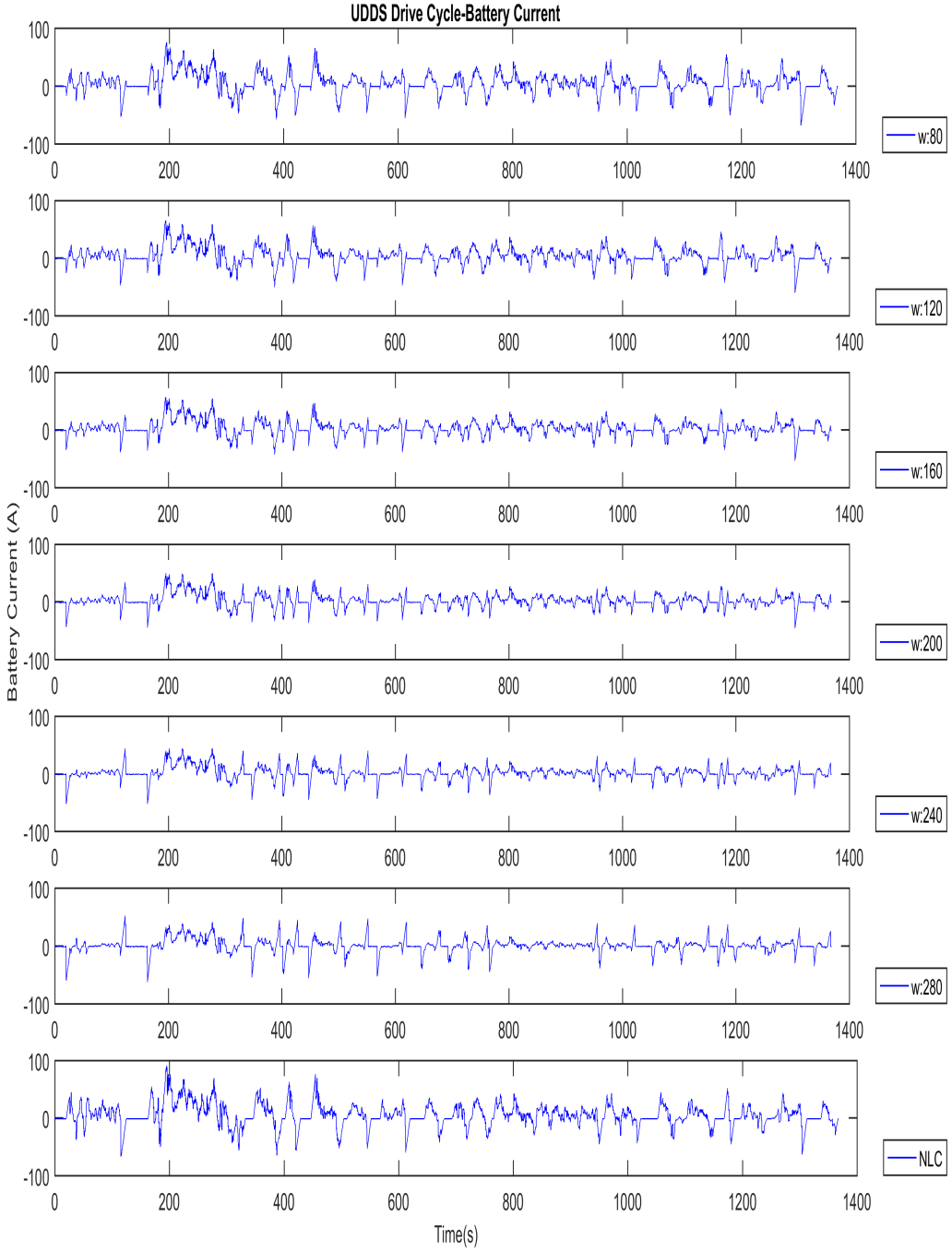

Figure 4.16: UDDS drive cycle battery current graph-effect of the flywheel initial speed

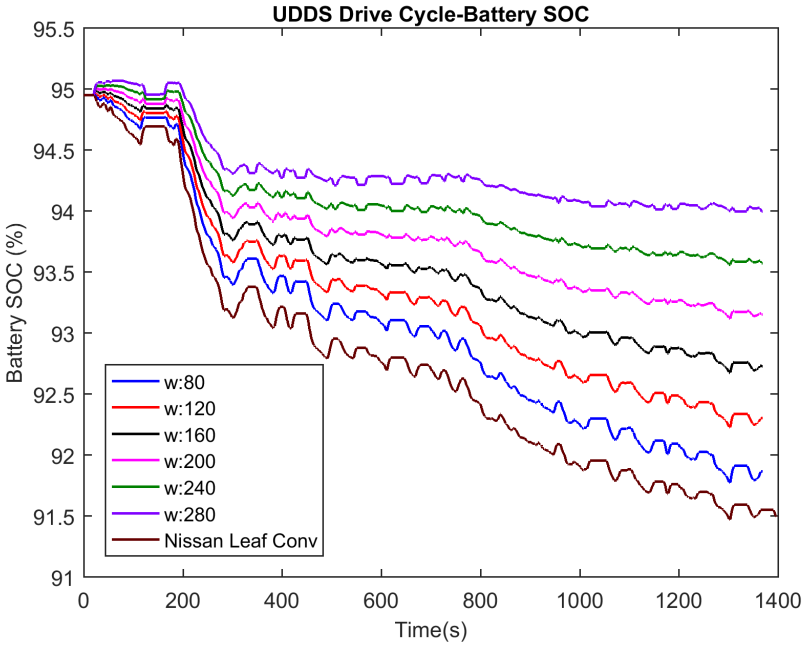

Figure 4.17: UDDS drive cycle SOC graph-effect of the flywheel initial speed

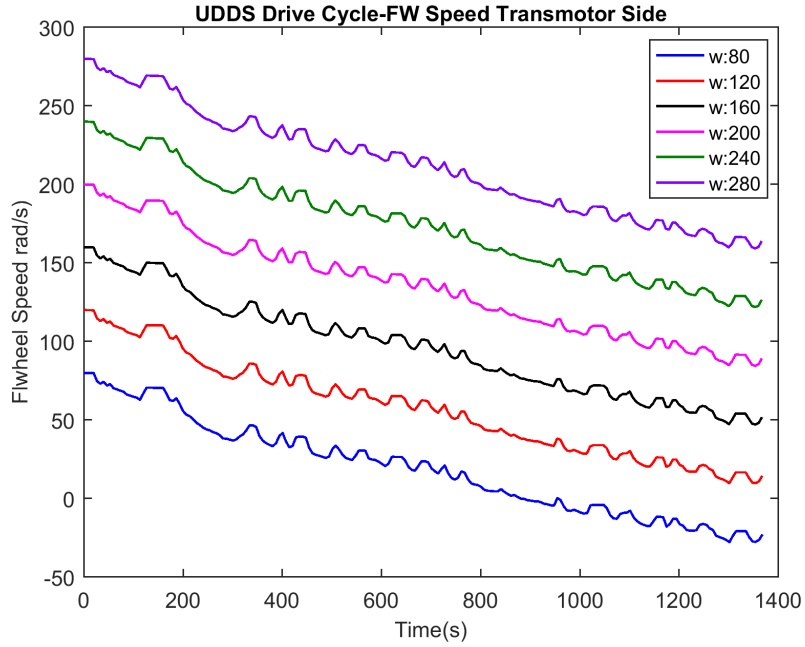

Figure 4.18: UDDS drive cycle FW speed graph-effect of the flywheel initial speed

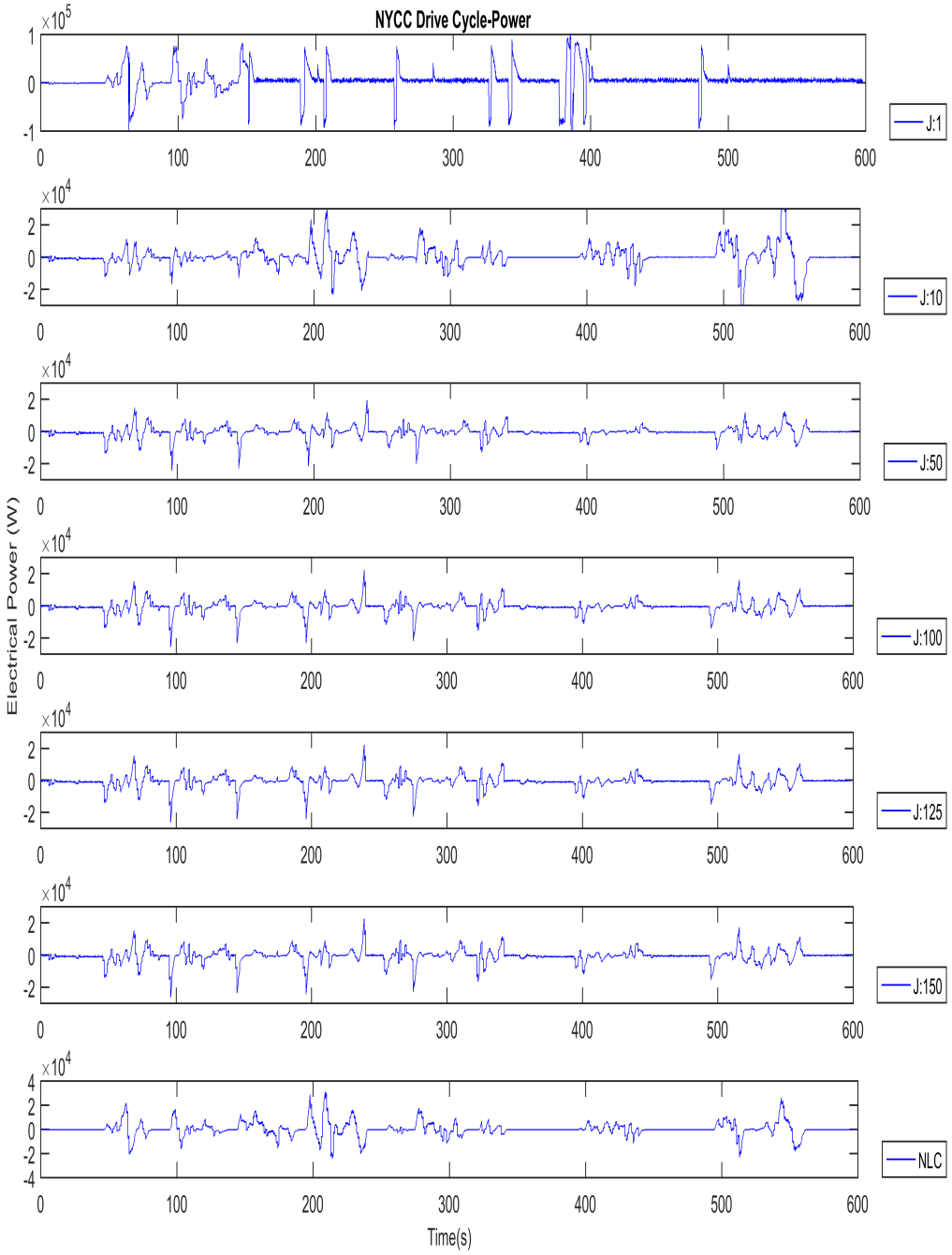

Figure 4.19: NYCC drive cycle power graph-effect of the moment of inertia

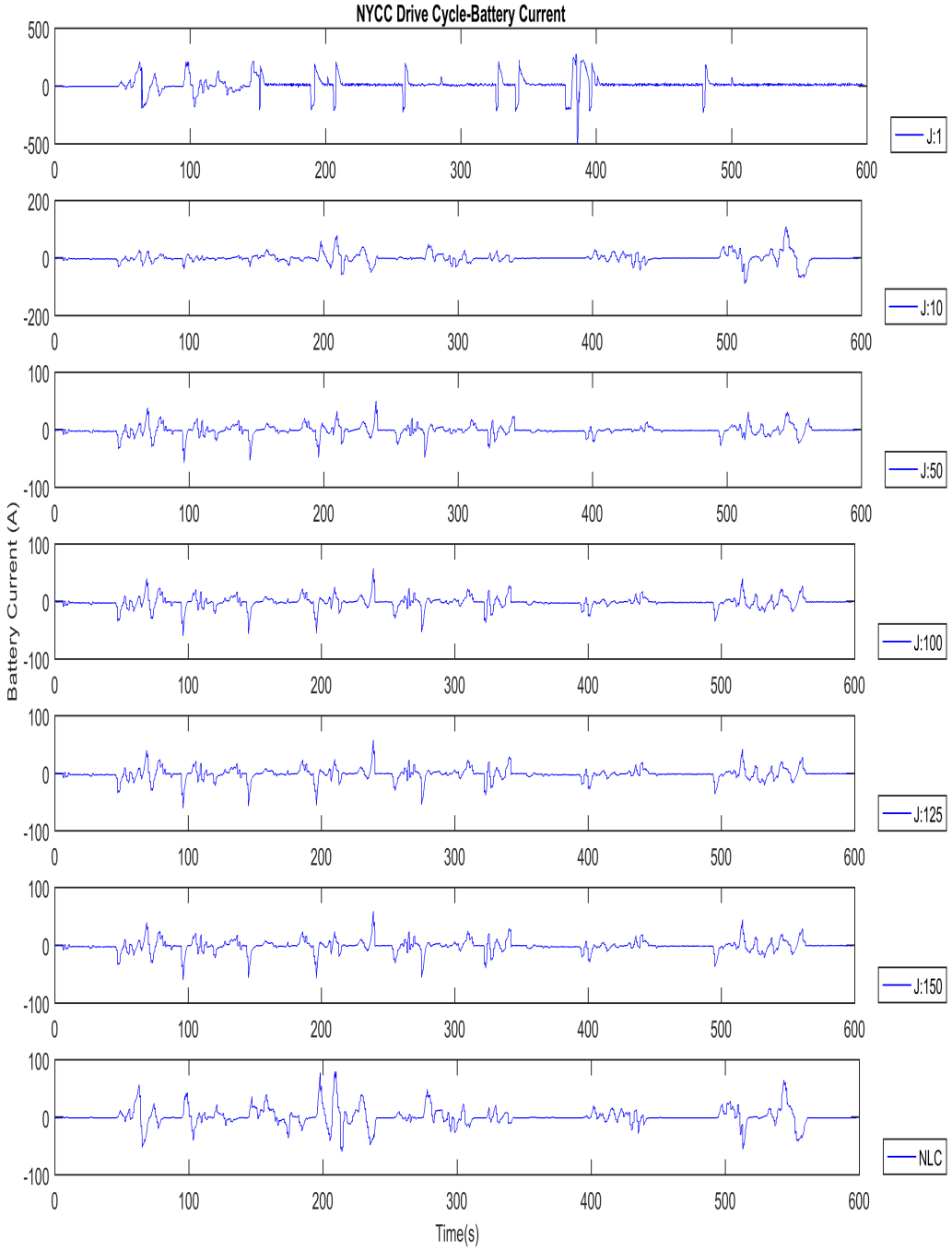

Figure 4.20: NYCC drive cycle battery current graph-effect of the moment of inertia

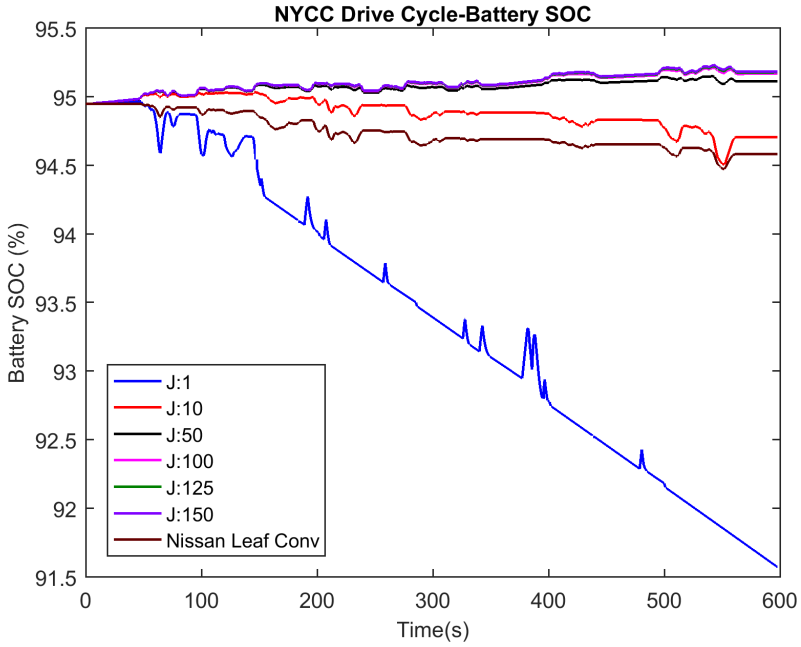

Figure 4.21: NYCC drive cycle SOC graph-effect of the moment of inertia J:1-150 kgm^2

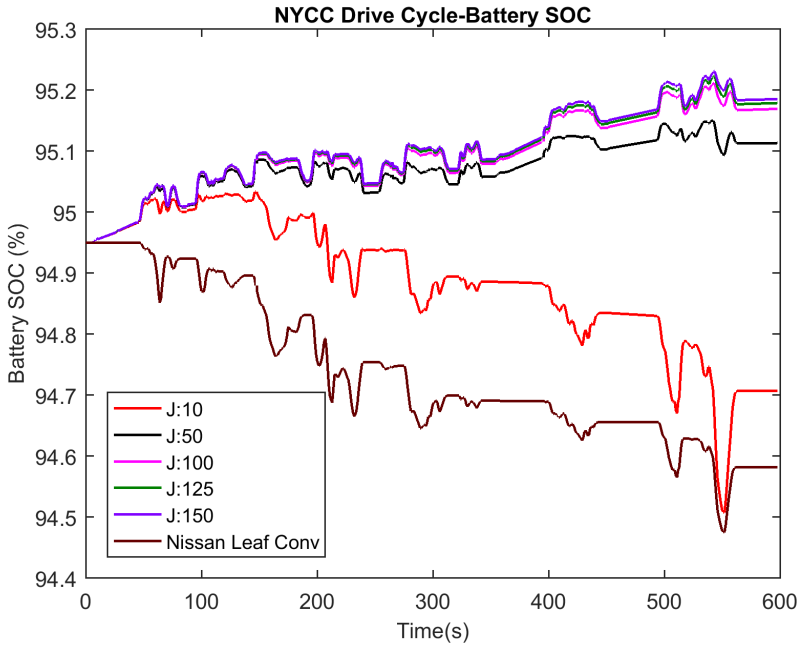

Figure 4.22: NYCC drive cycle SOC graph-effect of the moment of inertia J:10-150 kgm^2

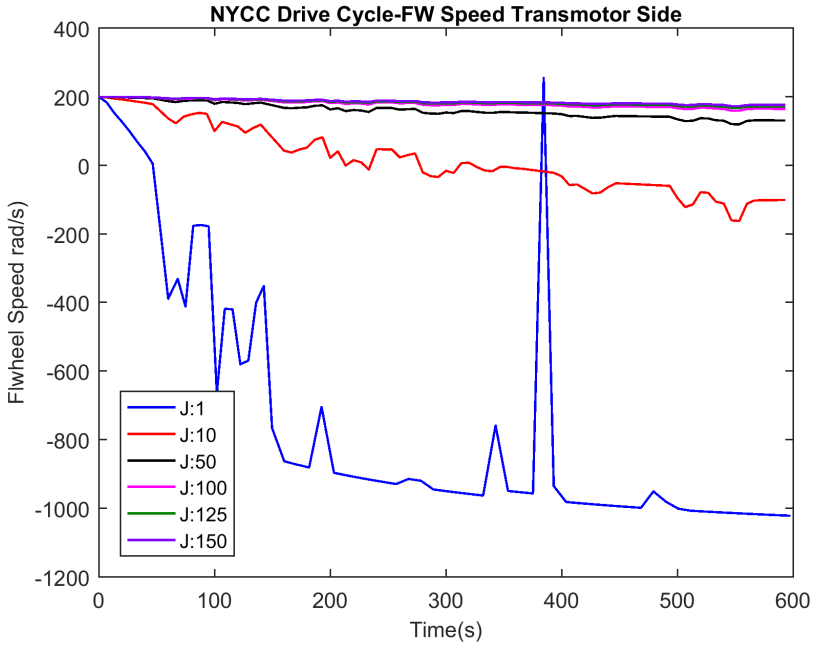

Figure 4.23: NYCC drive cycle FW speed graph-effect of the moment of inertia J:1-150 kgm^2

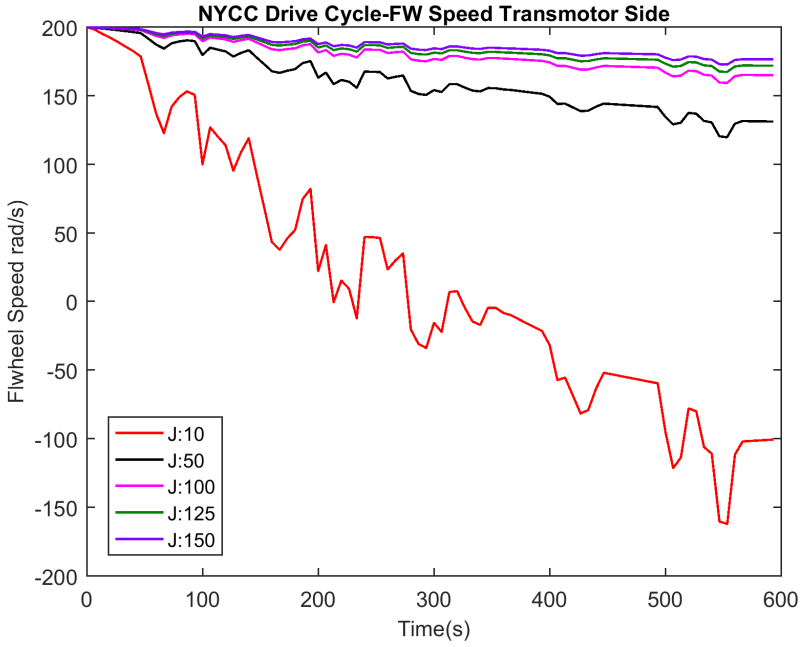

Figure 4.24: NYCC drive cycle FW speed graph-effect of the moment of inertia J:10-150 kgm^2

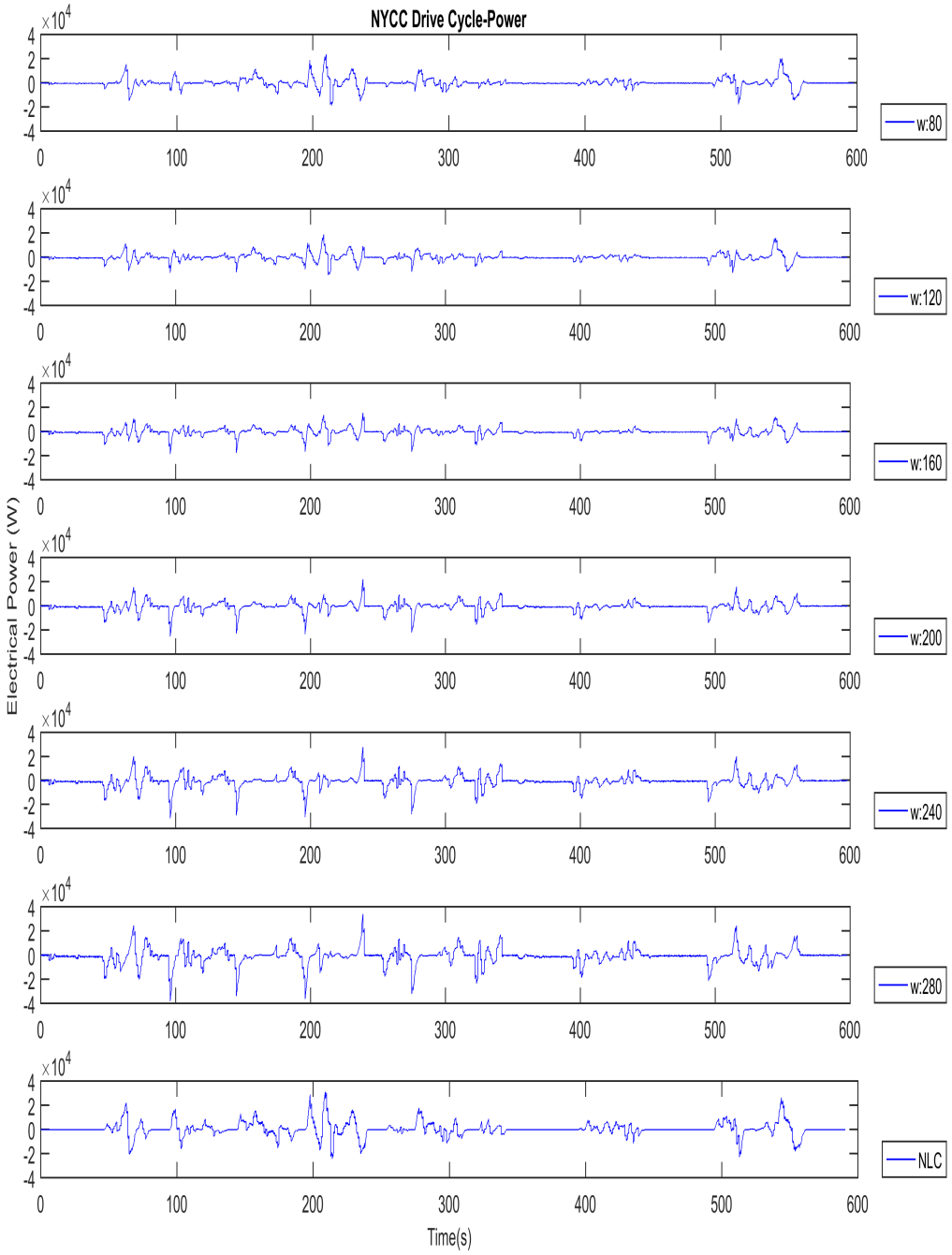

Figure 4.25: NYCC drive cycle power graph-effect of the flywheel initial speed

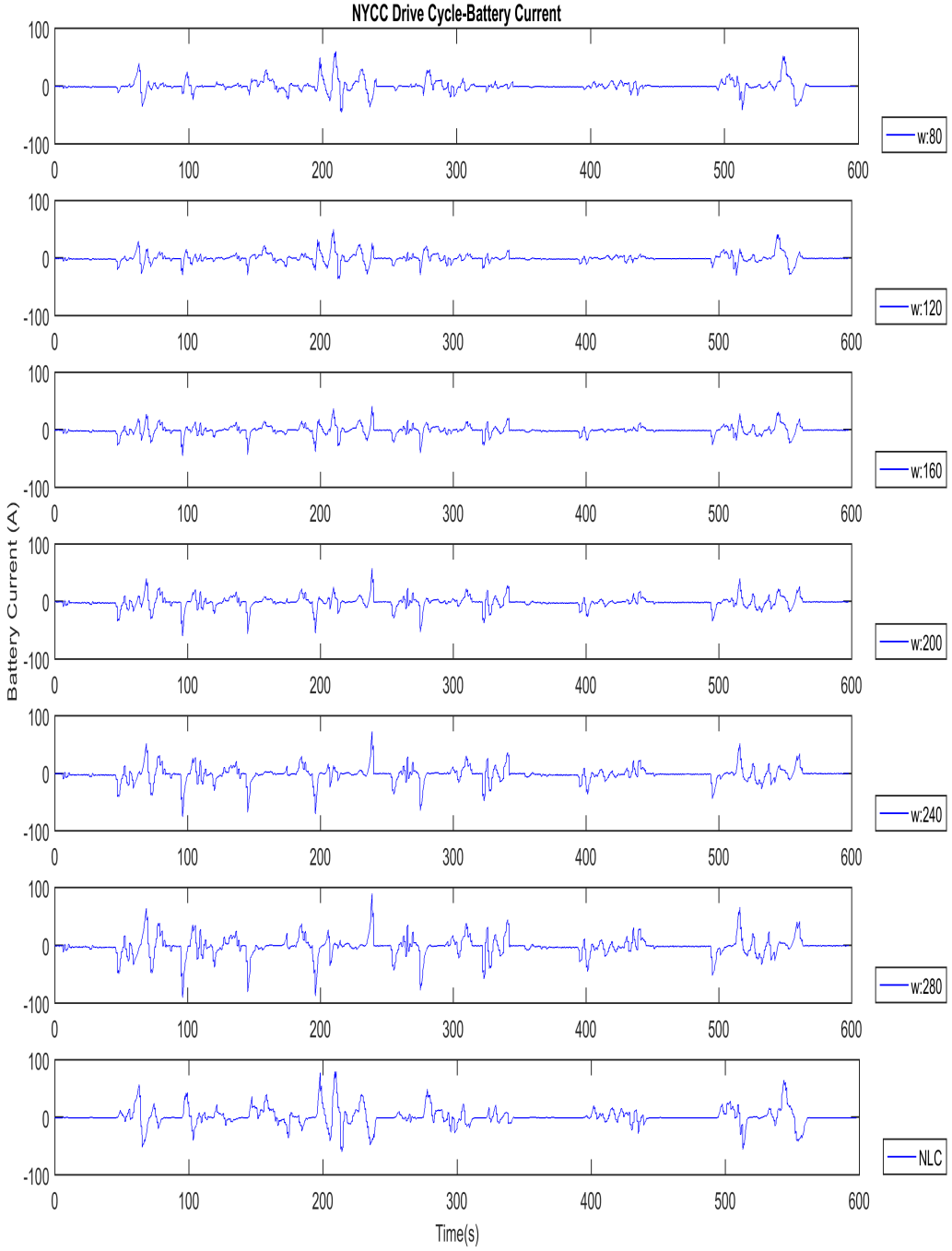

Figure 4.26: NYCC drive cycle battery current graph-effect of the flywheel initial speed

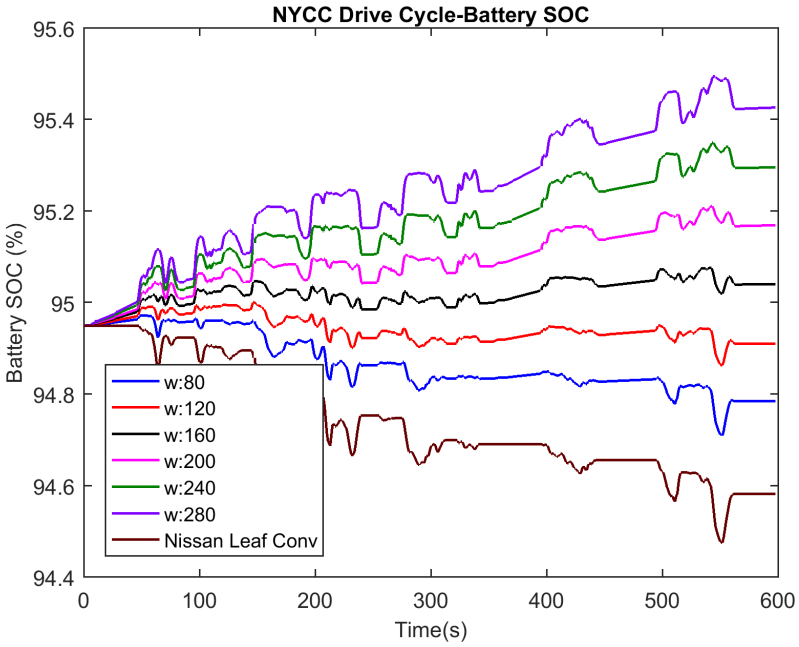

Figure 4.27: NYCC drive cycle SOC graph-effect of the flywheel initial speed

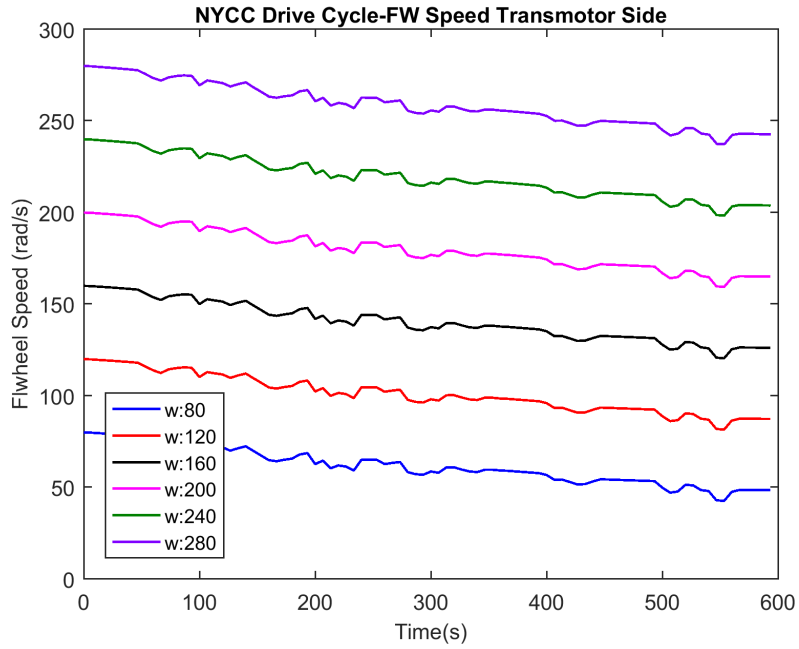

Figure 4.28: NYCC drive cycle FW speed graph-effect of the flywheel initial speed

inertia values at the end of driving schedules. However, for lower inertia values like 1,10, and 50 kgm^2, flywheel depletes too fast and starts to rotate in the opposite direction with the wheels (Figure 4.13,4.18,4.23,4.28). In that case, flywheel acts like a load in the system and demands extra power that is not a desired action. Higher inertia values like 100, 125, and 150 kgm^2, last longer and supplies sufficient energy to the vehicle. When we look at the pictures 4.13 and 4.23 we see that increasing inertia values does not change the flywheel final speed values dramatically. Moreover, increasing the inertia means increasing the mass of the flywheel. Since we want to keep the drivetrain simple and cheap, we want to use a single gear at the flyhwheel side. A realistic number for a gear ratio can be 1:10 at maximum. As a result, more mass would be required to increase the inertia of the flywheel. 100 kgm^2 is a reasonable number according to both drive cycle results. Considering the gear ratio and 100 kgm^2 inertia value, a flywheel with mass around 15-30 kg is enough for FWT powertrain application. In other words, 1-2% of a vehicle weight is enough for FWT powertrain application.

Hence, it can be said that flywheel inertia does not effect electrical ratings of the system but it is more a mechanical design parameter. It directly increases the vehicle weight. With a proper mechanical design, a reasonable flywheel can be added to an EV. Mechanical design of the flywheel is beyond this thesis.

The second parameter that is observed in the tests was rated speed of the flywheel. How to set the rated speed of flywheel was unclear before drive cycle and it is a very important parameter to determine. In the drive cycle test results, figure 4.15, 4.16, 4.25, and 4.26, we see that electrical power that is supplied by the transmotor and battery currents depend on flywheel speed. Flywheel speed values like 80 and 120 rad/s depletes too fast in UDDS drive cycle. Speed values higher than 120 rad/s are sufficient in terms of required energy. In figure 4.15, supplied power values are decreasing as we increase the flywheel speed until it reaches 200 rad/s. After this values peaking power values start increase again. Similar results can be observed in battery currents in figure 4.16. NYCC drive cycle tests also show the same trend with a slight difference that is peaking power and battery current start to increase after 120 rad/s in figures 4.25 and 4.26. From the simulation

results we can clearly understand that there is an optimum flywheel speed interval and it depends on the drive cycle. Then the question is how to determine or estimate this interval. Simulation results show that different drive cycles have different optimum points of rated flywheel speed. UDDS and NYCC drive cycles have different average speed values that are 19.59 mph and 7.1 mph respectively. Transmotor power equations show that higher speed difference between two shafts increases the required electrical power under a certain torque value. Then, the rated speed of the flywheel should always be close to the second shaft speed to minimize the electrical power in the powertrain. We know that vehicle speed changes from zero to different speed values but it definitely has an average speed value over the time. If we set the flywheel speed close to this average value, then we can minimize the electrical power rating in the system. Considering this fact, UDDS drive cycle average speed would become 219 rad/s at the transmotor shaft. Simulation result also shows that around this speed value power rating is minimum. This number is around 80 rad/s for NYCC drive cycle and simulation results support this result as well. As a result, rated speed of the flywheel affects power ratings of the powertrain and the optimum value of the rated speed depends on the drive cycle. Faster drive cycles requires higher speed values and flywheel speed should oscillate around the average speed to minimize the power ratings. Electrical power can be decreased up to 50% compared to conventional Nissan Leaf topology by adjusting the flywheel speed to optimum rated speed.

4.4.3 Performance Tests

Acceleration of a vehicle is a important performance sign. Because of this reason performance tests were performed. Effect of the flywheel inertia and flywheel rated speed on the performance was observed.

Simulation results show that acceleration time of Nissan Leaf 2012 with conventional powertrain topology from 0-60 mph is aroun 9.7 seconds. The actual number reported is 11.5 seconds. Since simulation model ignore some actual losses, obtained number is a reasonable performance number.

In figures 4.29-4.32 effect of the flyhwheel inertia on the performance can be seen. During

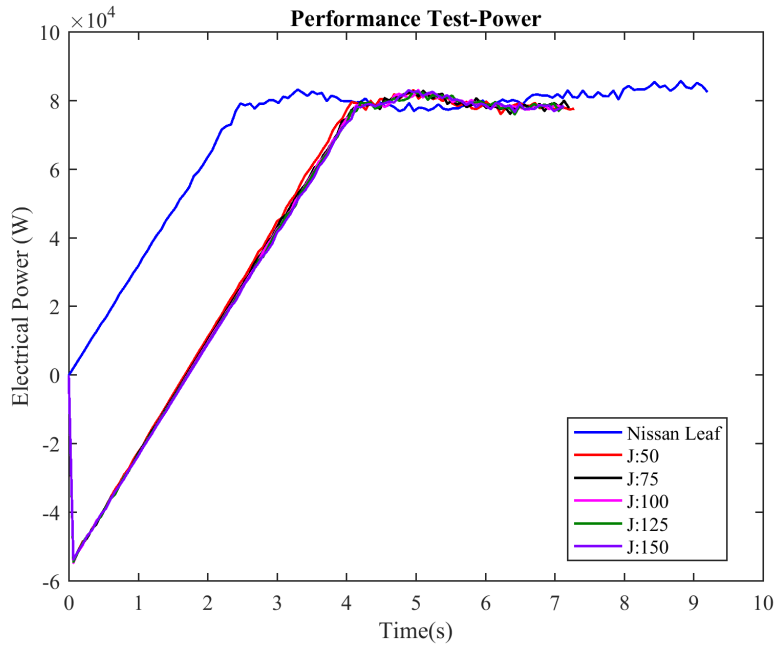

Figure 4.29: Performance tests power graph-effect of the moment of inertia

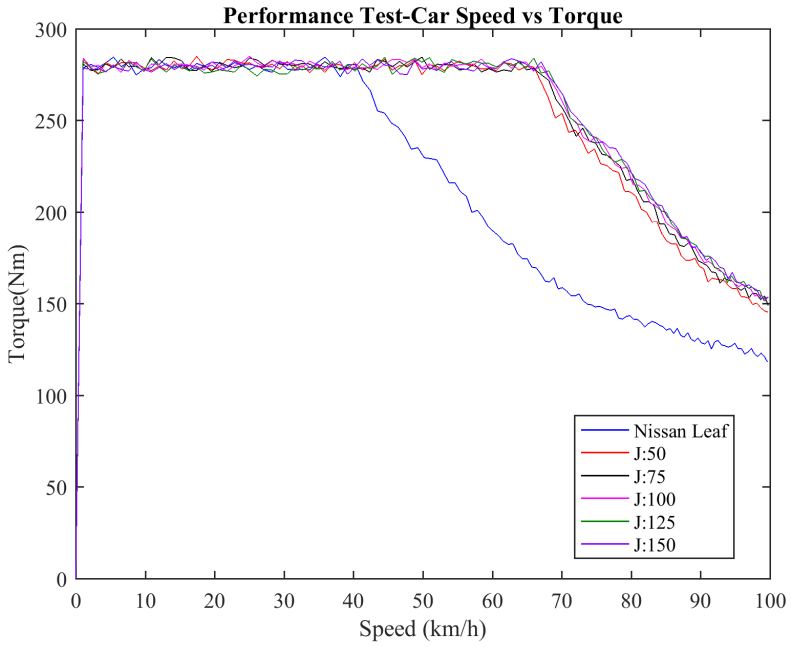

Figure 4.30: Vehicle speed-torque characteristic-effect of the moment of inertia

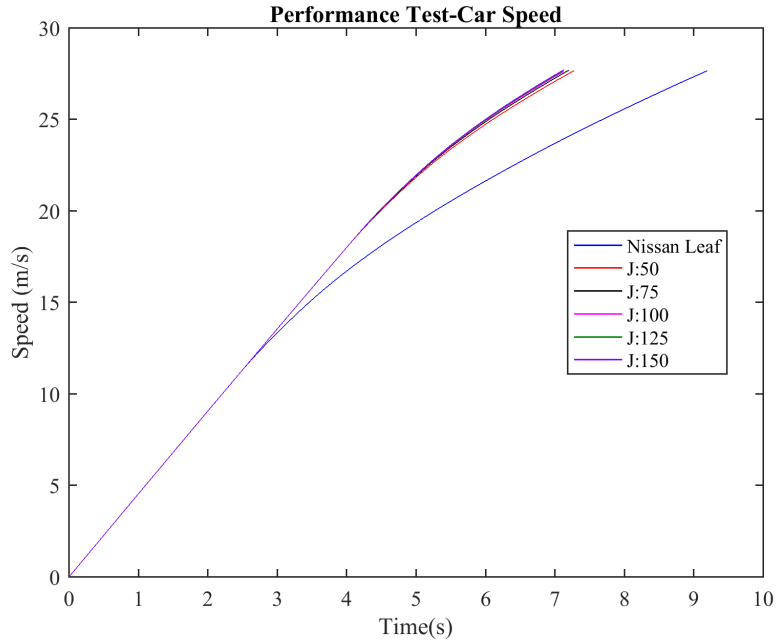

Figure 4.31: Vehicle acceleration-effect of the moment of inertia

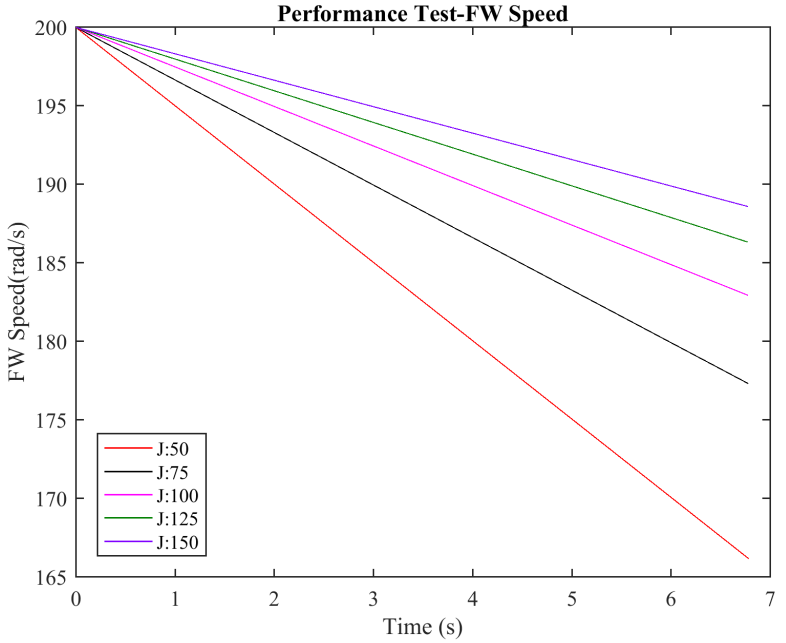

Figure 4.32: FW speed change-effect of the moment of inertia

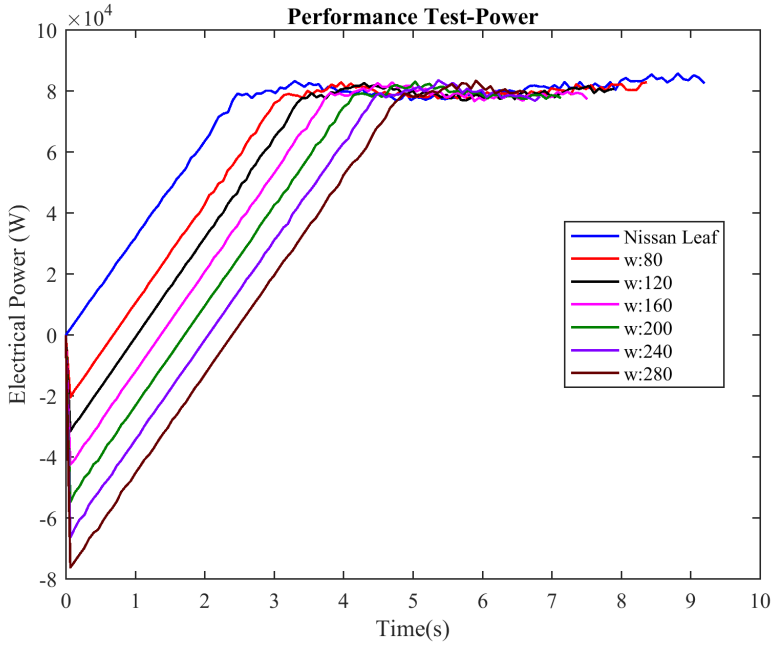

Figure 4.33: Output power graph-effect of the initial flywheel speed

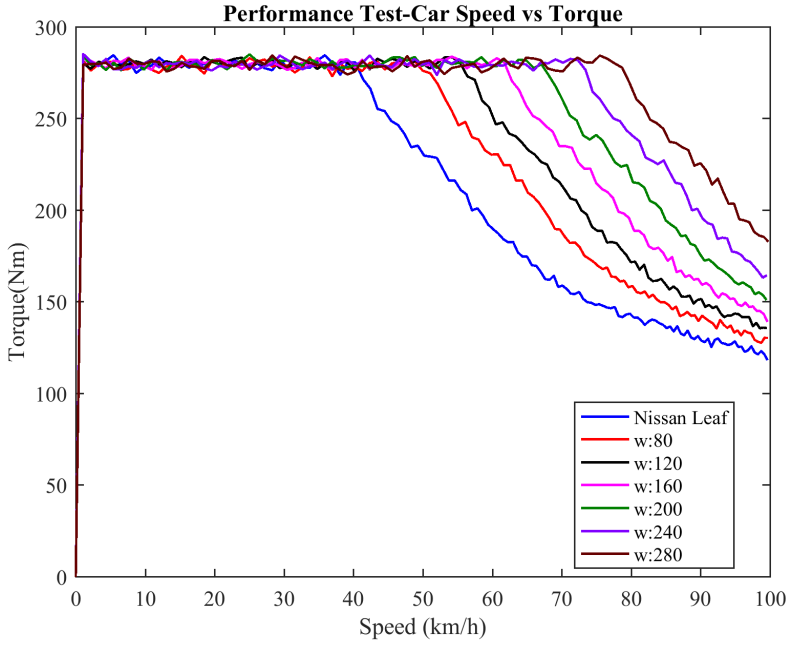

Figure 4.34: Vehicle speed-torque characteristic-effect of the initial flywheel speed

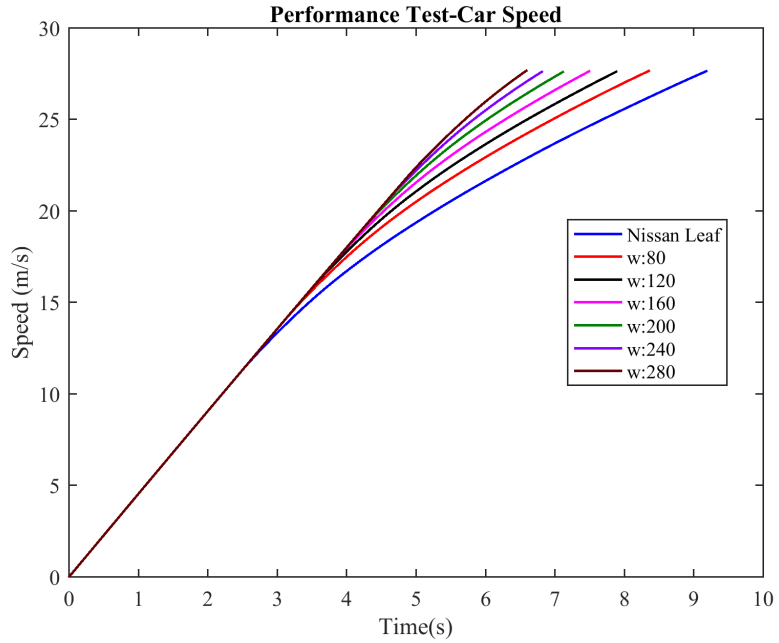

Figure 4.35: Vehicle acceleration graph-effect of the initial flywheel speed

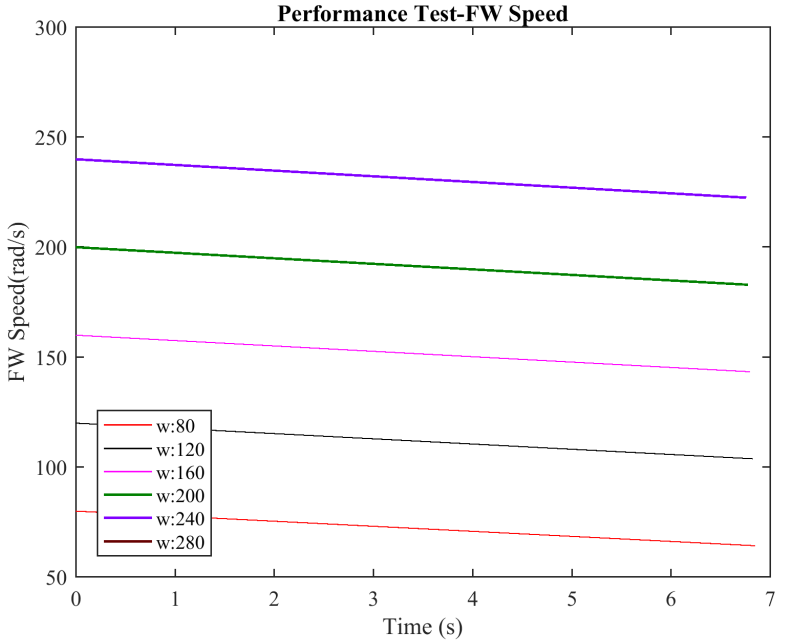

Figure 4.36: FW speed change-effect of the initial flywheel speed

performance tests, we used an 80 kW transmotor that has a flywheel speed of 200 rad/s. Increasing inertia values do not change the power profile. Electrical ratings remains almost constant. Acceleration time is do not change significantly. Flywheel speed change is different each case because higher inertia values show more resistance to speed change as expected. Even if we increase the flywheel inertia, which means flywheel mass, its effect in the vehicle performance is negligible. It is because mass of the vehicle is more dominant. An 80 kW transmotor with a flywheel spins at 200 rad/s accelerates the vehicle from zero speed to 60 mph in 7.2 seconds for different inertia values.

In figures 4.33-4.36 effect of the flyhwheel rated speed on the vehicle performance can be seen. Figure 4.33 shows that higher rated flywheel speed increases the peaking power received by the transmotor and the battery. As we know from the transmotor equations 2.1-2.3, increasing the angular speed under a constant torque scheme increases the power demand and it was observed in the simulation results as well. Figure 4.35 shows acceleration time values. In this figure we see that 80 rad/s rated flywheel speed powertrain accelerates the vehicle in 8.4 seconds and this number decreases to 6.5 seconds at 280 rad/s.

Acccording to these simulation results we understand that rated flywheel speed has an effect on both electrical power ratings and performance of the vehicle. This result can be interpreted in two ways. The first one is that an EV that has FWT powetrain can have different performance characteristic that depends on the charge level of the flywheel. Performance of the vehicle can be improved by spinning the flyhwheel at a higher speed if it is required. The second interpretation is about the design of the powertrain. Introducing the flywheel into the powertrain gives a flexibility while designing the transmotor. A new transmotor that develops lower torque with a charged flywheel can power the EV and satisfy demanded performance criteria.

Torque-vehicle speed characteristic results show us a significant finding. In figure 4.34, we see that constant torque region for the FWT powertrain is wider compared to the conventional Nissan Leaf 2012 powertrain. Higher rated speed values have wider constant torque region which explains the performance improvement. As we know transmotor supply current frequency is adjusted ac-

cording to the relative speed of the inner rotor to the outer rotor. Our base vehicle speed is 40 km/h. This base vehicle speed is higher because of the connected flywheel. The rotation of the flywheel extends the constant torque region. Higher flywheel rated speed increases the constant torque region and transmotor goes into flux weakening operation at higher vehicle speeds. As a result acceleration performance of the vehicle becomes better.

4.5 Optimized FWT Powertrain Designs

In the light of the previous simulations, we conceptually designed different transmotors and equipped them with different speed flywheels to maximize the range of the EV under UDDS driving scheme. We aimed to increase the mechanical energy transfer ratio with an acceptable vehicle performance. As we know, increasing the flywheel speed improves vehicle performance and it increases maximum electrical power. We can change the torque parameter in the transmotor and rated flywheel speed as design parameters. In table 4.5 different FWT powertrain information is given.

Table 4.5: Specifications of different transmotors in the FWT powertrain

	Transmotor Electrical Power (kW)	Torque (Nm)	FW Speed (rad/s)
Design 1	45	310	140
Design 2	60	300	200
Design 3	45	280	150
Design 4	60	280	150
Design 5	45	280	200
Design 6	60	280	200
Design 7	80	280	200

Simulation results for different FWT designs show that range of an EV can be increased around 8-14% with an optimized flywheel speed. Design 1 and design 2 are poor designs where torque is 10% higher than Nissan leaf 2012. This design tranmsotor design would require more magnetic material and would weigh heavier than the original motor. Besides range increase for the first two

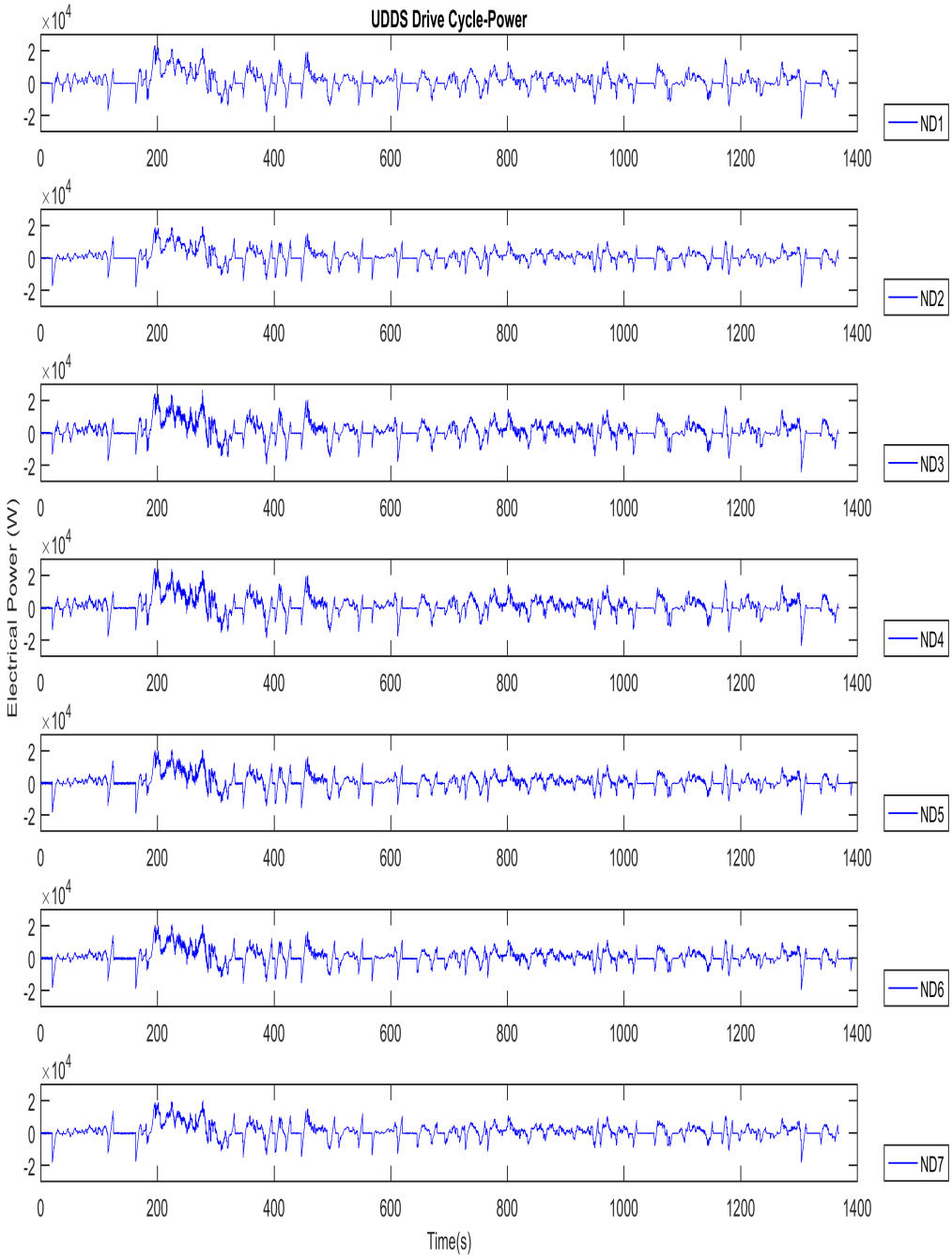

Figure 4.37: Comparison of different FWT powertrain designs-power graph

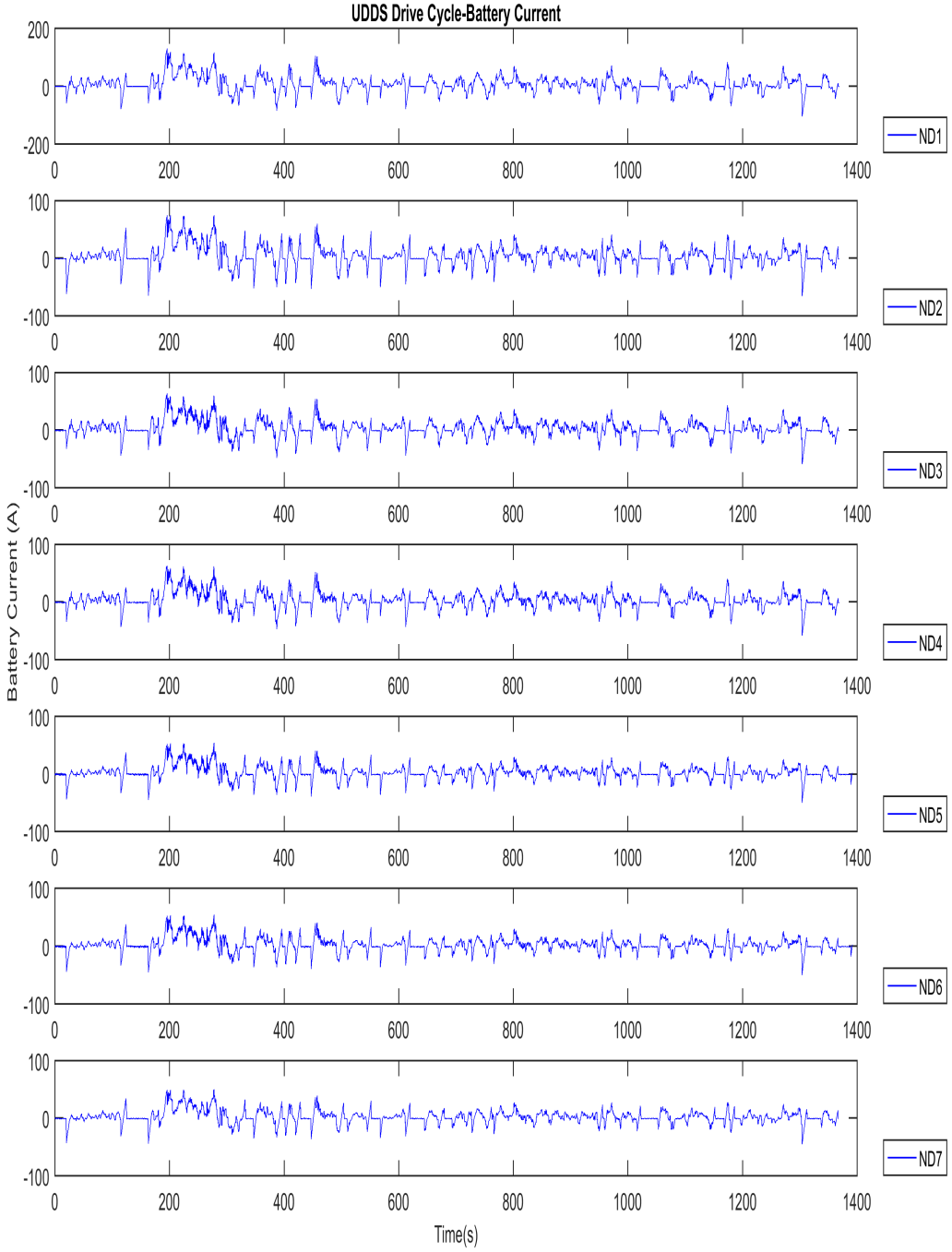

Figure 4.38: Comparison of different FWT powertrain designs-battery current graph

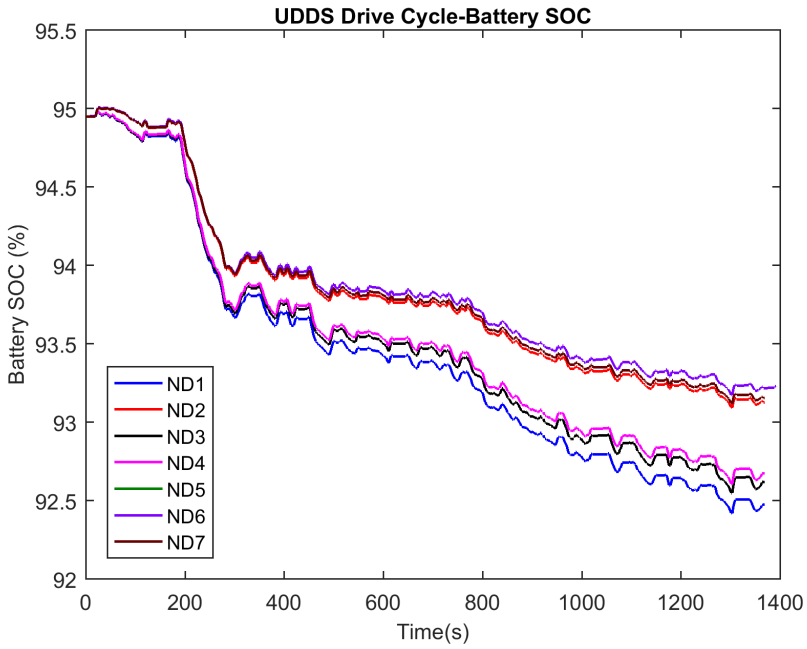

Figure 4.39: Comparison of different FWT powertrain designs-SOC graph

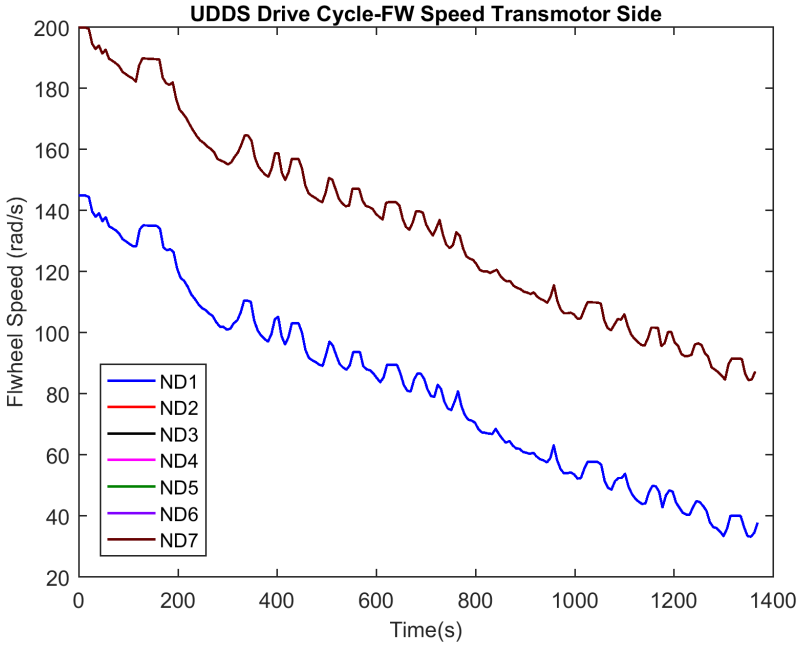

Figure 4.40: Comparison of different FWT powertrain designs-FW speed graph

Table 4.6: Energy consumption comparison

	E_e (Wh/cycle)	E_m (Wh/cycle)	E_e(Wh/mile)	E_m(Wh/mile)
Design 1	595.2	275.2	79.89	36.94
Design 2	436.8	449.6	58.63	60.35
Design 3	559.2	274	75.06	36.78
Design 4	547.2	274	73.45	36.78
Design 5	410	445	55.03	59.73
Design 6	412.8	448	55.4	60.13
Design 7	432	448	58	60.13
Nissan Leaf	958.2	0	128.62	0

Table 4.7: Comparison of different FWT powertrain designs

	E_{mech} (%)	Acceleration (s)	Perf. Change(%)	Range(mi)	Range Change (%)
Design 1	31.61	11.5	-21	160.7	+1
Design 2	50.8	9.5	-	159.6	+0.4
Design 3	32.9	14	-47.3	179.8	+13
Design 4	33.3	10.4	-9.47	181.5	+14.2
Design 5	52	12	-26.3	177	+11.3
Design 6	52	9.4	+1	174.6	+9.8
Design 7	51	7.2	+24	171.7	+8
Nissan Leaf	0	9.5	-	159	-

designs is 0.4-1% which is not a significant improvement. It can be said that higher torque design as an optimization is not a promising way to approach.

Design 7 is an over design for this vehicle. Range increase is 8% with a 7.2s 0-60 mi acceleration time. Performance of the vehicle significantly improved but achieving an acceptable acceleration time with low power transmotor designs is possible. Because of this reason we can say that design 7 can be used for a high performance expensive EV.

Design 3, 4,5 and 6 are proper options that increase vehicle range 11.3-14.2%. Design 4 is the best powertrain design with a 60 kW transmotor an a 200 rad/s rated flywheel speed. The range of Nissan Leaf 2012 with FWT powertrain can be improved 14.2%. The acceleration time for this

design is 10.4 s which is a moderate performance for a vehicle.

According to simulation results, higher mechanical energy transfer ratio results in better performance cars. In Table 4.7, we see that when the mechanical energy transfer ratio is around 50%, acceleration performance of the vehicle increases. An EV with a mechanical energy transfer ratio around 30% travels longer distance.

5. CONCLUSION

In this study, we developed a new powertrain for EVs. In this new powertrain configuration, we used a transmotor and a flywheel. Our goal was to introduce a new mechanical energy transfer to improve the range of an EV. The operation principal and mathematical model of the transmotor and control of the machine was introduced. MTPA operation with field weakening was used to control the machine at the highest possible efficiency.

Various applications of flywheels in ICE vehicles and EVs were investigated. Advantages and drawbacks of both full mechanical powertrains and EV powertrains were presented. Mechanical flywheel powertrains complicated components such as continuous variable tranmissions are used. In addition to that to implement energy recovery with a flywheel in mechanical powertrains extra components like clutches and actuators have to be used. As a result, complexity of the powertrain and cost of the vehicle increases. On the other side, EV powertrains utilize high technology electrical machines and multiple power converters in their topology that also increases the complexity of the control and cost of the vehicle.

In our topology we aimed to use benefits of both mechanical and electrical powertrains. In mechanical powertrains, the form of the energy does not change and efficiency of the energy transfer is higher as a result. EV powertrains do not require torque converters, response of the system is faster, regenerative braking occurs naturally, and maintenance requirement is significantly lower than mechanical systems. In this purpose, we used a dual rotor electrical machine, transmotor, and equipped the transmotor with a flywheel. FWT powertrain could benefit from both mechanical energy transfer and electrical energy transfer.

A transmotor can process very high power between its mechanical ports with a very low portion electrical power. We introduced the basics of the transmotor and a detailed analysis of energy transfer in Chapter 2. We showed that high power transfer between two identical flywheels with a lower electrical power rating. We emphasized the relative speed difference between the two mechanical ports is an important parameter to drive the transmotor and it is directly related to the

mechanical to mechanical energy power transfer ratio.

EV basics and a simple EV modeling was introduced in Chapter 3. In this chapter, we presented existing electric powertrains briefly. Energy storage devices and their issues were explained and a deeper insight was given for those devices.

FWT powertrain was presented and simple application was given in chapter 4. After developing the basic application, we applied this novel powertrain in a commercial EV that was Nissan Leaf 2012. A simulation model was developed and computer simulations were performed for this commercial product under standard drive cycles. In the light of the simulation results we discovered following design rules for the FWT powertrain.

- The moment of inertia of the flywheel has a very limited effect on the electrical power ratings and performance of the FWT. A flywheel that has a 1-2% of a vehicle weight is enough for regenerative braking.

- Rated speed of the flywheel is a significant parameter to determine electrical power ratings and performance of the vehicle. The rated speed of the flywheel should be set to a speed value that is close to the average speed of the driving schedule.

- The energy stored in the flywheel of the FWT powertrain should be around 2-3% of the main energy storage device's energy.

According to simulation results the range of a compact EV like Nissan Leaf 2012 can be increased upto 14.2% with an optimized powertrain design. In this design, electrical power of the traction motor and power electronics can be decrease 25%. These results clearly show that an EV with FWT powertrain can benefit from the mechanical power transfer to propel and brake vehicle. Since the power level is lower, peak current levels are decreased as well. Lower power level decreases the stress on the battery and can increase the battery life. In addition, FWT powertrain does not need a high DC bus voltage and utilizes only one bi-directional traction inverter. Traction is provided by a single electrical machine. The control complexity is lower compared to the other electric flywheel applications in the literature. Second mechanical port in the machine introduces

a second speed value in the system and transmotor is driven based on the relative speed between the two shafts of the machine. Because of this relative speed, a transmotor can be operated in a wider constant torque region that gives a significant room to a designer.

Although we have very beneficial outcomes for FWT powertrain , we introduce some drawbacks into the system as well. First of all, the transmotor in the system uses brushes and slip-rings which causes extra losses and needs extra maintenance. Because of the high flywheel speeds brushes and slip-rings would suffer from low lifetime. Because of this reason, they are mostly avoided in EV traction applications. Secondly, the transmotor in the powertrain has a torque constraint. Because of this constraint, charging the flywheel during the vehicle operation might require extra mechanical components such as a clutch and a mechanical lock. In addition to that, both of the mechanical shaft speeds should be measured. As a result, an extra speed sensor is required. Compared to the conventional electrical machine drives, control complexity of a transmotor drive is higher. Also, even though we have a relatively low speed flywheel in the powertrain, gyroscopic forces can cause failure in the operation of a flyhweel. Besides, during a tough road vehicle operation, the vertical forces on the flywheel can ruin the alignment of the machine and create extra safety and maintenance problems. Lastly, we should express that adding a flywheel in an EV powertrain creates an extra weight and cost in the vehicle.

Having said all of these drawbacks, we can suggest some solutions for certain issues. In our powertrain, we utilized a dual rotor transmotor and it has a torque constraint as we mentioned before. A three member transmotor that consists of two rotors and a stator can be developed to overcome this torque constraint. The stator in the new transmotor can be used to add or subtract torque during the operation. In this topology, we can also eliminate the need of brushes and slip-rings. As a future work, a three member transmotor can be developed and applied to an EV powertrain. This suggested three member transmotor could be very a promising alternative for EV applications. In our study, we discovered that flywheel rated speed should be around the drive cycle average speed to minimize the electrical power. In real world applications, drive cycles are not constant speed patterns. In this purpose, we can offer to use a dynamic flywheel speed charge

system that uses an online vehicle communication. By using the online traffic data, we can charge the flywheel at different speeds and we can have a more energy efficient. Using online vehicle communication in FWT powertrain can be a very challenging and pioneer research in EV area.

5.1 Discussion

As a result of this study, we have found out that the range of an EV can be increased 14.2% with a 25% lower electrical power. This outcome of the research can be used to design different vehicles. For example, this range increase can be used to shrink the battery in the EV. In this way, we can decrease the weight of the battery pack and cost of the battery pack as well. Also, lower power ratings can enable us to use low cost power electronic switches as well. As a result, a lower priced same range vehicle could be manufactured.

According to our study, we can sacrifice the performance of the vehicle a little more and can have even lower electrical power ratings. In the design 3 and 5 we see that a 45 kW transmotor can be used as an acceptable EV design. When the power level is this low, battery currents would be also significantly lower. In this case, charge/discharge efficiency of the battery could become less important. As it is known electric power level in hybrid EVs is lower. For example a Toyota Prius uses a 50 kW motor-generator and they prefer to use a NiMH battery in their powertrain. Admitting the fact that hybrid EVs full electric range is lower, a full EV could benefit from NiMH batteries if they run on low electric power. NiMH batteries can reach upto 120 Wh/kg energy density number whereas this number is 132Wh/kg in Nissan Leaf battery. A low power FWT powertrain topology could enable us to use NiMH batteries instead of high technology Li-Ion batteries. As a result, the cost of the vehicle could be significantly decreased. However, cost of the battery, FWT powertrain and an EV depends on many other parameters as well. We need more research and justification to make a clear comment about this issue.

REFERENCES

[1] D. A. Howey, R. Martinez-Botas, B. Cussons, and L. Lytton, "Comparative measurements of the energy consumption of 51 electric, hybrid and internal combustion engine vehicles," *Transportation Research Part D: Transport and Environment*, vol. 16, no. 6, pp. 459–464, 2011.

[2] "Plug-in electric vehicles: Market analysis and used price forecast," Tech. Rep. Q2, NADA, 2013.

[3] P. A. Nelson, K. G. Gallagher, I. Bloom, and D. W. Dees, "Modeling the performance and cost of lithium-ion batteries for electric-drive vehicles," Tech. Rep. ANL-12/55, Argonne National Laboratory, Argonne, IL, Dec. 2012.

[4] A. Emadi, *Advanced Electric Drive Vehicles*. Boca Raton, FL: CRC Press, Taylor & Francis, 2015.

[5] D. Bender, "Flywheels," Tech. Rep. SAND2015-3976, Sandia National Laboratory, Albuquerque, NM, May 2015.

[6] M. E. Amiryar and K. R. Pullen, "A review of flywheel energy storage system technologies and their applications," *Applied Sciences*, vol. 7, no. 3, p. 286, 2017.

[7] J. G. de Oliveira, H. Schettino, V. Gama, R. Carvalho, and H. Bernhoff, "Study on a doubly-fed flywheel machine-based driveline with an ac/dc/ac converter," *IET Electrical Systems in Transportation*, pp. 51–57, 2012.

[8] A. Dhand and K. Pullen, "Review of flywheel based internal combustion engine hybrid vehicles," *International Journal of Automotive Technology*, vol. 14, no. 5, pp. 797–804, 2013.

[9] G. Weisenberger, "Electric motor," Feb. 5 1900. US Patent 667,275.

[10] E. H. Wakefield, *History of the electric automobile battery-only powered cars*. Warrendale, PA: Society of Automotive Engineers SAE, 1993.

[11] L. Xu, "A new breed of electric machines-basic analysis and applications of dual mechanical port electric machines," in *Electrical Machines and Systems, 2005. ICEMS 2005. Proceedings of the Eighth International Conference on*, vol. 1, pp. 24–31, IEEE, 2005.

[12] L. Xu, Y. Zhang, and X. Wen, "Multioperational modes and control strategies of dual-mechanical-port machine for hybrid electrical vehicles," *IEEE Transactions on Industry applications*, vol. 45, no. 2, pp. 747–755, 2009.

[13] K. Ji, S. Huang, J. Zhu, Y. Gao, and C. Zeng, "A novel brushless dual-mechanical-port electrical machine for hybrid electric vehicle application," in *Electrical Machines and Systems (ICEMS), 2012 15th International Conference on*, pp. 1–6, IEEE, 2012.

[14] S. Cui, S. Han, X. Zhang, and Y. Cheng, "Design optimization for unified field permanent magnet dual mechanical ports machine," in *Vehicle Power and Propulsion Conference (VPPC), 2014 IEEE*, pp. 1–6, IEEE, 2014.

[15] F. Zhao, Z. Xingming, X. Wen, G. Qiujian, Z. Li, and Z. Guangzhen, "A control strategy of unified field permanent magnet dual mechanical port machine," in *Electrical Machines and Systems (ICEMS), 2013 International Conference on*, pp. 685–690, IEEE, 2013.

[16] M. Ghanaatian and A. Radan, "Modeling and simulation of dual mechanical port machine," in *Power Electronics, Drive Systems and Technologies Conference (PEDSTC), 2013 4th*, pp. 125–129, IEEE, 2013.

[17] S. Sodhi, "Electromagnetic gearing applications in hybrid-electric vehicles," Master's thesis, Texas A&M University, 1994.

[18] Y. Gao and M. Ehsani, "A mild hybrid vehicle drive train with a floating stator motor-configuration, control strategy, design and simulation verification," tech. rep., SAE Technical Paper, 2002.

[19] A. Ghayebloo and A. Radan, "Superiority of dual-mechanical-port-machine-based structure for series–parallel hybrid electric vehicle applications," *IEEE Transactions on Vehicular Technology*, vol. 65, no. 2, pp. 589–602, 2016.

[20] M. Hedlund, J. Lundin, J. de Santiago, J. Abrahamsson, and H. Bernhoff, "Flywheel energy storage for automotive applications," *Energies*, vol. 8(10), pp. 10636–10663, 2015.

[21] R. Whitelaw, *Two new weapons against automotive air pollution: the hydrostatic drive and the flywheel-electric LDV.[Local-Duty Vehicle (LDV)].* New York, NY: ASME, 1972.

[22] G. C. Kugler, "Electric vehicle hybrid power train," Tech. Rep. 730254, SAE Technical Paper, Feb. 1973.

[23] G. Chang, J. Swisher, and G. Pezdirtz, "DOE's flywheel program," in *Flywheel Technology Symp*, 1977.

[24] B. H. Rowlett, "Flywheel drive system having a split electromechanical transmission," Nov. 18 1980. US Patent 4,233,858.

[25] H. H. Braess and K. N. Regar, "Electrically propelled vehicles at BMW-experience to date and development trends," tech. rep., SAE, 1991.

[26] P. Jefferies and A. Corbett, "The petro-electric drive train," in *IEE Colloquium on Motors and Drives for Battery Powered Propulsion*, pp. 7–1, IET, 1993.

[27] U. Schaible and B. Szabados, "A torque controlled high speed flywheel energy storage system for peak power transfer in electric vehicles," in *Conference Record of the 1994 IEEE Industry Applications Society Annual Meeting*, pp. 435–442, IEEE, 1994.

[28] P. Mellor, N. Schofield, and D. Howe, "Flywheel and supercapacitor peak power buffer technologies," in *Electric, Hybrid and Fuel Cell Vehicles (Ref. No. 2000/050), IEE Seminar*, pp. 8/1–8/5, IET, 2000.

[29] M. Flynn, J. Zierer, and R. Thompson, "Performance testing of a vehicular flywheel energy system," tech. rep., SAE, 2005.

[30] T. S. Saitoh, D. Ando, and K. Kurata, "A grand design of future electric vehicle with fuel economy more than 100 km/liter," tech. rep., SAE Technical Paper, 1999.

[31] T. Saitoh, A. Yoshimura, and N. Yamada, "An evaluation of future energy conversion systems including fuel cell," *WIT Transactions on The Built Environment*, vol. 75, 2004.

[32] T. S. Saitoh, H. Ogasawara, and N. Yamada, "Study of flywheel energy storage system and application to electric vehicle," *Nippon Kikai Gakkai Ronbunshu B Hen(Transactions of the Japan Society of Mechanical Engineers Part B)(Japan)*, vol. 16, no. 9, p. 2482, 2004.

[33] T. S. Saitoh, N. Yamada, D. Ando, and K. Kurata, "A grand design of future electric vehicle to reduce urban warming and co 2 emissions in urban area," *Renewable Energy*, vol. 30, no. 12, pp. 1847–1860, 2005.

[34] J. Lundin, *Flywheel in an all-electric propulsion system*. PhD thesis, Uppsala University, Uppala, June 2011.

[35] J. de Oliveira, *Power control systems in a flywheel based all-electric driveline*. PhD thesis, Uppsala University, Uppsala, Sept. 2011.

[36] R. C. Clerk, "The utilization of flywheel energy," tech. rep., SAE Technical Paper, 1964.

[37] L. J. Lawson, "Design and testing of high energy density flywheels for application to flywheel/heat engine hybrid vehicle drives," in *Intersociety Energy Conversion Engineering Conf*, 1971.

[38] G. Dugger, A. Brandt, J. George, and L. Perini, "Flywheel and flywheel/heat engine hybrid propulsion systems for low-emission vehicles," in *Intersociety Energy Conversion Engineering Conf*, 1971.

[39] A. Frank and N. Beachley, "Improved fuel economy in automobiles by use of a flywheel energy management system," in *Flywheel Technology Symp*, DTIC Document, 1975.

[40] W. V. Loscutoff, "Flywheel-heat engine power for an energy-economic personal vehicle," tech. rep., Battelle Pacific Northwest Labs., Richland, Wash.(USA), 1976.

[41] F. Hagin, S. Martini, and R. Zelinka, "The use of hydrostatic braking and flywheels systems in buses hydrobus and gyrobus: Their future applications in hybrid electric vehicles to

reduce energy consumption, and to increas," *Electric Vehicle Develompent Group International*, 1981.

[42] C. Greenwood, "Integration of a commercial vehicle regenerative braking driveline," *Leyland Vehicles, Leyland, Preston, Lancashire*, no. C191/86, 1986.

[43] N. Schilke, A. DeHart, L. Hewko, C. Matthews, D. Pozniak, and S. Rohde, "The design of an engine-flywheel hybrid drive system for a passenger car," *Proceedings of the Institution of Mechanical Engineers, Part D: Transport Engineering*, vol. 200, no. 4, pp. 231–248, 1986.

[44] R. Van der Graaf, "An IC engine flywheel hybrid drive for road vehicles," in *EAEC Conf*, 1987.

[45] S. Shen, A. Serrarens, M. Steinbuch, and F. Veldpaus, "Coordinated control of a mechanical hybrid driveline with a continuously variable transmission," *JSAE review*, vol. 22, no. 4, pp. 453–461, 2001.

[46] U. Diego-Ayala, P. Martinez-Gonzalez, N. McGlashan, and K. Pullen, "The mechanical hybrid vehicle: an investigation of a flywheel-based vehicular regenerative energy capture system," *Proceedings of the Institution of Mechanical Engineers, Part D: Journal of Automobile Engineering*, vol. 222, no. 11, pp. 2087–2101, 2008.

[47] D. Cross and J. Hilton, "High speed flywheel based hybrid systems for low carbon vehicles," in *IET HEVC 2008 - Hybrid and Eco-Friendly Vehicle Conference*, pp. 1–5, Dec 2008.

[48] K. van Berkel, S. Rullens, T. Hofman, B. Vroemen, and M. Steinbuch, "Topology and flywheel size optimization for mechanical hybrid powertrains," *IEEE Transactions on Vehicular Technology*, vol. 63, no. 9, pp. 4192–4205, 2014.

[49] G. Choi and T. Jahns, "Design of electric machines for electric vehicles based on driving schedules," in *Electric Machines & Drives Conference (IEMDC), 2013 IEEE International*, pp. 54–61, IEEE, 2013.

[50] K. Pullen and C. Ellis, "Kinetic energy storage for vehicles," in *Hybrid Vehicle Conference, IET The Institution of Engineering and Technology, 2006*, pp. 91–108, IET, 2006.

[51] J. G. De Oliveira, H. Schettino, V. Gama, R. Carvalho, and H. Bernhoff, "Study on a doubly-fed flywheel machine-based driveline with an ac/dc/ac converter," *IET Electrical Systems in Transportation*, vol. 2, no. 2, pp. 51–57, 2012.

[52] M. Ehsani, Y. Gao, and A. Emadi, *Modern Electric, Modern Hybrid, and Fuel Cell Vehicles*. Boca Raton, FL: CRC Press, second ed., 2010.

[53] A. Dehkordi, A. Gole, and T. Maguire, "Permanent magnet synchronous machine model for real-time simulation," in *International Conference on Power Systems Transients (IPST 2005)*, vol. 5, pp. 19–23, 2005.

[54] F. Niu, B. Wang, A. S. Babel, K. Li, and E. G. Strangas, "Comparative evaluation of direct torque control strategies for permanent magnet synchronous machines," *IEEE Transactions on Power Electronics*, vol. 31, no. 2, pp. 1408–1424, 2016.

[55] C. Capitan, "Torque control in field weakening mode," Master's thesis, Aalborg University, Aalborg, June 2009.

[56] D. Martinez, "Design of a permanent magnet synchronous machine with non–overlapping concentrated windings," *KTH, Stockholm, Master Thesis XR-EE-E2C*, vol. 2012, p. 020, 2012.

[57] P. Vaclavek and P. Blaha, "Interior permanent magnet synchronous machine high speed operation using field weakening control strategy," in *WSEAS International Conference. Proceedings. Mathematics and Computers in Science and Engineering*, no. 12, WSEAS, 2008.

[58] Y. Yang, S. M. Castano, R. Yang, M. Kasprzak, B. Bilgin, A. Sathyan, H. Dadkhah, and A. Emadi, "Design and comparison of interior permanent magnet motor topologies for traction applications," *IEEE Transactions on Transportation Electrification*, vol. 3, no. 1, pp. 86–97, 2017.

[59] Y. kang Chin, "A permanent magnet synchronous motor for an electric vehicle - design analysis," Master's thesis, Royal Institute of Technology, Stockholm, SWEDEN, Apr. 2004.

[60] T. M. Jahns, S.-H. Han, A. M. El-refaie, J.-H. Baek, M. Aydin, M. K. Guven, and W. L. Soong, "Design and experimental verification of a 50 kw interior permanent magnet synchronous machine," in *Industry Applications Conference, 2006. 41st IAS Annual Meeting. Conference Record of the 2006 IEEE*, vol. 4, pp. 1941–1948, IEEE, 2006.

[61] B. Y. Liaw and M. Dubarry, "From driving cycle analysis to understanding battery performance in real-life electric hybrid vehicle operation," *Journal of power sources*, vol. 174, no. 1, pp. 76–88, 2007.

[62] Y. Sato, S. Ishikawa, T. Okubo, M. Abe, and K. Tamai, "Development of high response motor and inverter system for the nissan leaf electric vehicle," tech. rep., SAE Technical Paper, 2011.

[63] J. G. Hayes and K. Davis, "Simplified electric vehicle powertrain model for range and energy consumption based on epa coast-down parameters and test validation by argonne national lab data on the nissan leaf," in *Transportation Electrification Conference and Expo (ITEC), 2014 IEEE*, pp. 1–6, IEEE, 2014.

[64] H. Kawamura, K. Ito, T. Karikomi, and T. Kume, "Highly-responsive acceleration control for the nissan leaf electric vehicle," tech. rep., SAE Technical Paper, 2011.

[65] Y. Ishihara, H. Takagi, and K. Asao, "Aerodynamic development of the newly developed electric vehicle," tech. rep., SAE Technical Paper, 2011.

[66] M. Ikezoe, N. Hirata, C. Amemiya, T. Miyamoto, Y. Watanabe, T. Hirai, and T. Sasaki, "Development of high capacity lithium-ion battery for nissan leaf," tech. rep., SAE Technical Paper, 2012.

[67] Y. Kinoshita, T. Hirai, Y. Watanabe, Y. Yamazaki, R. Amagai, and K. Sato, "Newly developed lithium-ion battery pack technology for a mass-market electric vehicle," tech. rep., SAE Technical Paper, 2013.

[68] T. Burress, "Benchmarking state-of-the-art technologies," *Oak Bridge National Laboratory, ORNL report*, 2013.

[69] H. Lohse-Busch, M. Duoba, E. Rask, and M. Meyer, "Advanced powertrain research facility avta nissan leaf testing and analysis," *Argonne National Laboratory*, 2012.

[70] T. Nakada, S. Ishikawa, and S. Oki, "Development of an electric motor for a newly developed electric vehicle," tech. rep., SAE Technical Paper, 2014.

[71] H. Shimizu, T. Okubo, I. Hirano, S. Ishikawa, and M. Abe, "Development of an integrated electrified powertrain for a newly developed electric vehicle," tech. rep., SAE Technical Paper, 2013.